INTERCRYSTALLINE SOLUTION ION ACTIVITY PRODUCT BASIS OF SUBSURFACE DISSOLUTION IN A HYDROXYAPATITE SYSTEM

by

David Henry Bergstrom

A dissertation submitted to the faculty of
The University of Utah
in partial fulfillment of the requirements for the degree of

Doctor of Philosophy

Department of Pharmaceutics

The University of Utah

June 1985

THE UNIVERSITY OF UTAH GRADUATE SCHOOL

SUPERVISORY COMMITTEE APPROVAL

of a dissertation submitted by

David Henry Bergstrom

This dissertation has been read by each member of the following supervisory committee and by majority vote has been found to be satisfactory.

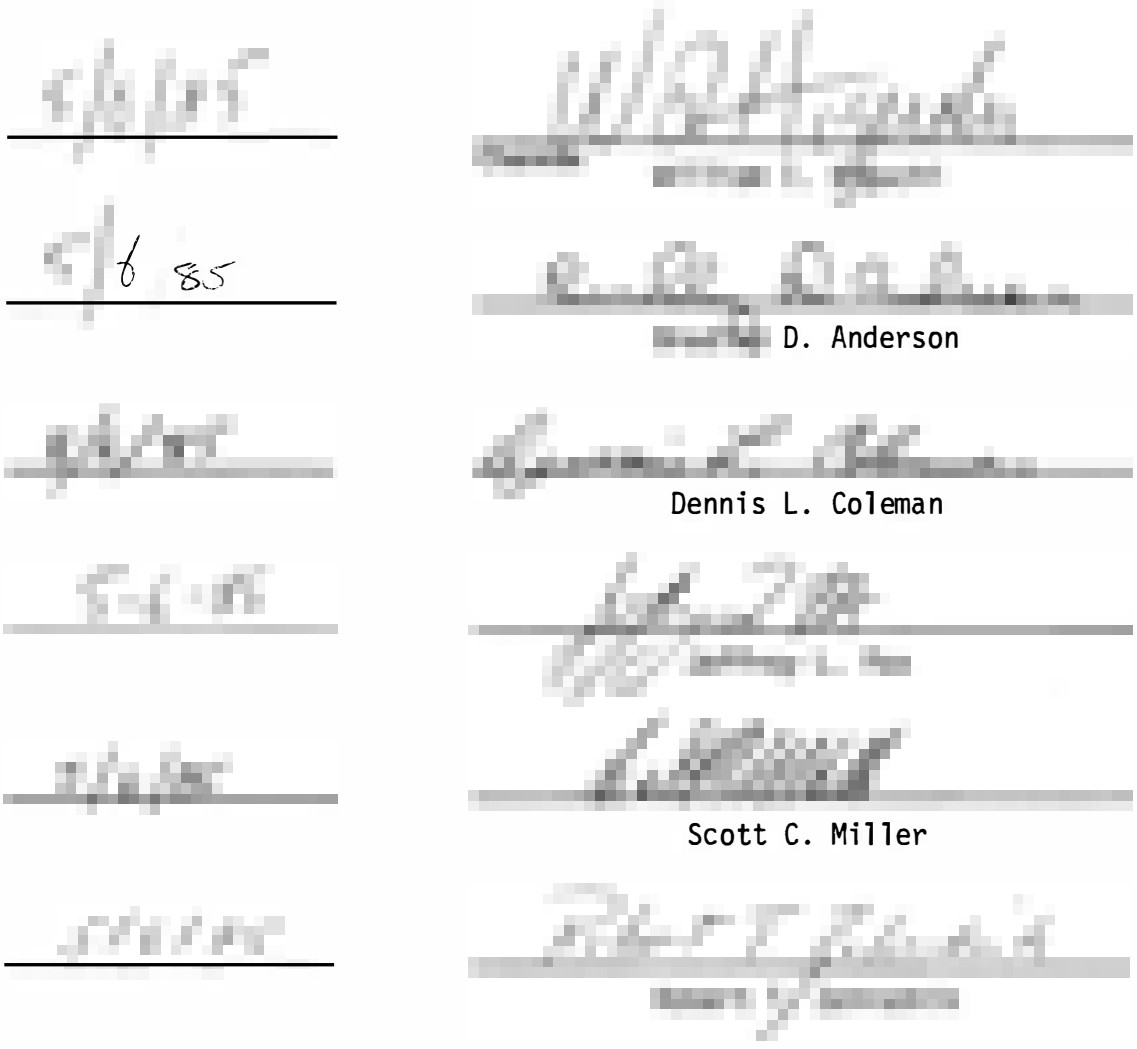

D. Anderson

Dennis L. Coleman

Scott C. Miller

THE UNIVERSITY OF UTAH GRADUATE SCHOOL

FINAL READING APPROVAL

To the Graduate Council of The University of Utah:

I have read the dissertation of David [redacted] in its final form and have found that (1) its format, citations, and bibliographic style are consistent and acceptable; (2) its illustrative materials including figures, tables, and charts are in place; and (3) the final manuscript is satisfactory to the Supervisory Committee and is ready for submission to the Graduate School.

May 10, 1985
Date

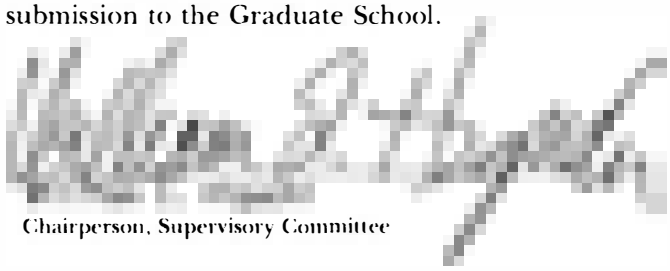

Chairperson, Supervisory Committee

Approved for the Graduate Council

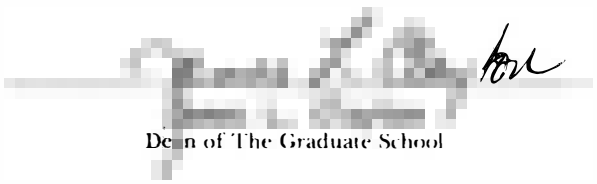

Dean of The Graduate School

ABSTRACT

Recognition of the importance of low level solution fluoride on the propensity of bovine enamel to form an intact surface layer with concomitant subsurface dissolution in an in vitro bovine enamel model hydroxyapatite system has led to the development of a comprehensive physical and mathematical model capable of predicting experimental observations over a wide range of solution chemistries and hydrodynamics. It has been found that as bulk solution fluoride diffuses into the enamel matrix it is adsorbed by the hydroxyapatite crystallites in the surface region. Upon saturation of the available adsorption sites in this surface region the intercrystalline solution ion activity product ($K_{FAP} = a_{Ca}^{10} \cdot a_{PO_4}^{6} \cdot a_{OH}^{2}$) is elevated above a critical value ($pK_{FAP} = 115.0 \pm 1.0$) and further dissolution of this surface region is inhibited. At the same time because of the adsorption/depletion mechanism, dissolution may prodeed at a finite rate beyond the advancing fluoride front resulting in subsurface dissolution with simultaneous preservation of the crystallites in the surface region. Consideration of the appropriate diffusion, reaction and chemical equilibria equations has enabled theoretical computer simulation of the subsurface dissolution phenomenon. Calculations have shown that the theoretical model is semi-quantitatively descriptive of the mineral density changes occurring within the hydroxyapatite matrix as a function of time and position.

To my wife, Tamie

TABLE OF CONTENTS

LIST OF FIGURES

LIST OF TABLES

ACKNOWLEDGMENTS

The author wishes to acknowlege the following individuals for their contributions in the completion of this dissertation.

Dr. William I. Higuchi, whose scientific guidance, insight and personal effort greatly assisted in achieving this goal. It has been a privilege to have studied under the direction of a scientist of his reputation.

Dr. Jeffrey L. Fox, for his scientific contribution in all phases of this project. In particular, acknowlegment is given for the computational aspects of the theoretical simulation of the problem.

Dr. Robert T. Zahradnik, whose interest and scientific appreciation of the problem made his comments and recommendations particularly valuable.

Dr. Bradley D. Anderson, whose scientific perspective on the problem forced critical examination of the hypotheses tested.

Dr. Dennis L. Coleman and Dr. Scott C. Miller, for their helpful comments during the development of the project.

My mother and father, for their continued support and encouragement throughout all of my college years.

Dr. Tamie Kurihara, my wife, whose own personal strength and determination has been and will continue to be, a constant source of inspiration. For her patience, understanding and unabated encouragement during my graduate studies, I owe a sincere thank you.

CHAPTER 1

INTRODUCTION

Subsurface demineralization, a phenomenon uniquely characteristic of dental enamel incipient caries formation, has been the subject of numerous studies. Despite the intensity of research in this area a mechanistic understanding of this subsurface dissolution process has remained elusive. It is generally accepted that enamel caries are the result of loss, through dissolution, of the enamel mineral component, hydroxyapatite. The dissolution process is initiated by the penetration of organic acids into the porous enamel matrix. These acids are metabolic by-products of the microbial flora and fermentable carbohydrates present in the oral cavity.

Dissolution studies conducted over the past quarter century with biological apatites and synthetic apatites, both in powder and block pellet form, have revealed that this area of research is extremely complex. Attempts by various research groups at describing the dissolution behavior of hydroxyapatite have had limited usefulness. It was not the two-site model was proposed for describing hydroxyapatite dissolution kinetics that many of the previously unexplained observations of hydroxyapatite dissolution could be rationalized over a wide range of solution conditions (Fox et al., 1978). While undoubtedly considered a breakthrough, the model is deficient in that although the observed zonal dissolution of enamel caries is predicted

the concomitant formation of an intact surface layer is not.

The principal goal then of this research was to understand the mechanism subsurface dissolution in bovine enamel and to predict semiquantitatively, using the physical model approach, the intercrystalline solution conditions giving rise to this unusual morphological pattern observed in incipient caries.

In order to characterize lesion morphology changes a method of quantifying the observed changes in mineral density had to be developed. The method of contact microradiography, with the appropriate internal standardizing and quantifying methods, developed herein provides this ability. The development of this technique then provided this laboratory with a quantitative technique capable of following mineral density changes occurring within the enamel directly rather than extrapolating conclusions from changes occurring within the solution chemistry with time. This technique and other previously established techniques made possible a systematic study to delineate the requisite variables determining subsurface dissolution in vitro.

The great degree of variability observed in human enamel in its tendency toward acid dissolution and caries formation makes it an unsuitable model system for basic in vitro studies. Bovine enamel, although containing more carbonate than human enamel, is chemically and morphologically similar. In addition to being readily available, bovine enamel obtained from calves fed a restricted, uniform diet has been found to be a suitable experimental model system to study the enamel dissolution process in vitro.

The implications of the results of this research in the in vivo clinical situation are apparent. In particular, is the need for fluoride in solution within the microenvironmental pores, in addition to sufficient calcium and phosphate, to inhibit the dissolution kinetics of enamel in the surface region. This finding is considered significant and will be an important consideration in the rational future development of therapeutic systems for the prevention or palliative treatment of dental caries.

CHAPTER 2

REVIEW OF THE LITERATURE

An inordinate amount of literature has been published in the area of hydroxyapatite dissolution. The literature cited herein pertains specifically to the clinically observed subsurface dissolution associated with incipient caries in dental enamel. The literature review is divided into four subheadings.

1. Enamel Composition in General: This will include a discussion of the inorganic mineral component, foreign ion gradients, porosity and organic matrix considerations.

2. Acid Demineralization of Enamel in General: This section will present an overview of previous studies into the dissolution kinetics of hydroxyapatite systems in the presence and absence of foreign ions, in particular fluoride. Emphasis will be placed on the dissolution studies performed in these laboratories examining the influence of solution fluoride on the enamel dissolution rate.

3. Enamel Dissolution Pertaining to Subsurface Demineralization Specifically: The various hypotheses proposed by different investigators will be reviewed. Attention will be drawn to the point of whether or not solution fluoride was a consideration.

4. Nature of the Intact Surface Layer: A series of questions will be addressed. What is the intact surface layer? Is the surface enamel inert and consequently stays behind after dissolution by de-

fault? Is the intact surface dynamic and forms with time? If so, what is this new phase? Or, is the intact surface layer nothing more than fluoride inhibition of the enamel dissolution rate (Mir, 1967).

Enamel Composition in General

By weight, dental enamel is composed almost entirely of the mineral hydroxyapatite, a calcium phospate compound of chemical formula $Ca_{10}(PO_4)_6(OH)_2$. The remaining few percent by weight are accounted for by water and less than 1% by organic material (Driessens, 1980). Hydroxyapatite serves as a prototype of the inorganic component of enamel. However, other calcium phosphates like whitlockite, are known to be present (Driessens, 1980). Nonetheless, the majority of research results presented in the literature have assumed the inorganic component of enamel to be a single phase of hydroxyapatite crystallites.

Hydroxyapatite has the rather unusual property of being able to incorporate into its crystalline lattice a large number of foreign ions. By spark source mass spectroscopy, 35 elements were found to be present in human enamel in detectable and quantifiable concentrations (Losee, et al., 1974). Minor elements occurring in greatest concentration (> 10 micrograms/g. dry weight) were F, Mg, S, Cl, K, Zn and Sr. Baseline levels for F were determined to be approximately 300 micrograms/gram. The influence of these trace elements on the solubility and dissolution kinetics has been studied by many investigators. In particular, fluoride ion has received a great deal of attention due to its purported anti-caries activity.

A major impurity ion, carbonate, has been found to have a strong preference for incorporation in only one calcium phosphate, hydroxyapatite (Driessens, 1980). The amount of carbonate in mature human enamel varies greatly between individuals from near 0 to approximately 3%. The exact role carbonate plays in affecting thermodynamic and kinetic properties of hydroxyapatite is not known. Solubility studies have shown that carbonate produces an effect only under certain conditions. It increased the solubility of apatite when present in solution and when incorporated into precipitated apatite. Unexpectedly, it did not change the solubility when acquired through exposure of apatite to bicarbonate solutions (Gron et al., 1963). A selective loss of carbonate occurs during the early stages of caries formation and carbonate has therefore been implicated as a possible source of "weakness" in enamel, so far as carious attack is concerned. Several authors have shown that carious enamel contains less carbonate than does sound tissue (Coolidge and Jacobs, 1957; Johansen, 1963). The carbonate content of sound bovine enamel is between 3 and 4% (Driessens and Verbeeck, 1982).

Concentration gradients have been found to exist for several of the minor ions within the enamel. Qualitatively, fluoride concentration is found to decrease with distance from the enamel surface to the dentino-enamel junction (Little and Barrett, 1976). A reverse gradient in exists in mature enamel (Driessens and Verbeeck, 1982). Variation in the enamel concentrations of these ions between individuals is observed.

Zahradnik determined porosity, specific surface area and pore volume distribution by an isothermal water vapor sorption technique (Zahradnik and Moreno, 1975). Assuming a value of 3 grams/cm^3 for the density of enamel, the apparent porosity was reported to be about 1.8%. Specific surface areas were reported to be approximately 4 $meter^2$/gram.

The nonmineral component of enamel is referred to under the general term organic matrix. This organic matrix is proteinaceous in nature. It has an amino acid composition characterized by a high content of proline (25%) and relatively high concentrations of glutamic acid, histidine and leucine. The carbohydrate content of the matrix is about 1%. The principal carbohydrates are hexose and hexosamine. Acid mucopolysaccharides and glycopeptides are minor components.

Acid Demineralization of Enamel in General

Simplistically, incipient caries of dental enamel are the result of dissolution of the inorganic component of enamel, hydroxyapatite, in an acidic media. Because of the complexity of this process all attempts at achieving a fully comprehensive understanding of enamel dissolution behavior have met with varying degrees of failure. Only now is a unified model describing hydroxyapatite dissolution behavior over a wide range of bulk solution conditions (degree of saturation and foreign agent presence and hydroxyapatite "type") being developed.

One hundred years ago it was postulated that dissolution due to acids was an important step in the initiation of dental caries (Mil-

ler, 1884). This hypothesis of caries formation remains the keystone around which the physical chemical studies of dental caries are designed. Despite the century of work centered on this hypothesis the basic parameters determining the nature of carious lesion formation under various conditions have remained elusive to all investigators. To reconcile these heretofore disparate in vitro results, a mechanistic basis for subsurface demineralization is needed.

It was postulated that acid dissolution of enamel may be a diffusion controlled process (Stalfors, 1958; Gray, 1962). Gray's work suggested that an approach based on the use of mathematical modeling might be applied to the kinetics of dental enamel dissolution. Eventually this led other investigators (Higuchi, Gray, Hefferren and Patel, 1965) to develop a model for enamel dissolution which included a dissolution driving force equated to the solubility of hydroxyapatite and a first order kinetic rate constant related to the hydrodynamics and diffusivities of the reacting chemical species. This model as formulated rationalized the dependency of dissolution rate on solution pH, buffer concentration, buffer pK_a and concentrations of calcium or phosphate common ion. Experiments performed over a range of solution conditions showed that the model described the data remarkably well. The solubility of enamel was a fitted parameter in this model, its value corresponding to a solubility product of about 10^{-124}, which is considerably below the accepted value of the thermodynamic solubility of 10^{-116}. Experiments conducted with both block enamel and powdered enamel suspensions yielded similar results.

In order to perform more well defined kinetic studies than those obtainable with biological apatite, synthetic hydroxyapatite was compressed into pellets and employed as a model apatite system (Wu, Higuchi, Fox and Friedman, 1976). The pellets were mounted in a rotating disk apparatus which had quantitatively well defined hydrodynamics. These controlled hydrodynamics enabled dissolution rates to be calculated on an absolute basis as a function of solution composition and angular velocity of the rotating disk. Such calculations showed that NBS-hydroxyapatite had an apparent solubility corresponding to a solubility product of around 10^{-125}, suggesting this material to be a suitable synthetic model for dental enamel. At the same time, it was observed that the dissolution kinetics were intermediate between strictly surface controlled and diffusion controlled. That is, both aqueous diffusion and surface kinetics contributed significantly to the rate constant, k. At low angular velocity, k was predominantly diffusion controlled; at high angular velocity, k was only 30 to 50% diffusion controlled.

Since the model yielded an apparent solubility or ion activity product dissolution threshold considerably below the thermodynamic solubility of hydroxyapatite, it followed that there would be no dissolution expected if hydroxyapatite were exposed to a solution supersaturated with respect to this apparent solubility or dissolution threshold. Experiments designed to test this prediction refuted the model predictions as dissolution occurred into solutions supersaturated with respect to this dissolution threshold.

Extensive experimentation subsequent to this observation led to a postulate of two distinct types of dissolution sites, each characterized by a rate constant and an ion activity product dissolution threshold demarcating the regime of solution composition in which dissolution occurs from that in which there is no dissolution (Fawzi, Fox, Dedhiya, Higuchi and Hefferren, 1978; Fox, Higuchi, Fawzi and Wu, 1978; Griffith, Katdare, Fox and Higuchi, 1978). The two-site model and accompanying mathematics assumed that NBS-hydroxyapatite crystal dissolution may occur at two sites each characterized by an apparent solubility, C_s and a first order crystal surface-solution kinetic reaction rate constant, k_c. This model adequately described the dissolution kinetics of hydroxyapatite over a wide range of solution compositions.

This early work on the two-site model used compressed pellets of hydroxyapatite and a physical model that accounted for both dissolution and diffusion in the intercrystalline spaces in the pellet. The model was used to deduce the dissolution kinetic properties of hydroxyapatite, even though the crystals in the pellets encountered a range of microenvironmental solution compositions dependent on their locus in the pellet. These deduced parameter values were later critically examined in carefully designed dissolution kinetic experiments with hydroxyapatite suspensions and found to be in quantitative agreement (Higuchi et al., 1983). This demonstrated not only the validity of the kinetic parameters but also that the quantitative correlations were possible between data from suspension experiments and data from

experiments using pellets (and possibly for experiments using block enamel as well).

Acid demineralization of enamel in the presence of solution fluoride has been studied by many investigators. Fluoride has been implicated in making the enamel more resistant to acid dissolution (Dean, Arnold and Elvove, 1942; Volker, 1939; Armstrong and Brekhus, 1938). The findings of these studies were supported in that fluoride prevents caries by combining directly with the enamel surface to increase its resistance to the effect of acid (Bibby, 1944 a,b). The importance of the effect of solution fluoride on the dissolution kinetics of hydroxyapatite has been recognized by few investigators. At low solution fluoride concentrations (less than 100 ppm) the following mechanism has been postulated for the reaction of fluoride with dental enamel in which fluorapatite is the only reaction product:

$$Ca_{10}(PO_4)_6(OH)_2 + 2\ F^- \longrightarrow Ca_{10}(PO_4)_6F_2 + 2\ OH^-$$

The fluoride ions in solution exchange with the hydroxyl groups of the hydroxyapatite crystal surface. It has been shown that there is no liberation of, nor exchange with phosphate (Falkenheim and Hodge, 1947; Neuman, Neuman, Main, O'Leary and Smith, 1950). There is however, competition between solution hydroxyl and fluoride ions for the limited number of surface sites of the apatitic crystal. The reaction between fluoride ions and hydroxyapatite is not entirely reversible (Leach, 1959). Furthermore, the uptake of fluoride by hydroxyapatite at calcium and fluoride concentrations too low to form calcium fluo-

ride is extremely pH dependent (Mir, 1967). At low pH, significant amounts of fluoride are fixed by the apatite crystal, the reaction being not readily reversible (Neuman et al., 1950; Malaowalla and Myers, 1962). Brudevold, 1963 has shown that fluoride in acid solutions containing phosphate has the dual effect of depressing both calcium fluoride formation as well as the kinetics of enamel dissolution. This mechanism uniquely permits exposure of enamel to acidic fluoride containing solutions without resultant demineralization. The findings of Brudevold were confirmed by other investigators, albeit only qualitatively (Koulourides and Reed, 1964). It was not until 1967 when Mir et al. proposed a quantitative model that the inhibitory effect of low levels of solution fluoride upon enamel demineralization was understood mechanistically. The key assumption in this model is that the exposure of hydroxyapatite to a low concentration of solution fluoride in acidic buffers results in the formation of a thin layer of fluorapatite around the hydroxyapatite crystal. Thus, fluorapatite and not hydroxyapatite becomes the thermodynamically governing phase during dissolution. The results show that fluoride in solution decreased the rate of enamel dissolution. Dental enamel powder dissolution kinetics in the presence of low solution fluoride concentration were described by a solution ion activity product (K_{FAP}) of 10^{-119}. Similarity in the magnitude of the K_{FAP} and K_{HAP} for bovine enamel implies that the fluorapatite was formed by the isomorphous substitution of surface hydroxyls by fluoride ions rather than bulk precipitation of a new fluorapatitic phase.

Enamel Dissolution Pertaining to Subsurface Demineralization Specifically

Enamel dissolution as related to "white spot" formation or subsurface demineralization is a very complex and often times controversial subject. The histology of incipient caries has been reported in detail by many investigators. The most striking characteristic of incipient caries is the presence of a relatively unaltered surface enamel layer with an underlying zone where substantial demineralization has occurred. There is no clear reason why the lesion forms at some distance from and not at the enamel surface itself.

Theories attempting to delineate the mechanism of "white spot" or the subsurface dissolution phenomenon of enamel have centered on either a biological or physical basis and in some instances a combination of both.

The enamel surface was considered as a semipermeable membrane with resulting membrane equilibria of the type described by Donnan being responsible for carious decalcification (von Bartheld, 1961). In this model, which remains extant, enamel is regarded as a water containing gel of very dense structure. Because of its "density" it is assumed only to admit small molecules and ions from the oral fluid, remaining impenetrable to macromolecules such as proteins. In the immediate proximity of the enamel surface positively charged ions too large to diffuse into enamel (e.g., salivary mucins) are presumed to accumulate. A Donnan ionic distribution is set up resulting in a drop in pH within the enamel. An excess of hydrogen ions develops within the enamel and the ensuing decalcification proceeds as long as the

predominantly positively charged macromolecules remain in true or colloidal solution.

Of the various hypotheses put forth, two main lines of reasoning are most common. On the basis of the results obtained in these studies some have dealt primarily with the driving forces involved in the process (von Bartheld, 1958); others have focused attention on the kinetics of the process and the derivation of pertinent equations based on diffusion theory (Gray, 1966; Holly and Gray, 1968). Both approaches, however, have been only partially successful because they fail to explain fully all experimental observations.

One of the controversies among studies on the formation of the lesion pertains to the preservation of the surface layer. Many investigators have concluded that during in vivo or in vitro demineralization the surface is rendered less soluble due to the accumulation of fluoride (Larsen and Fejerskov, 1977), polyphosphate-like compounds (Francis, Briner and Gray, 1973; Featherstone, Duncan and Cutress, 1978), or other salivary components (Zahradnik, Moreno and Burke, 1976). Alternatively, it has been argued that the surface enamel is in some way intrinsically different than the bulk of the enamel by virtue of its lower carbonate content or high baseline fluoride levels and that for these reasons less mineral is lost during dissolution (Weatherell, Robinson and Hallsworth, 1974; Driessens, Dijk, Borggreven and Verbeeck, 1980). A gradient in the apparent solubility with enamel depth was proposed to account for subsurface dissolution (Theuns, Dijk, Driessens and Groeneveld, 1983). In a study on the

influence of fluoride in solution on enamel demineralization (Cate and Duijsters, 1983a), the authors have shown that the rate of enamel demineralization at a given pH is a function of the fluoride content in solution. From these data, it was concluded that the presence of fluoride at the time of acid attack on the enamel may considerably slow the rate of decay. Their mechanistic interpretation of these results is that during initial stages of demineralization, fluoride is adsorbed or bound onto the enamel surface, the result being an increased resistance of the surface enamel to acid attack. The authors go on to state that as an alternative or possibly additive mechanism, fluoride present in the lesion pores (near the enamel surface) may stimulate redeposition of mineral dissolved in the interior of the lesion.

Summarizing the currently plausible hypotheses concerning intact surface layer formation, first, the surface layer may be due to a protective agent rendering the outer enamel insoluble resulting in the preservation of the original surface (Gray and Francis, 1963; Featherstone, Duncan and Cutress, 1979). Gray has suggested that every system capable of forming an artificial lesion involves a component making the surface insoluble (Gray, 1977). Secondly, the surface layer may be the result of a combination of dissolution and/or reprecipitation processes resulting in a regeneration of the surface layer (Moreno and Zahradnik, 1974; Dijk, Borggreven and Driessens, 1979).

Nature of the Intact Surface Layer

A great deal of controversy centers upon chemical definition of the exact nature of the intact surface layer. The fact that the intact layer is on a microscale, analytical limitations and the probability of multiple phase presence all confound the problem of chemical composition determination. Certain physical characteristics of the intact surface layer have been reported; these will be reviewed here. Some conceptions that are more conjecture than fact will also be discussed.

A number of questions arise when discussing the intact surface layer. Does it grow? That is, is it dynamic, increasing in mineral density as a function of time? What exactly is it? Or, is it inert, staying behind by default? From the literature the answer is yes to all these questions. The conclusion is that the facts are not known at this time.

Gray, 1966 states that there is limited demineralization and then remineralization of the outer layer from accumulated reaction products to form less soluble coatings on the surface region crystallites. Numerous reports suggest that the intact layer is the result of gross precipitation of a less soluble phase, fluorapatitic in nature or an insoluble polyphosphonate salt (White and Nancollas, 1980; Larsen and Fejerskov, 1977; Cate and Duijsters, 1983b).

Growth of the intact layer was determined by following its increase in thickness (Groeneveld, Purdell-Lewis and Arends, 1975; Langdon, Elliott and Fearnhead, 1980). Remineralization during lesion

formation was observed over a period of several days not only as increased surface layer thickness but also as increased radio-opacity of surface relative to control enamel.

Brown (1978) interpreted this phenomenon as being due in part to variable thermodynamic solubility as well as kinetic factors or to the formation of brushite.

A more dynamic concept of the intact surface layer was proposed by Moreno and Zahradnik (1974). In their model there is a critical balance between thermodynamic and kinetic factors which under specified conditions can result in phase transformations in the surface enamel. In particular, slight dissolution of the surface enamel occurs, followed by precipitation of solid phases $CaHPO_4 2H_2O$ (DCPD) and $Ca_5F(PO_4)_3$ (FA). The trace levels of fluoride needed for this to occur were presumed to be liberated from the enamel itself. Thus the surface layer was presumed to be composed of three solid phases DCPD, FA and bulk hydroxyapatite of the enamel. Implicit in this model is the reasonable assumption that a quasi-equilibrium exists between these three solid phases and the solution in the microenvironmental pores of the surface layer.

Crystallographic analysis of the surface layer of synthetic hydroxyapatite pellets shows improved crystallinity of apatitic material in this surface region after dissolution (Aoba, Okazaki, Takahashi and Moriwaki, 1978). X-ray fluoresence of bovine enamel demineralized in solutions containing 1-hydroxy-1-ethane-1,1-diphosphonic acid (HEDP) or fluoride suggest that the enamel surface is

protected from dissolution by the slow formation of an insoluble HEDP salt or fluorapatite (White and Nancollas, 1980).

The redistribution of indigenously bound fluoride in surface enamel during dissolution in the absence of exogenous fluoride indicates that the bound fluoride of the surface region does not confer any special property to the surface enamel (Clarkson, Wefel and Silverstone, 1981). In the same study using human enamel, an exogenous source of fluoride deposited more fluoride (1000 to 2000 ppm) in the surface zone of the lesion relative to baseline levels (500 to 1000 ppm).

Although solution fluoride has been implicated by many in rendering the surface enamel less soluble due to precipitation of fluorapatite or adsorption of fluoride reducing the apparent solubility of the surface enamel, nowhere in the literature has it been explicitly stated that it is the solution fluoride that is important in preserving the surface layer during subsurface dissolution of enamel by maintaining the prevailing solution ion product within the enamel above a critical value and thereby resulting in an inhibition of the dissolution rate in this surface region.

CHAPTER 3

STATEMENT OF THE PROBLEM

Subsurface dissolution uniquely characteristic of incipient caries in dental enamel is observed in vitro as well as in vivo. A review of the literature indicates great need for a basic physical chemical study of this process. Although there have been numerous attempts to explain the observed phenomenon, a comprehensive mechanistic understanding of subsurface dissolution has not evolved.

In the present study, a physical model has been proposed and experimentally studied based on an awareness of the influence of trace levels of solution fluoride on the propensity of bovine enamel to form an intact surface layer. The influence of trace levels of solution fluoride on subsurface lesion formation phenomenon were quantified and the following hypotheses were tested:

1. Trace levels of solution fluoride have a dissolution retarding effect primarily upon those crystallites in the surface region (i.e., 10 to 20 micrometers from the surface) where the microenvironmental solution fluoride levels would be appreciable.

2. The advancing front of fluoride in solution within the enamel is limited by complete saturation of available adsorption sites in the surface region; therefore, the prevailing microenvironmental solution fluoride levels in the deeper recesses of the enamel would be negligibly low and dissolution would be able to take place in these

regions.

3. Trace levels of solution fluoride would have their maximal effect at low pH and high K_{HAP}, e.g., $K_{HAP} > 1 \times 10^{-120}$ because under these conditions, $K_{FAP} = a_{Ca}\, a_{PO}\, a_F$ would also be maximal.

4. A critical value of the intercrystalline solution ion activity product exists, above which dissolution is inhibited and below which dissolution will proceed at an appreciable rate.

The experimental design employed to test these hypotheses has focused on the interdependency of bulk solution fluoride, thermodynamics and hydrodynamics. The following experiments were designed to test these hypotheses:

1. The influence of solution fluoride was examined at two solution K_{HAP}'s and four solution K_{FAP}'s. These studies were conducted to test whether or not fluoride presence itself is both necessary and sufficient for intact surface layer formation. Limited kinetic studies under different hydrodynamic conditions yielded dissolution rates and tested whether or not the intact surface layer is the result of dissolution inhibition or the result of precipitation as a new phase. Bulk solution fluoride concentration was followed to estimate fluoride uptake rates as well as allowing rigorous calculation of surface fluoride concentration.

2. Biopsies of enamel were taken as a function of distance from the surface and analyzed for fluoride content to determine whether or not significantly more fluoride is concentrated in the surface region as expected if an adsorptive/depletion mechanism is operating and from

the fluoride levels obtained whether the intact surface layer is the result of fluoride adsorption or precipitation as a fluorapatitic phase. Fluoride equilibrium adsorption isotherms were generated with synthetic hydroxyapatite powder to test whether or not significant fluoride adsorption could occur at the very low fluoride concentrations expected at the advancing front of the microenvironmental solution fluoride.

3. Microradiographic analysis of the resulting lesions produced at constant bulk solution fluoride concentrations and two different K_{HAP}'s tested whether solution fluoride exhibits its maximal influence when the solution ion activity product is high.

Equilibrium fluoride adsorption isotherms were generated at two different pH's to determine whether or not there is a competitive influence of solution hydroxyl ion for fluoride ion isomorphous substitution for the hydroxyapatite crystal surface hydroxyls and also allow estimation of the extent of adsorption at pH = 4.5.

4. Theoretical physical model development allowed analysis of the experimental data and tested whether or not it is possible to specify a single critical microenvironmental solution ion activity product that would be sufficient in and of itself for predicting intact surface layer formation and concomitant subsurface dissolution in bovine enamel.

The studies outlined above provided the necessary data for determining the mechanism by which low level solution fluoride exerts its influence on the formation of an intact surface layer during bovine

enamel dissolution in weak acid buffer. Albeit limited to the in vitro bovine enamel model system, the conclusion drawn from these studies may also apply qualitatively to formation of clinically observed incipient caries.

CHAPTER 4

THEORETICAL CONSIDERATIONS

Physical Model

The development of a satisfactory physical model depicting the subsurface dissolution phenomenon was not feasible until realization was made of the importance of the presence of low level solution fluoride in this process. The model (Figure 4.1) considers the bovine enamel to be a homogeneous single phase of hydroxyapatite crystallites in the form of a porous matrix, extending from $x = 0$ to $x = \infty$. It is assumed that at a sufficient depth in the enamel the saturation solubility of enamel, C_s is reached. At the interface between the enamel surface and the bulk solution is an aqueous boundary layer of thickness "h".

The bulk solution dissolution media contains calcium and phosphate resulting in some degree of saturation with respect to the enamel solubility. Within a matter of seconds (< 10 seconds) after exposure to the dissolution media a steady-state concentration profile is established for calcium, phosphate and pH.

Fluoride ions present in the bulk solution diffuse into the porous enamel matrix and are adsorbed onto the hydroxyapatite crystallite surfaces. This adsorptive process, probably Langmuirian, then depletes the intercrystalline solution fluoride until such time as all sites are saturated and the fluoride front advances. Remaining behind

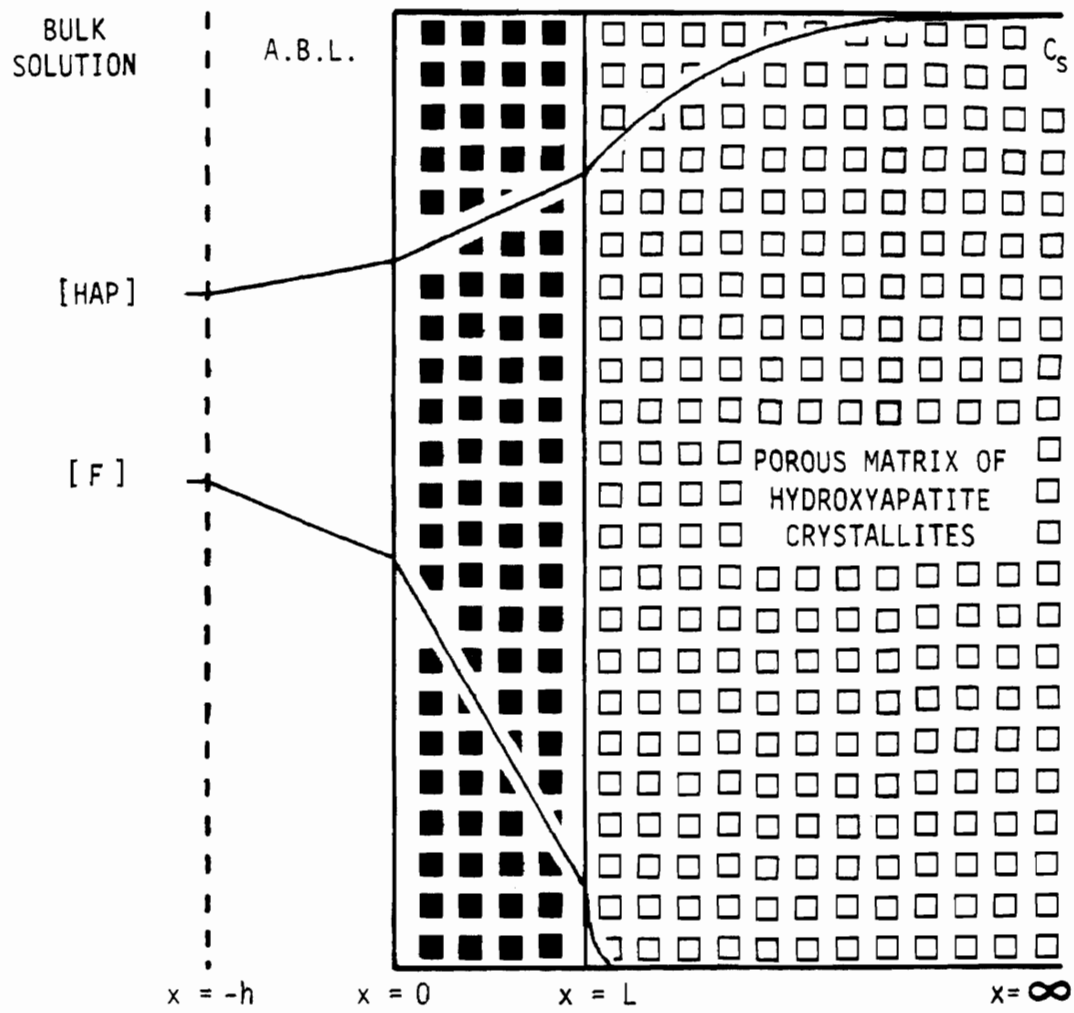

Fig. 4.1. Schematic representation of the physical model, not presented to scale.

is a region in which the crystals now have a "monolayer" coverage of fluorapatite extending from x = 0 to x = L and at the same time are no longer able to deplete solution fluoride as it diffuses in from the bulk, thereby allowing the intercrystalline solution fluoride concentrations behind the moving front to rise to substantial levels. This elevated solution fluoride then provides the basis for the proposed model.

It has been established (Mir, 1967) that hydroxyapatite dissolution kinetics in the presence of low levels of solution fluoride may be reconciled if it is assumed that there is a fluorapatitic monolayer coverage of the hydroxyapatite crystallites which becomes the thermodynamically governing phase. Therefore, in order to understand the dissolution behavior within the enamel matrix it is necessary to consider the following two cases. First, the dissolution kinetics of hydroxyapatite crystals exposed to a microenvironmental solution void of fluoride will be described according to a K_{HAP} function. Secondly, in the surface region and to a depth L, i.e., where solution fluoride is present in sufficiently high concentration, the dissolution kinetics will be described by a K_{FAP} function.

Since it is not possible to determine the microenvironmental solution chemistry experimentally without the use of microelectrodes, etc., and to provide a more rigorous theoretical understanding of the processes involved, the appropriate diffusion equations have been employed to allow calculation of the microenvironmental solution ion activity product as a function of distance within the enamel.

Calculation of this ion activity product provides a rational basis for predicting where and when subsurface dissolution will occur in bovine enamel.

Mathematical Model

Rigorous Development

Hydroxyapatite dissolution and diffusion can be described by Fick's Second Law of diffusion modified to include a term for the dissolution component.

$$\frac{\partial C}{\partial t} = \frac{\partial}{\partial x}\left[D_{(m)}\ \frac{\partial C}{\partial x}\right] + R_{DISS} \qquad (4.1)$$

C, is the concentration of hydroxyapatite (or fluorapatite, if in the presence of solution fluoride) in solution; t, is the time; x is distance; and $D_{(m)}$ is the diffusivity of all species within the porous enamel matrix and defined as

$$D_{(m)} = D_o \cdot \varepsilon \qquad (4.2)$$

where D_o is the aqueous diffusivity and ε is the porosity at any x. Since conditions of high partial saturation result in the enamel porosity varying with position, the porosity is then a function of hydroxyapatite mass, (m) at x.

$$\varepsilon = \varepsilon_o + \left(1 - \varepsilon_o\right)\cdot\left(1 - \frac{m}{m_o}\right) \qquad (4.3)$$

where ε_o and m_o are the time zero porosity and mass respectively.

The dissolution component, R_{DISS}, is defined per unit volume of

enamel as

$$R_{DISS} = k_d \cdot \frac{A_{(m)}}{V} \cdot \left(C_s - C\right) \tag{4.4}$$

k_d, is the rate constant, units (cm/second); V, is the volume, units (cm^3); C_s is the apparent solubility; C is the concentration of hydroxyapatite at (x,t). A_m is the hydroxyapatite surface area, unit ($meter^2$/gram) defined according to

$$A_{(m)} = A_o \cdot \left(\frac{m}{m_o}\right)^{\rho} \tag{4.5}$$

where A_0 is the time zero area, and ρ is a factor relating surface area change with volume assuming an elongated hexagonal geometry for the hydroxyapatite crystals. This C term of equation (4.4) is defined according to whether dissolution is goverened by a K_{HAP} or K_{FAP} function; the R_{DISS} used in the calculation is determined by the smaller of the two ΔC's.

The change in mass with time is described by

$$\frac{\partial m}{\partial t} = - R_{DISS} \tag{4.6}$$

Simultaneously, the inward diffusion of solution fluoride must be considered. Again, this is described by Fick's Second Law modified to account for loss of fluoride from solution due to the adsorption component.

$$\frac{\partial F}{\partial t} = \frac{\partial}{\partial x}\left[D_{(m)} \frac{\partial F}{\partial x}\right] - R_{ADS} \tag{4.7}$$

F, is the molar concentration of fluoride in solution, R_{ADS} is the adsorption term.

R_{ADS} is defined, assuming Langmuirian adsorption behavior, as

$$R_{ADS} = F \cdot A_{(m)} \cdot \frac{k_1 N_{sites}}{1 + k_3/k_4 [OH]} - \frac{F \cdot F_{ADS} \cdot k_1}{1 + k_3/k_4 [OH]} - k_2 \cdot F_{ADS} \quad (4.8)$$

where k_1, k_2 and k_3, k_4 are the forward and reverse rate constants for the adsorption and desorption of fluoride and hydroxyl for hydroxyapatite respectively; N_{sites}, is the maximum number of sites available for adsorption, units (moles/meter^2); F_{ADS} is the amount of adsorbed fluoride per unit volume of enamel defined according to

$$\frac{\partial F_{ADS}}{\partial t} = R_{ADS} \quad (4.9)$$

The time dependent partial differential equations were solved by the method of lines. The mesh points in the space variable were spaced nonuniformly, with points being more densely distributed at the enamel surface. Partial derivatives with respect to the space variable were approximated using the centered differences described by Sincovec and Madsen (1975). That is, at the $i^{\underline{th}}$ mesh point

$$\frac{\partial C}{\partial t} = \frac{2}{h_i + h_{i+1}} \left[D_{i+\frac{1}{2}} \left(\frac{C_{i+1} - C_i}{h_{i+1}} \right) - D_{i-\frac{1}{2}} \left(\frac{C_i - C_{i-1}}{h_i} \right) \right] \quad (4.10)$$

where $D_{i\pm\frac{1}{2}} = D \cdot (m_{i\pm\frac{1}{2}})$

$m_{i\pm\frac{1}{2}} = \dfrac{m_{i\pm1} + m_i}{2}$ (m is the mineral density)

$h_i = x_i - x_{i-1}$

The other terms in the space discretized set of ordinary differential

equations follow in a straightforward manner from the partial differential equations. The resulting system of ordinary differental equations was solved using a PASCAL translation (by Dr. J.L. Fox) of the EPISODE integrator described by Hindmarsh and Byrne (1975). This technique works well until such time as the surface crystals become saturated with respect to fluoride adsorption. At this point the problem becomes one of a moving boundary problem and the integration becomes intolerably slow.

This type of moving boundary problem may best be handled by a moving finite element technique described by Gelinas, et al., (Gelinas, Doss and Miller, 1983). Nevertheless, to overcome the present problem of computational speed by existing techniques it was necessary to assume instantaneous and irreversible binding which affords of an analytic solution for the time dependent fluoride diffusion problem. On the basis of electrophoretic mobility data of human enamel crystals, Seleeb and de Bruyn (1972), concluded F^- rapidly substitutes for OH^- and found this ion-exchange process to be irreversible. The experimental conditions were different than used here however. Also assumed is a quasi-steady-state profile for calcium, phosphate and pH profiles for the uniform density situation, taking into account the added diffusional distance of an intact surface layer thickness increasing with time. It was possible then to calculate linear fluoride concentration profiles approximating the curvilinear rigorous solutions.

Approximating Function

The fluoride concentration change with position in the enamel is related to the bulk driving force by the following expressions

$$S \cdot \frac{dx}{dt} = - D_m \cdot \frac{\partial C}{\partial x} = P_{aq} \cdot \left(C_b - C_{o,t} \right) \qquad (4.11)$$

(x) is the distance (cm), D_m is the diffusivity within the hydroxyapatite crystal matrix (cm^2/sec.), P_{aq} is the aqueous permeability (cm/sec.), C_b is the bulk concentration, $C_{o,t}$ is the concentration at the surface, S is the number of adsorption sites per unit volume, (moles/cm^3).

When the moving front is at $x = X_{(t)}$, where, $X_{(t)}$ is the position of the moving front along (x) where $C_{(x)} = 0$, the quasi-steady state is given by

$$C_{(x,t)} = C_{(o,t)} \cdot \frac{X_{(t)} - x}{X_{(t)}} \qquad (4.12)$$

Partial differentiation with respect to "x" and substituting into equation (4.11) gives the expression for $C_{(o,t)}$

$$C_{(o,t)} = \frac{C_b \cdot P_{aq}/D_m \cdot X_{(t)}}{1 + P_{aq}/D_m \cdot X_{(t)}} \qquad (4.13)$$

Substitution of equation (4.12) into equation (4.11) and integration yields the expression for the position of $X_{(t)}$ with time.

$$\frac{P_{aq}}{2\ D_m} \left[X_{(t)} \right]^2 + X_{(t)} = \frac{P_{aq}\ C_b}{S} \cdot t \qquad (4.14)$$

It is noteworthy that this development leads to an expression that

would predict, under conditions of high aqueous permeability, a square root time dependence for the position of the advancing fluoride front. This is in agreement with quantitative expressions for lesion progression developed by Featherstone and Mellberg (1981) who suggested lesion depth "r" was proportional to the square root of demineralization time, (t)

$$r^2 = D \cdot t \tag{4.15}$$

and also in agreement with Holly and Gray (1968) who proposed a relationship

$$r = (a^2 + bt)^{1/2} - a \tag{4.16}$$

where a and b are constants.

Christoffersen and Arends (1982) however, found that lesion depth is about proportional to the third root of demineralization time.

CHAPTER 5

EXPERIMENTAL CONSIDERATIONS

Materials

Bovine Enamel

Enamel slabs of the desired dimensions were cut from incisors of six week old calves. This enamel is from calves fed a uniform, rigidly controlled diet. It is therefore consistent in chemical composition from tooth to tooth, especially for a biological sample. The carbonate content was determined to be 3 to 4% by weight[1]. Baseline fluoride content was found to be 50 to 300 ppm by abrasion. A flat fluoride profile was found in ground samples. Prior to use, selected relatively flat specimens were visually inspected for any obvious defects in structure, color etc.. The pellicle and surface debris was removed by first grinding with 400 then 600 grit silicon carbide paper. Extreme care was taken in all steps of sample preparation to ensure no contamination with water or other material adulterated with fluoride.

Hydroxyapatite

Hydroxyapatite, (UM-A) was used in generating the fluoride adsorption isotherms. This sample was synthesized in these laboratories

---

[1]Galbraith Laboratories, Inc. Knoxville, TN.

as a low temperature preparation yielding a low carbonate containing apatite with good stoichiometry.

Bio-Gel® HTP[2] hydroxyapatite, a high surface area commercial preparation was used as obtained in all extraction procedures for removing trace levels of fluoride in dissolution buffers.

Dissolution Media

Weak acid buffers were prepared from calculated quantities of acetic acid and sodium acetate. All dissolution studies were with 0.1 M acetate buffer at pH = 4.5 and ionic strength = 0.5 M, adjusted with added NaCl. When desired, fluoride was added from a 100 ppm stock solution. Desired stoichiometric quantities of $CaCl_2$ and NaH_2PO_4 were added. The ion activity product of these solutions was calculated by the method described by Fox (1977). The pH was measured to an accuracy of ± 0.01 pH unit using an Altex® 71 pH meter. Chemicals of reagent grade were used in all studies with no further purification. Extreme care was taken to avoid fluoride contamination from water or glassware. All water used in buffer preparation was 18 megohm cm water from a Milli-Q® deionizing system[3].

Adsorption Media

Barbital buffer (0.01 M) was prepared from calculated amounts of sodium barbital and concentrated HCl. The pH was adjusted to 7 or 8 as desired with concentrated HCl or NaOH. NaCl was added to give an

---

[2]Bio-Rad Laboratories, Richmond CA.
[3]Millipore Corp., Bedford, MA.

ionic strength of 0.5 M.

Methods

Dissolution

Ground bovine enamel slabs were mounted in the rotating disk apparatus with beeswax. An enamel surface area of 0.09 cm^2 was exposed to the demineralizing solution. Fifty ml of the acetate buffer was pipetted into a water jacketed beaker at 30^o C. All glassware and sample holders were meticulously cleaned to ensure no fluoride contamination.

Adsorption

Fifty mg of hydroxyapatite was placed in 50 ml of 0.01 M barbital buffer containing fluoride. The slurry was sonicated[4] for 3 minutes before being magnetically stirred at 600 rpm. Evaporation was minimized by closing the system with Parafilm[5]. At adsorption equilibrium, samples withdrawn by a pipette were passed through a 0.22 micrometer Millipore filter[6]. The filtrate was assayed for fluoride concentration. Control experiments indicated no loss of fluoride due to adsorption by the beaker or stirrer.

Bulk Fluoride Depletion

Uptake of fluoride by the enamel was followed by monitoring the solution fluoride concentration as a function of time. One-half ml

---

[4]Bransonic 321 Utrasonic Cleaner.
[5]American Can Co., Greenwich, CT.
[6]Millipore Corp., Bedford, MA.

samples of solution were withdrawn by pipette. Appropriate control experiments were performed using an identical experimental protocol, except for the absence of the enamel slab. Results indicated no loss of fluoride to the polypropylene beaker or rotating disk assembly.

Enamel Abrasion

The sample to be abraded was left in the rotating disk holder with one flat surface exposed. Adhesive tape was placed over the demineralized sample exposing a 0.14 cm^2 window. The sample and holder was placed on a triple beam balance with a 200 gram counterload. The foam cylinder used for abrading was coated with 400 grit silicon carbide powder suspended in glycerin. The silicon carbide and glycerin contained negligible fluoride compared to the samples. The foam rubber cylinder was found not to adsorb significant fluoride. The silicon carbide coated foam cylinder was placed in a holder and mounted to a constant speed motor shaft. Abrasion was accomplished by placing the foam cylinder, rotating at 1500 rpm, against the sample for the desired period of time. After each abrasion the sample was wiped with a cotton pledget which together with the foam cylinder was placed in a polyethylene vial. The cotton pledget is calcium and phosphate free. Each enamel surface was serially abraded until the desired depth was obtained.

To each of the vials, one ml of 0.5 M $HCLO_4$ was added. The abraded material was left to sit for one hour with intermittent shaking. Aliquots were then taken for fluoride and phosphate analysis.

Buffer Extraction

A stoichiometric buffer having an ion activity product of 10^{-117} at pH = 4.5 was prepared as previously described. To this was added 2 g./100 ml of Bio-Gel® hydroxyapatite. The flask was placed in a wrist action shaker (160 agitations/minute) at room temperature. The slurry was redispersed every 30 minutes by inversion. After two hours the slurry was passed through a 0.2 micrometer Metricel® membrane filter[7]. The filtrate was analyzed for calcium and phosphate and the solution ion activity product was reestablished. The desired pK_{HAP} solution was obtained by dilution with "sink" buffer of the appropriate ionic strength. The pH was adjusted to 4.5 immediately prior to the experiment. Extreme vigilance was used to avoid fluoride contamination from any source once the extraction had taken place.

Analytic Methods

Phosphate. Phosphate concentrations were determined according to the method of Gee et al., (1954). The phosphoammonium molybdate complex formed was reduced by stannous chloride. The absorbance of the resulting color was read under visible light at wavelength = 720 nm on a Perkin-Elmer Lambda-7® spectophotometer.

Calcium. Calcium concentrations were determined by atomic absorption. Strontium chloride was added to samples and standards to prevent phosphate interference. The absorbance was read at wavelength = 422.7 nm on a Perkin-Elmer 305A spectophotometer.

---

[7]Gelman Sciences, Ann Arbor, MI.

Fluoride. A fluoride ion selective electrode was used to determine solution fluoride concentration. Samples were buffered with low level TISAB buffer. The calibration standards used were of the same pH and ionic strength as the samples.

Quantitative Microradiography. The enamel sample is mounted in a circular saw fitted with a high concentration diamond wafering blade. Sections approximately 200 micrometers thick were cut through the exposed window perpendicular to the enamel surface. The section to be examined was then ground planoparallel using 600 grit silicon carbide paper to a thickness of exactly 100 micrometers as determined by a micrometer. Any small aberrations resulting from the grinding were removed during a final polishing using diamond paste on a rayon cloth.

The thin section was placed in direct contact with the emulsion on a 2" x 2" high resolution glass photographic plate[8]. A wedge of bovine enamel was placed adjacent to the surface to be analyzed. This untreated enamel wedge is used as an internal standard to factor out any artifacts resulting from deviations from linearity in the time/temperature dependent film development process.

The sample was placed in the center of an X-ray beam for 25 minutes[9]. The instrument settings used were 40 kVp and 30 mA. The negative was developed in D-19 developer[10] according to manufacturers instructions.

---

[8]Type 1-A, Eastman Kodak Co, Rochester, NY.
[9]Faxitron, Hewlett-Packard, McMinnville, OR.
[10]Eastman Kodak, Rochester, NY.

Density profiles were quantified from the microradiographic images by using a Leitz microscope photometer equipped with a scanning stage. The sample image was analyzed by moving it in 0.25 micrometer steps and at each step measuring the transmitted light. The stage movement was controlled by a microcomputer which also recorded the transmitted light by means of an analog to digital converter connected to the photomultiplier head of the microscope. The range of stage travel was 100 micrometers so that each image consisted of some 400 separate readings, each of which was an average of one to eight individual readings as selected. The image of the enamel wedge internal standard was recorded in a similar fashion.

The raw data from the image scan was processed in the following way. A calibration curve (ADC reading versus enamel thickness) was constructed for the enamel wedge by fitting a fourth degree polynomial to the logarithm of ADC reading versus enamel thickness raw data. This procedure also included an algorithm that precisely locates the edge of the wedge based on an examination of the data. This calibration curve for the wedge was then used to convert the ADC versus position data for the sample to equivalent enamel thickness (or percent of original mineral remaining) versus thickness. The data at each stage of this process (sample raw data, wedge raw data and calibration curve, sample density versus position) were then plotted as a hard copy when desired. In addition, the mineral density profile was saved on a floppy disk for possible subsequent use in correcting the fluoride profile (as determined by the abrasion technique) for the

positional variation in mineral density.

Numerical point by point integration allowed calculation from the area above the curve, a good estimate of the amount of hydroxyapatite dissolved, expressed as "equivalent micrometers of enamel dissolved".

Results and Discussion

Reproducibility Considerations

Before introducing the experimental results, reproducibility issues will be addressed so as to determine the extent to which conclusions are warranted based on these limitations.

The quantitative microradiographic procedure has been thoroughly scrutinized as to its limitations. In this regard, precision assessments were made by making multiple scans over the same region of a sample image. It was determined from visual examination of the mineral density profiles that the system precision limitations are much less than 1%.

An assessment of the uniformity in mineral density changes within a lesion has also been made. In this test, 4 equally spaced sections were cut from a lesion produced in a single tooth. Each thin section was scanned at approximately the midpoint of the lesion. The results indicate approximately ±3% variation in the calculated amount dissolved values and about ±5% variation in the mineral density of the intact surface layer.

The uniformity of the lesion within a single section was also examined. Sections were chosen from microradiographic images that

visually appeared uniform in mineral density across the lesion and also from images that appeared nonuniform. It was concluded that visual examination of the microradiographic image may lead to erroneous conclusions about the mineral density of the sample as it was determined that for both the visually uniform and nonuniform samples the mineral density variations were within ±5% based on amount dissolved calculations and within ±2 to 3% for the mineral density at the enamel surface.

Most importantly, since many conclusions are based on data obtained from different teeth, an evaluation was made of the tooth to tooth reproducibility limitations. Two teeth from two different experiments were used in this study. It was determined that the variability in the mineral density of the intact surface layer may be as much as 10% but the calculated amount dissolved, based on integration of the mineral density profiles, was better, usually within 5%.

The conclusions deduced from the experimental results in this study have been interpreted in terms of the limitations imposed by the reproducibility assessment presented.

Mineral Density Profiles

Mineral density changes occurring within the enamel matrix during dissolution have been assessed by the quantitative microradiographic technique developed in these laboratories. The essence of this technique is that mineral density is, quantitatively, determined as a function of position in the tooth.

Uncommon, but not totally unique to hydroxyapatite systems is the

zonal dissolution observed in enamel when the dissolution is accomplished into fluoride free acetate buffer having an ion activity product of 10^{-120}, approximately 50% saturated on a molar basis with respect to hydroxyapatite assuming a thermodynamic solubility of 10^{-116} (Figure 5.1). Figure 5.1 is typical of the mineral density profile obtained in a fluoride free environment. The mineral density is near zero at the surface and increases monotonically until at sufficient depth the mineral density reaches that of sound enamel (assumed to be unaffected to a significant degree by the dissolution procedure). Figures 5.2 and 5.3 represent the extremes obtained in the mineral density profiles of enamel samples under these conditions. The enamel used in these experiments contained < 300 ppm baseline fluoride concentration and therefore dissolution of the enamel would liberate fluoride into the bulk solution with the potential for resulting in bulk fluoride levels significant enough to affect the enamels dissolution behavior. Nevertheless, in the absence of solution fluoride the mineral density profile obtained after 24 hours dissolution in a buffer having a pK_{HAP}=120 is typified by Figure 5.1 ; where the profile obtained exhibits zonal dissolution with near zero mineral density at the surface.

The pronounced effect that low levels of solution fluoride had on the propensity of a sample to form an intact surface layer was recognized and became useful as a tool in investigating the hypothesis that it was the intercrystalline solution ion activity product that was important in determining subsequent intact surface layer formation.

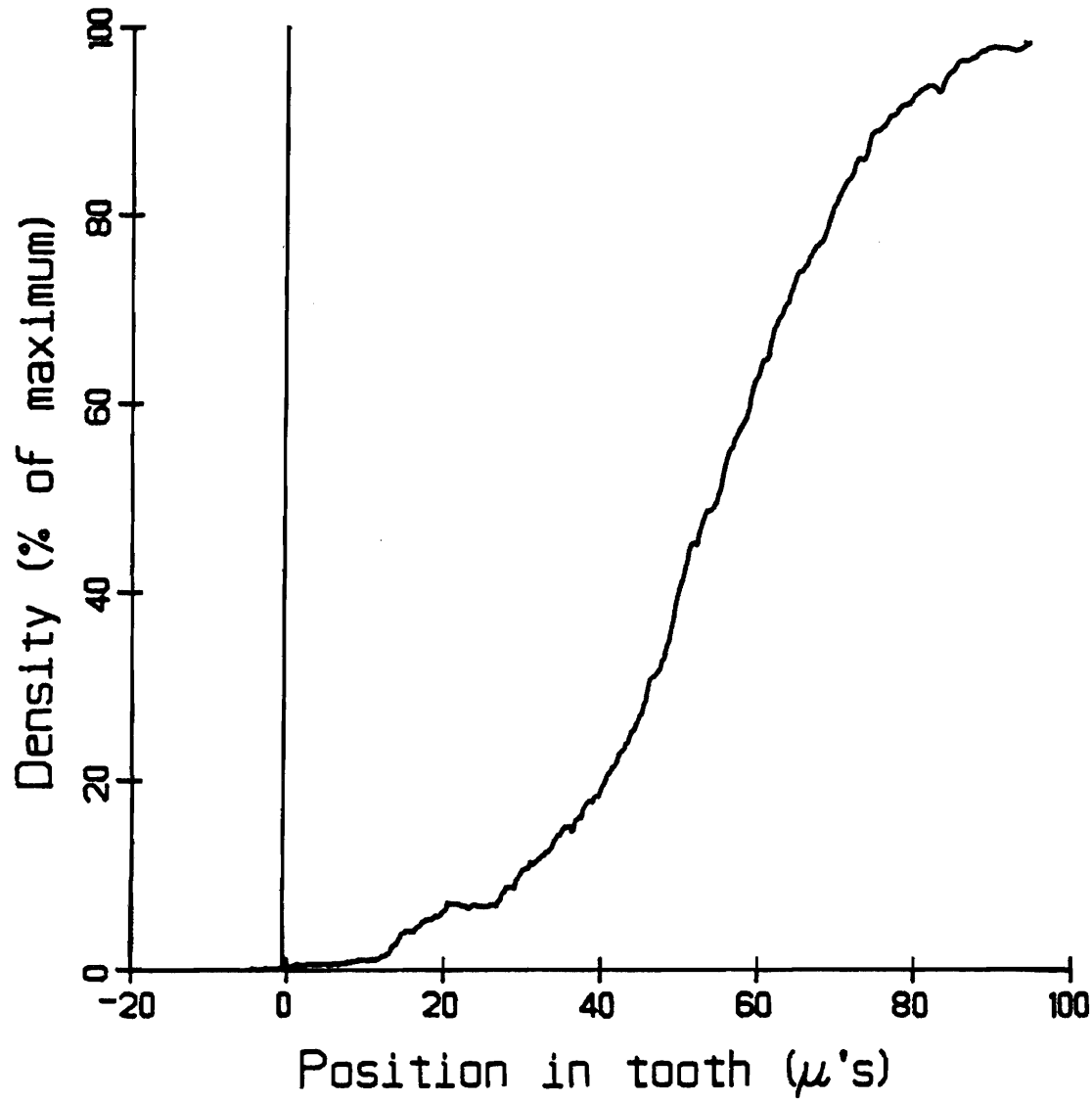

Fig. 5.1. Mineral density profile after 24 hours of dissolution in pK_{HAP} = 120.0 buffer at 10 rpm, 59.1 equivalent micrometers of enamel dissolved.

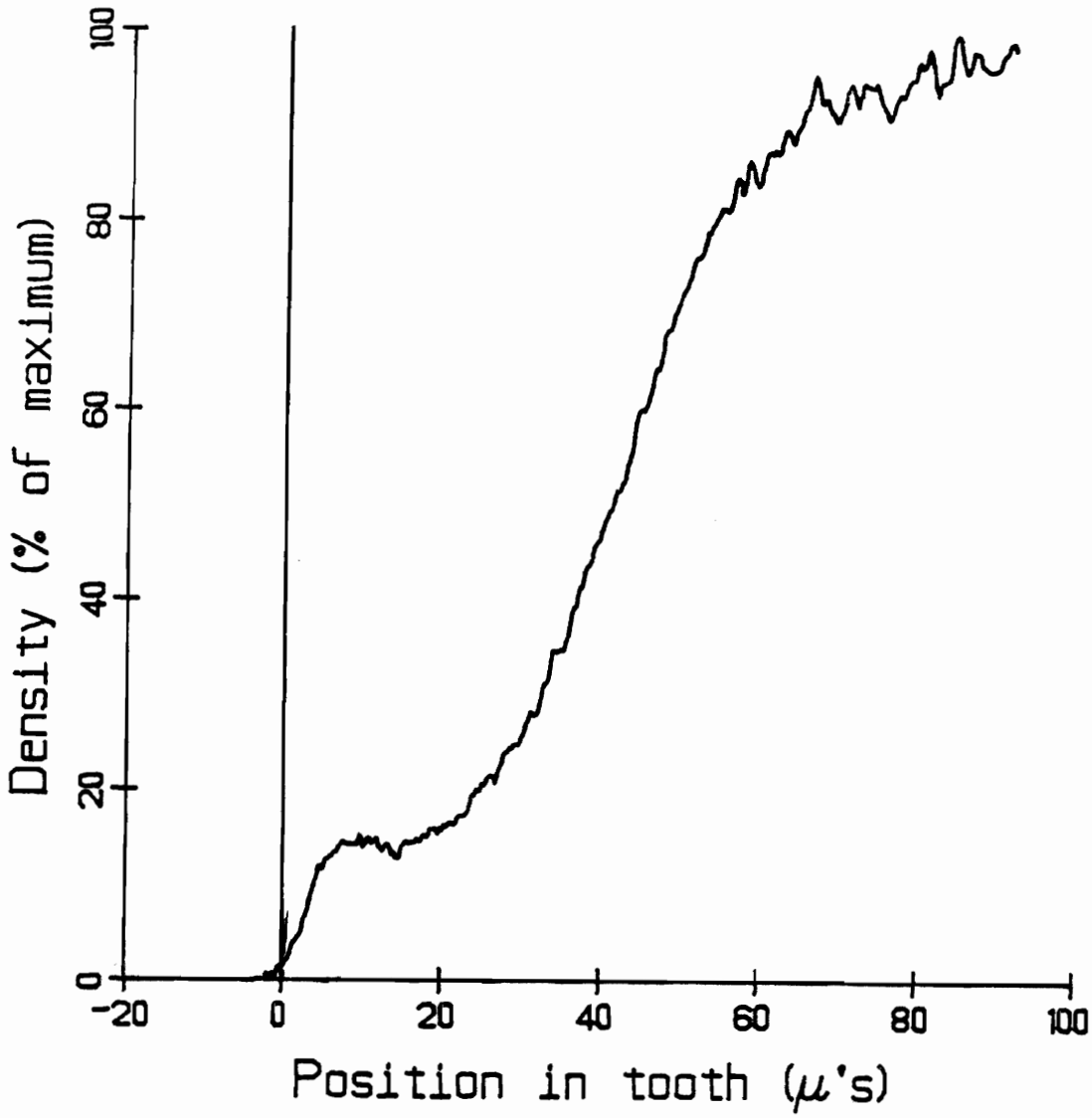

Fig. 5.2. Mineral density profile after 24 hours of dissolution in pK_{HAP} = 120.0 buffer at 10 rpm, h = 227 micrometers, 46.1 equivalent micrometers of enamel dissolved.

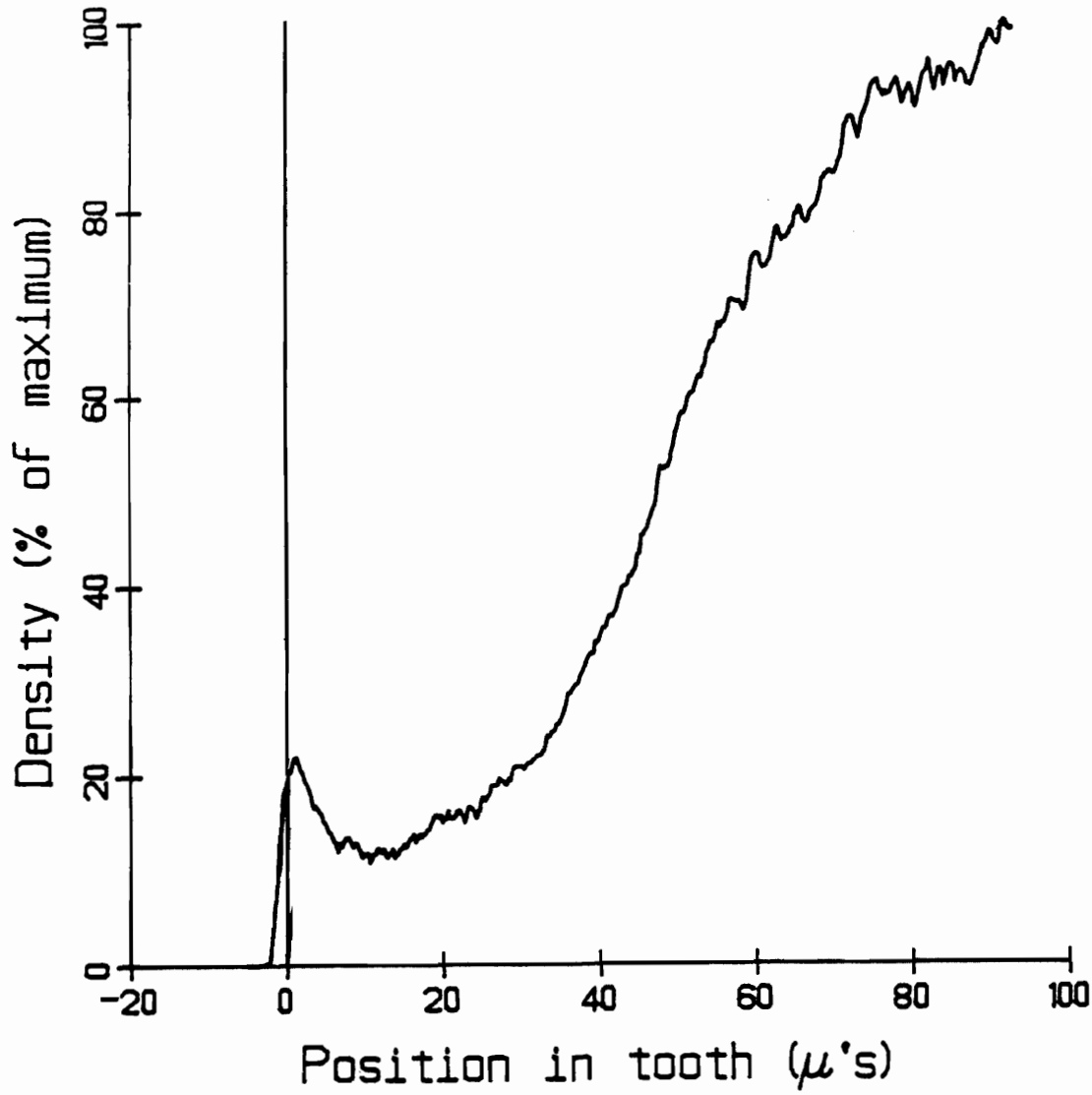

Fig. 5.3. Mineral density profile after 24 hours of dissolution in pK_{HAP} = 120.0 buffer at 10 rpm, h = 227 micrometers, 51.0 equivalent micrometers of enamel dissolved.

Bulk conditions were chosen to cover a range of fluoride, calcium and phosphate concentrations. These conditions covered a range of solution ion activity products; $K_{HAP} = 10^{-124}$ and 10^{-120} and four different bulk K_{FAP}'s, $K_{FAP} = 10^{-112}$ to 10^{-118}, Table 5.1. A common concentration of fluoride was included to test the hypothesis that it was the ion activity product that is important and not a given level of bulk solution fluoride concentration.

Figures 5.4 - 5.7 depict the mineral density profiles obtained under four different bulk solution K_{FAP}'s. The multiple profiles for identical experimental conditions using different bovine enamel specimens indicate good reproduciblity. As estimated by area above the curve measurements the mineral density changes are within $\pm$ 10% for repeat experiments. This is considered quite satisfactory for a biological sample. Qualitatively, the reproducibility in the shape of the profile is even better.

Dissolution under bulk conditions having a relatively high pK_{FAP} ($pK_{FAP} \gtrsim 116$) has consistently resulted in either surface recession or at the most, a very low degree of mineralization at the enamel surface, with the absence of an intact surface layer (Figures 5.4 and 5.5). Dissolution experiments performed under bulk conditions having a $pK_{FAP} < 114$ result in the formation of an intact surface layer with concomitant subsurface dissolution (Figures 5.6 and 5.7). The theoretically calculated surface $pK_{HAP's}$ and $pK_{FAP's}$ after the surface mineral content has been eroded by 3 hours of dissolution are $pK_{HAP/FAP} = 118.69/126.01$ for the bulk solution $pK_{FAP} = 117.93$ and h =

TABLE 5.1

SOLUTION COMPOSITION OF DISSOLUTION MEDIA*

Calcium (mM)	Phosphate (mM)	Fluoride (mM)	pK_{HAP}	pK_{FAP}
8.26	4.95	-	124.0	-
14.8	8.88	-	120.0	-
8.26	4.95	5.26×10^{-3}	-	115.93
8.26	4.95	2.63×10^{-3}	-	114.53
14.8	8.88	5.26×10^{-6}	-	117.93
14.8	8.88	5.26×10^{-3}	-	111.93

* All solutions contain 0.1 M acetate buffer, ionic strength = 0.5 M and pH = 4.5.

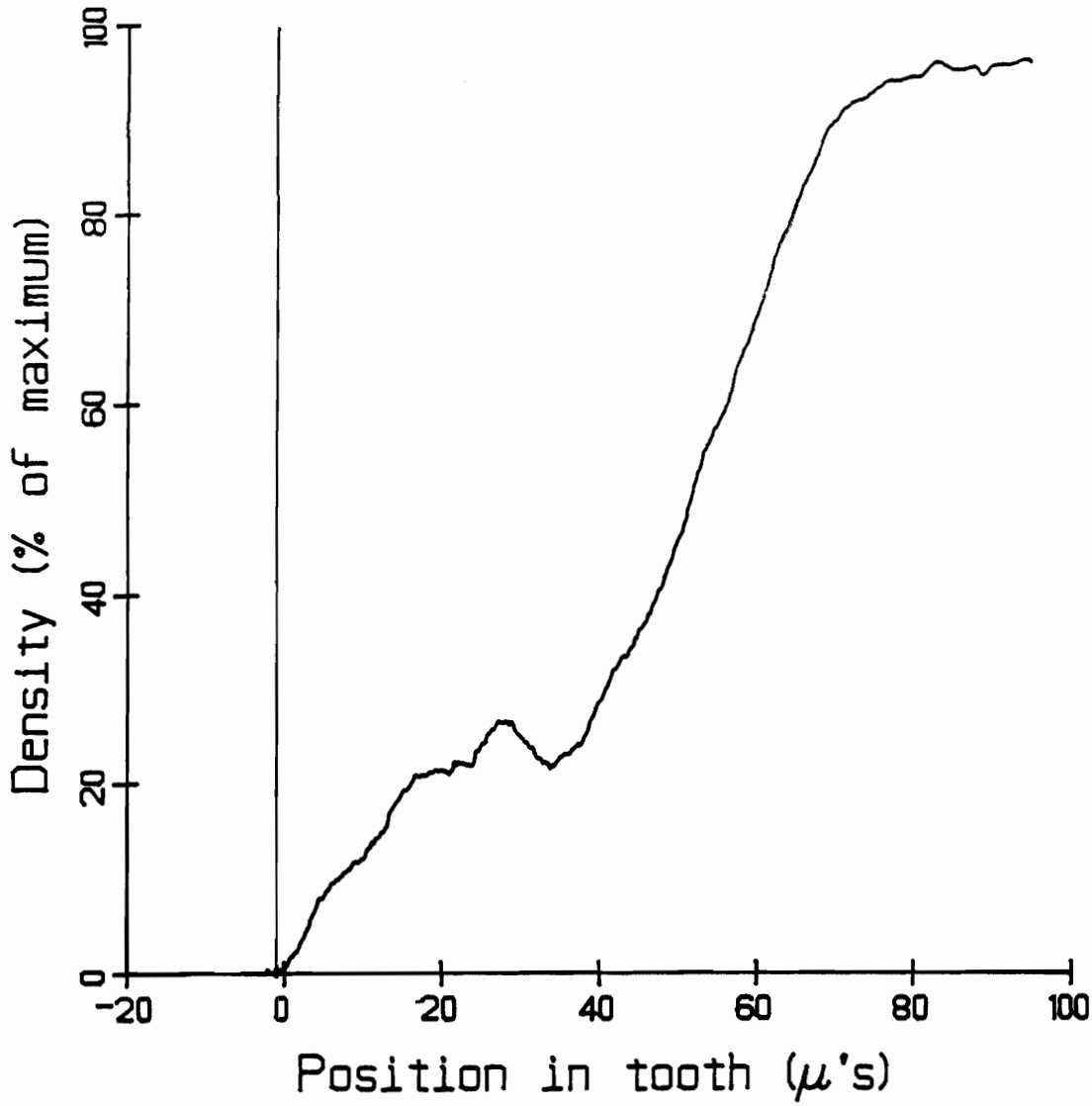

Fig. 5.4. Mineral density profile after 24 hours of dissolution in pK_{FAP} = 117.93 buffer at 10 rpm, h=227 micrometers, 51.6 equivalent micrometers of enamel dissolved.

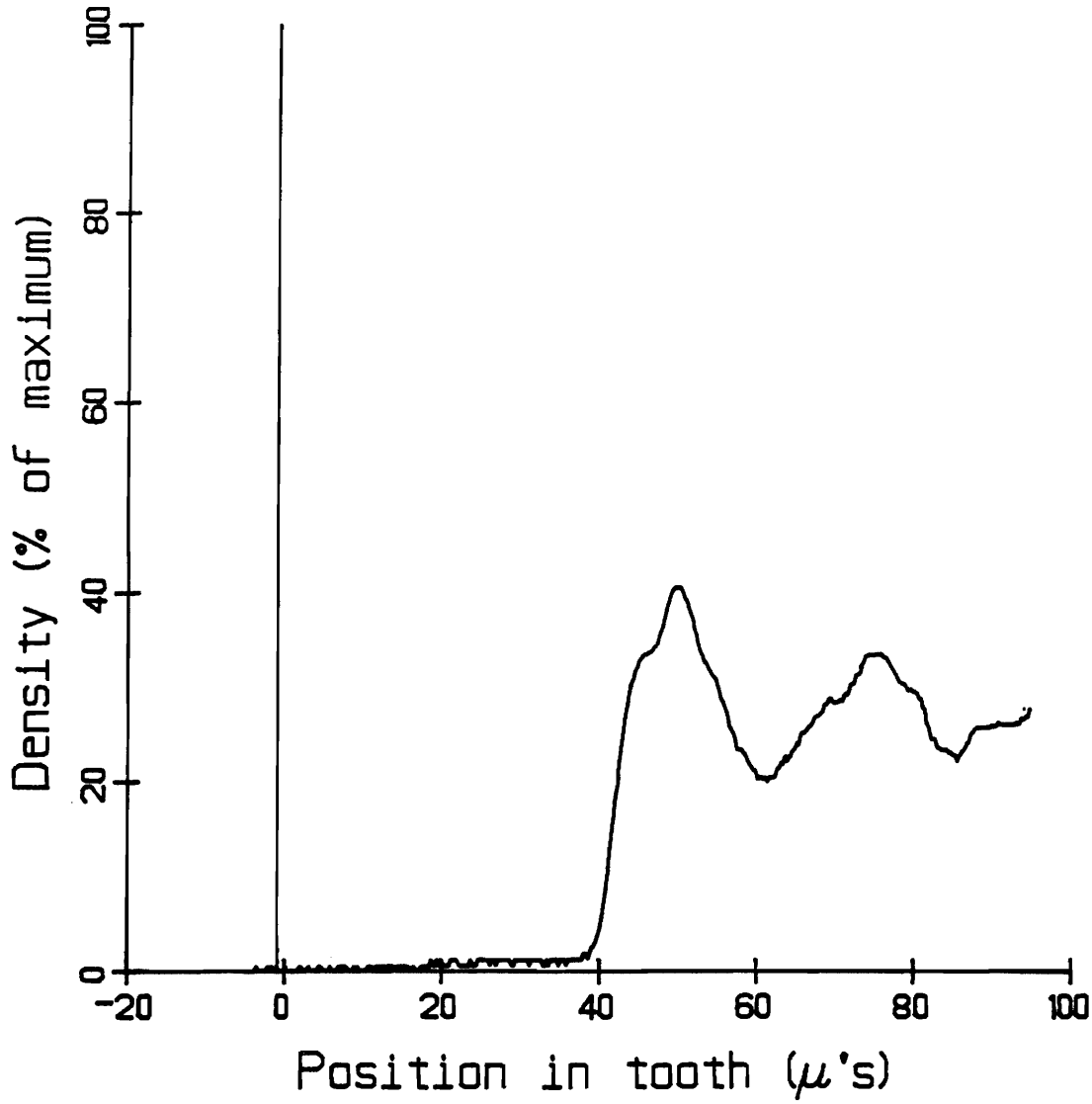

Fig. 5.5. Mineral density profile after 24 hours of dissolution in pK_{FAP} = 115.93 buffer at 10 rpm, h=227 micrometers, 84.4 equivalent micrometers of enamel dissolved.

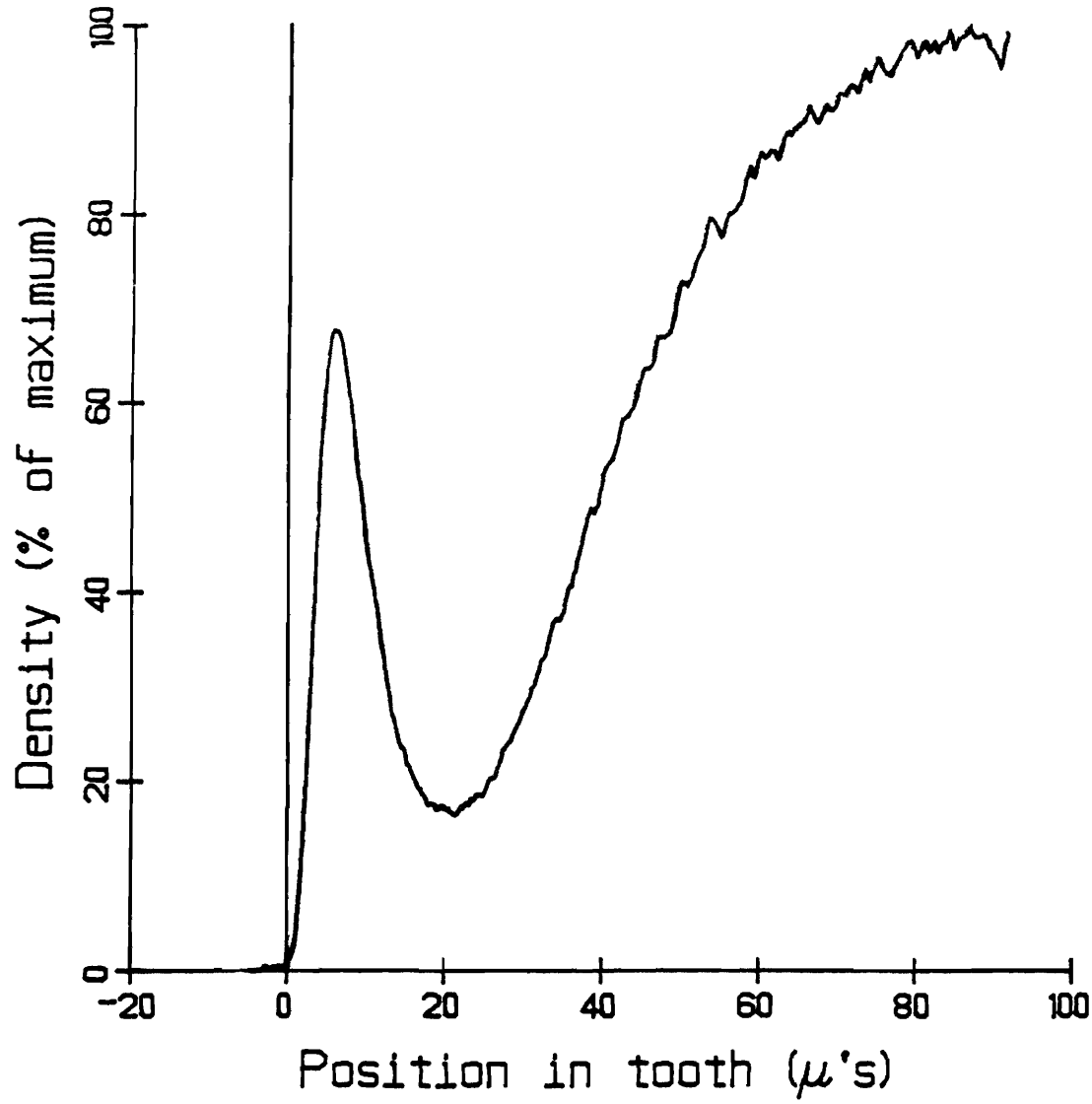

Fig. 5.6. Mineral density profile after 24 hours of dissolution in pK_{FAP} = 111.93 buffer at 10 rpm, h = 227 micrometers, 41.2 equivalent micrometers of enamel dissolved.

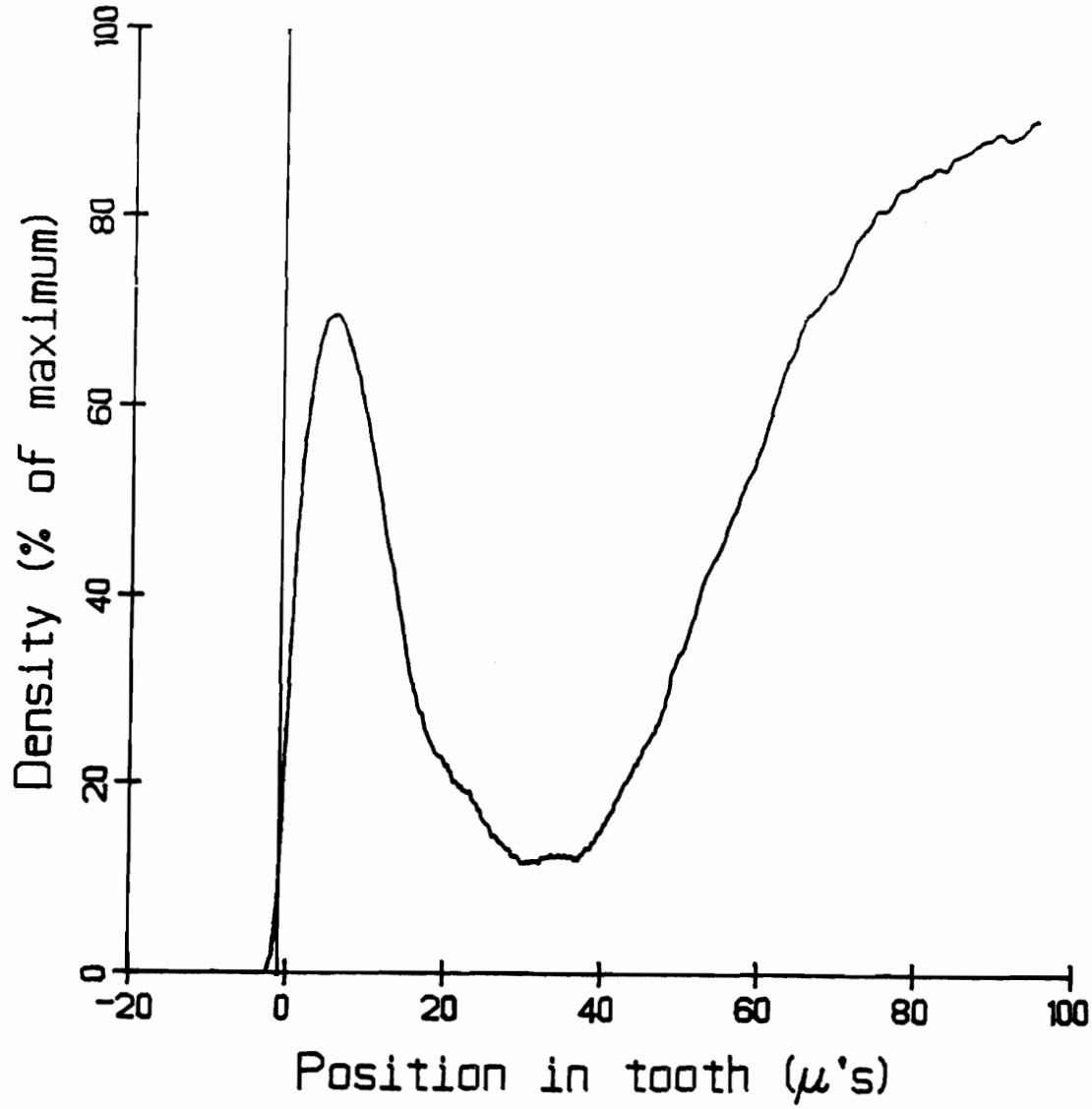

Fig. 5.7. Mineral density profile after 24 hours of dissolution in pK_{FAP} = 114.53 buffer at 10 rpm, h=227 micrometers, 52.5 equivalent micrometers of enamel dissolved.

227 micrometer case and $pK_{HAP/FAP}$ = 120.18/115.53 for the bulk solution pK_{FAP} = 115.93 case. These experimental and theoretical observations suggest that a microenvironmental solution pK_{FAP} = 114 or 115 represents a minimum criteria for determining when dissolution results in surface recession or formation of an intact surface layer. These experiments clearly implicate solution fluoride as having a major role in intact surface layer formation characteristic of the "white-spot" lesion observed clinically.

Bulk Solution Fluoride Uptake by Enamel

The bulk changes in fluoride concentration were followed as a function of time at two different initial fluoride concentrations and under two different hydrodynamic conditions (Figures 5.8 and 5.9). The uptake rates for the 0.09 cm^2 enamel slabs were calculated by a nonlinear least squares minimization procedure[11] method. This involves fitting the experimental data to the function

$$A_i = A_\infty \cdot (1 - e^{-k t_i}) \qquad (5.1)$$

and extracting the instantaneous initial rate constant, k.

Results of this analysis for the data presented in Figures 5.8 and 5.9 are summarized in Table 5.2. The uptake of fluoride by the enamel is not linear in time, a consequence of the fact that as the surface region sites become saturated they no longer participate in

---

[11]Dr. J. L. Fox, Department of Pharmaceutics
The University of Utah, Salt Lake City, UT.

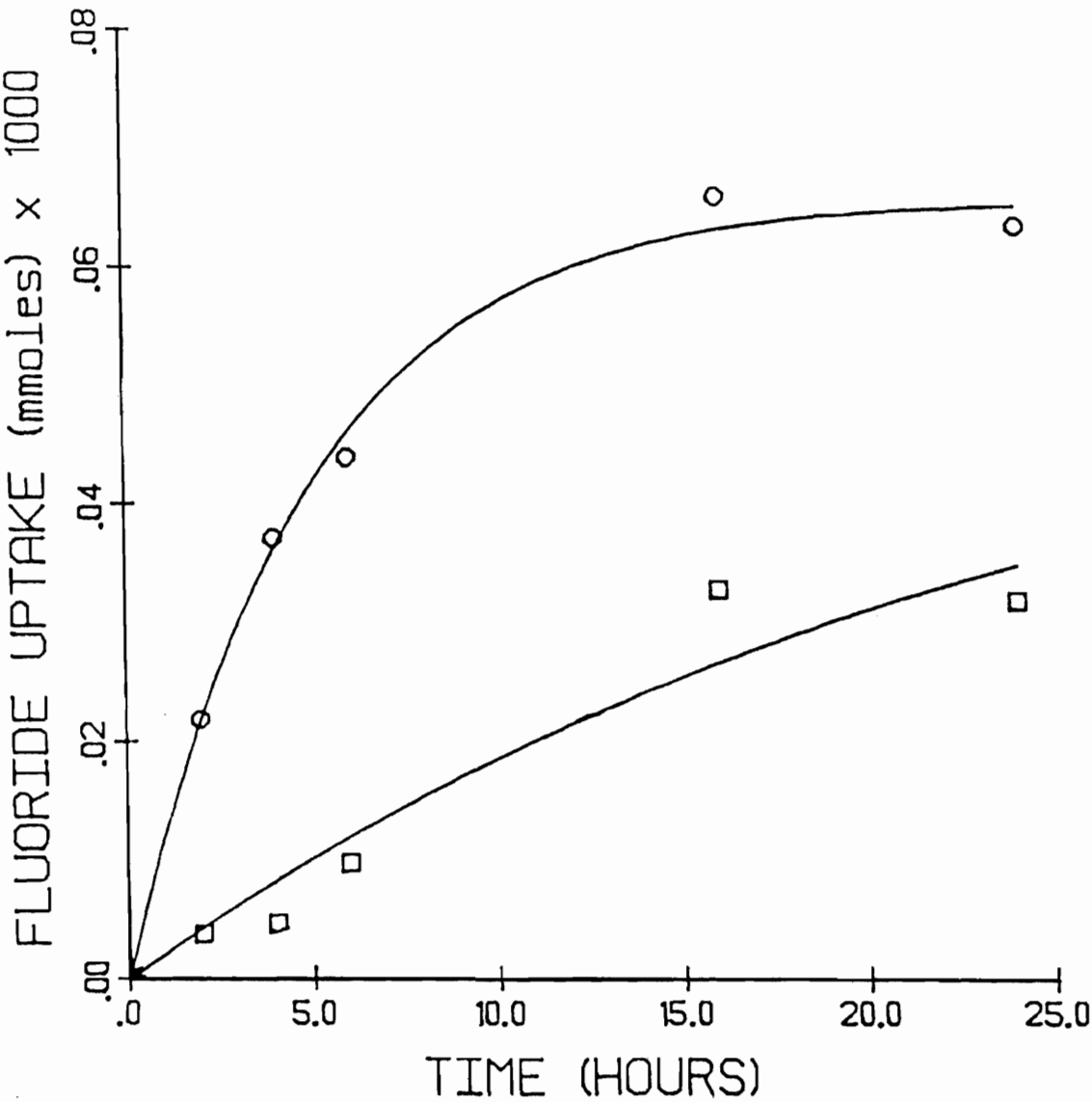

Fig. 5.8. Uptake of fluoride by the enamel under conditions known to produce an intact surface layer, bulk solution pK_{FAP}= 114.53, □ 10 rpm and ○ 500 rpm.

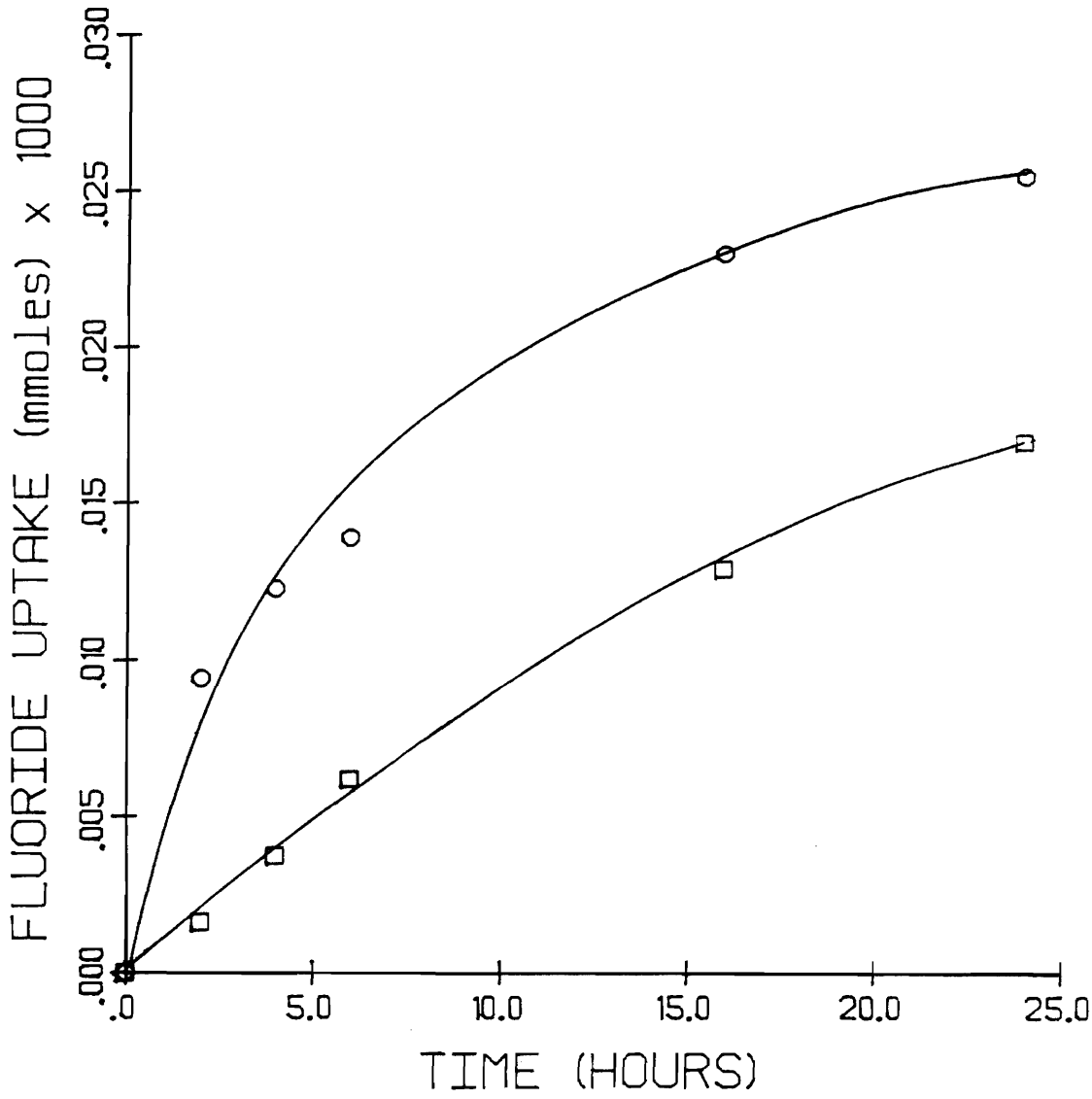

Fig. 5.9. Uptake of fluoride by the enamel under conditions known to produce an intact surface layer, bulk solution pK_{FAP}= 111.93, □ 10 rpm and ○ 500 rpm.

TABLE 5.2

FLUORIDE UPTAKE RATES AND SURFACE FLUORIDE CONCENTRATION*

Bulk Fluoride Concentration (M)	Uptake Flux ($mmoles/cm^2$ sec.)	Aqueous Boundary Thickness (micrometers)	Surface Fluoride Concentration (M)
2.63×10^{-5}	4.04×10^{-8}	32.1	1.33×10^{-5}
2.63×10^{-5}	6.91×10^{-9}	227.0	1.06×10^{-5}
5.26×10^{-6}	1.21×10^{-8}	32.1	1.37×10^{-6}
5.26×10^{-6}	3.33×10^{-9}	227.0	0

*Fluoride diffusivity used in calculations was 1.0×10^{-5} $cm^2/sec.$ (Liang, 1971).

the adsorptive process and only serve then to effectively increase the boundary layer effect on the uptake rate, hence a decreased slope at longer times.

From the measured flux of fluoride into the enamel it is possible to calculate the concentration of fluoride at the enamel surface rigorously using expression (5.2).

$$J = -\frac{D}{h} \cdot \Delta F \qquad (5.2)$$

The concentration of fluoride drops significantly across the boundary layer (Table 5.2). This is indicative of a high affinity of hydroxyapatite for adsorption of fluoride, the enamel slab initially acting as a sink for fluoride ions as they approach the enamel surface.

The results of these fluoride uptake studies are consistent with the concept of solution fluoride being important in modulating the dissolution rate behavior of the enamel in the surface region.

Abrasion Biopsy of Enamel

Serial abrasion and chemical analysis allow compositional determination of the enamel as a function of depth.

The raw data obtained from the abrasion procedure consists of quantities of fluoride and phosphate present in etchings from successive layers of enamel. The appropriate cumulative sums of this data are calculated to construct a table of cumulative amount of fluoride versus cumulative amount of phosphate. A smooth interpolating curve, Stineman interpolation (Stineman, 1980) is passed through these points to yield a continuous representation of cumulative fluoride versus

cumulative phosphate. The first derivative of this smooth curve then is proportional to the fluoride content profile taken as a function of cumulative phosphate rather than as a function of position.

If mineral density were assumed to be uniform, then a simple proportionality conversion of the independent variable from cumulative phosphate to position would yield the fluoride profile. Since the mineral density is not necessarily uniform, its positional variation must be taken into account to correctly effect the change in variable from cumulative phosphate to position. This transformation is a straightforward one. The mineral density versus position information saved on a floppy disk during the quantitative microradiography procedure is transformed via the appropriate summations to a table of cumulative phosphate versus position. This table then can be used in conjunction with the fluoride level versus cumulative phosphate calculated as described in the paragraph above to yield the desired fluoride profile as a function of position. The procedure has been described in more detail elsewhere (Fox, Muhammad, Bergstrom and Higuchi, 1984).

Baseline levels of fluoride in the enamel used in these studies was determined to be < 300 ppm. In addition, after the grinding procedure, the fluoride was found to have a rather flat distribution with distance from the abraded enamel surface. If bound fluoride is important in enamel reactivity towards acid dissolution, then its effect should be constant with position in enamel. Subsequent studies have implicated solution fluoride as being more important than bound

fluoride in its effect on the enamel dissolution rate.

Figures 5.10 - 5.14 represent the levels and distribution of fluoride in an enamel slab subjected to dissolution conditions known to produce an intact surface layer for various times of dissolution and under different hydrodynamic conditions. Clearly the data show that the levels of fluoride decrease rapidly with distance from the enamel surface, particularly in the early time case. Analysis of the mineral in the surface region above the subsurface lesion shows a low level of bound fluoride (2000-3000 ppm) suggesting that fluoride uptake in these experiments is likely an adsorptive phenomenon rather than growth of an apatitic phase (pure fluorapatite contains ~37,000 ppm fluoride). This finding is consistent with carbonate-apatite crystal suspension studies in which solid phase analysis showed no crystal growth in solutions with a pK_{FAP} of 114 to 116.

Time dependence studies of bound fluoride indicate an initial steep gradient which becomes more broadly distributed at longer times. Implicit in these findings is that the levels of solution fluoride at the advancing front of the solution fluoride diffusing in from the bulk must be extremely low. Assuming fluoride to have a high adsorption affinity for apatite, then complete saturation of available adsorption sites would occur before the fluoride front advances further. Taking these considerations into account, as the levels of bound fluoride approach baseline levels at sufficient enamel depth, then levels of solution fluoride must correspondingly be approaching zero. Since experimental determination of the intercrystalline solu-

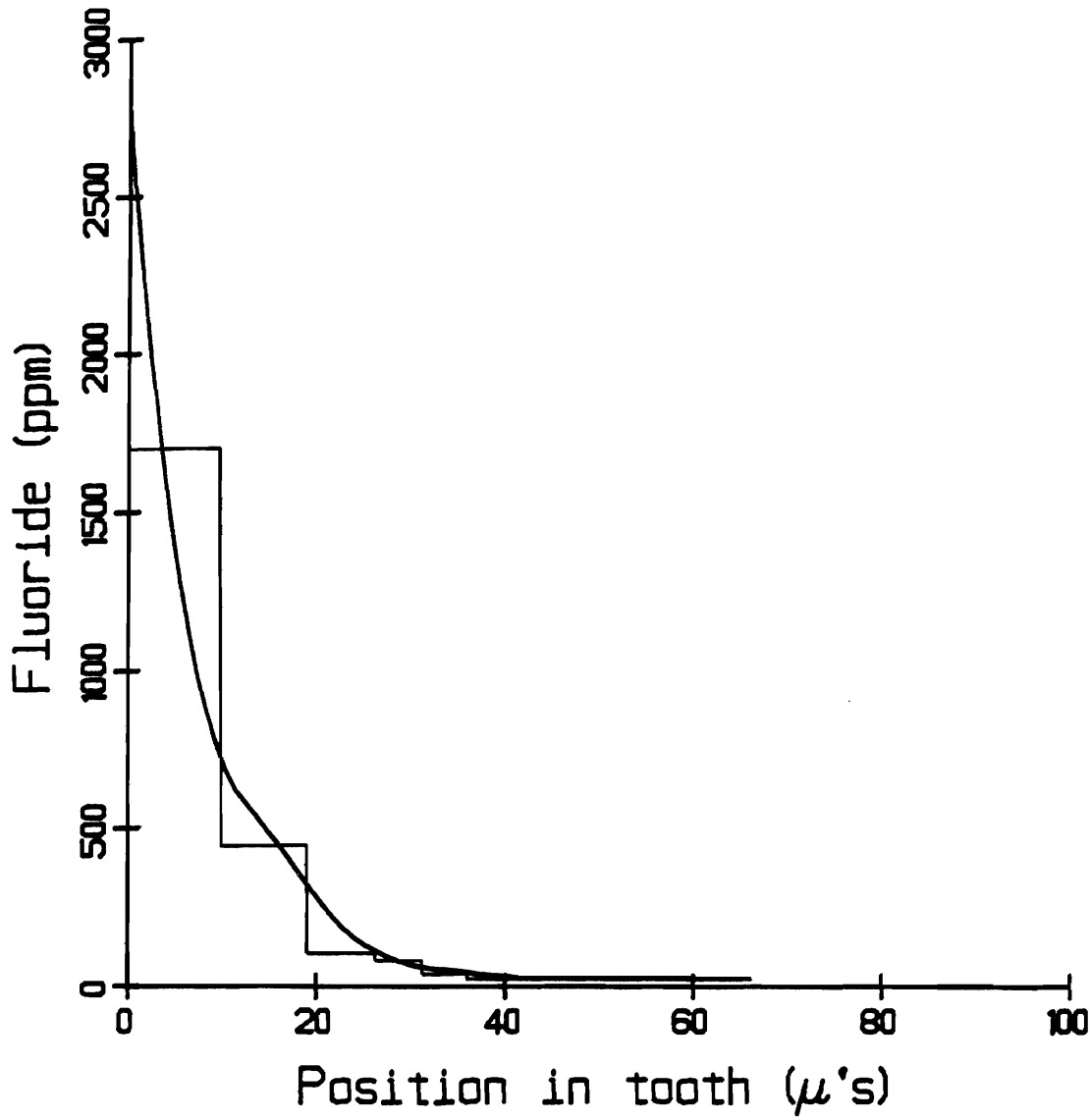

Fig. 5.10. Adsorbed fluoride distribution of dissolution for 3 hours case in pK_{FAP}= 114.53 buffer at 10 rpm, h = 227 micrometers. The smooth curve represents the fluoride profile corrected for mineral density and the histogram represents the raw data.

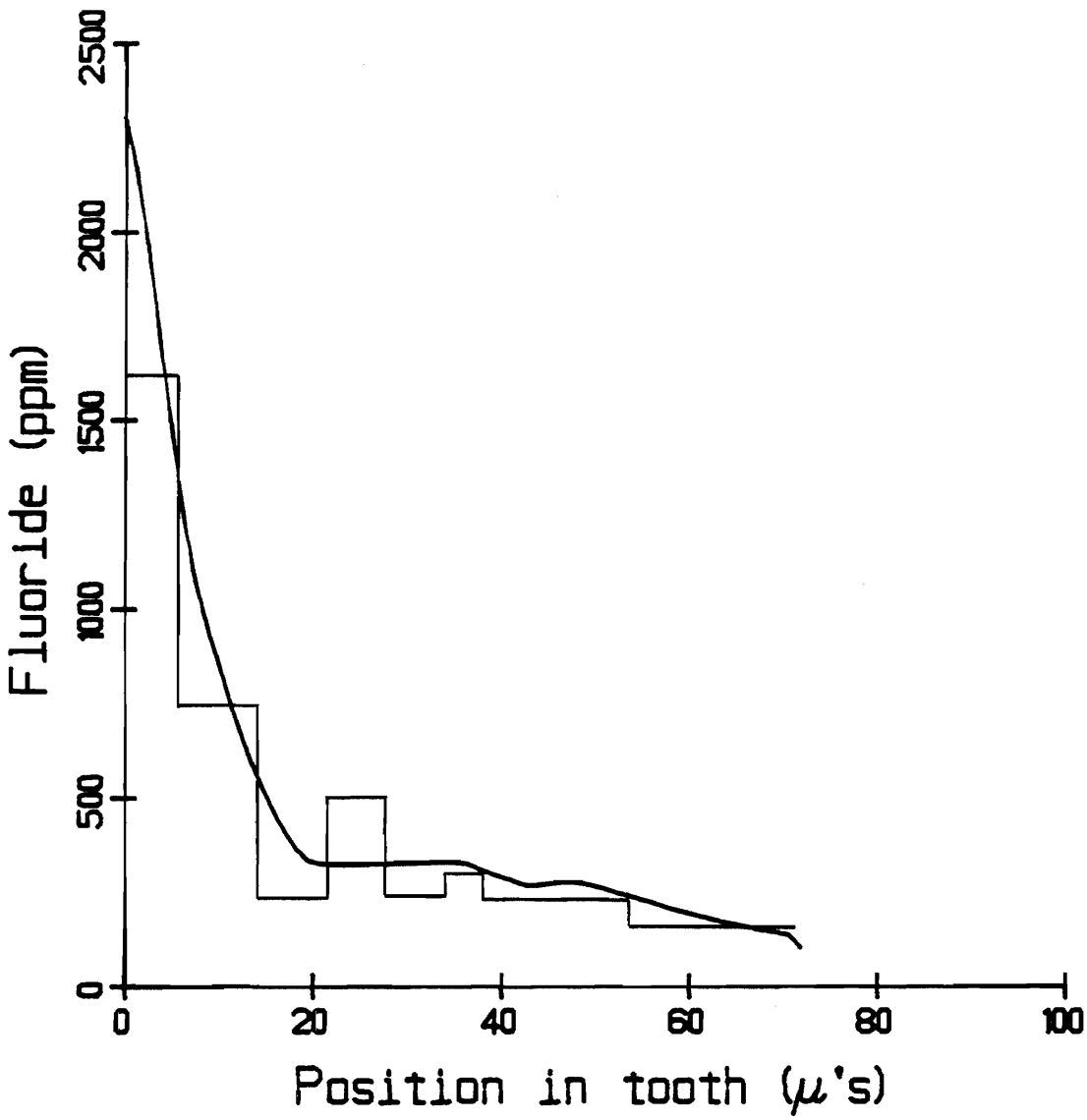

Fig. 5.11. Adsorbed fluoride distribution of dissolution for 6 hours case in pK_{FAP} = 114.53 buffer at 10 rpm, h = 227 micrometers. The smooth curve represents the fluoride profile corrected for mineral density and the histogram represents the raw data.

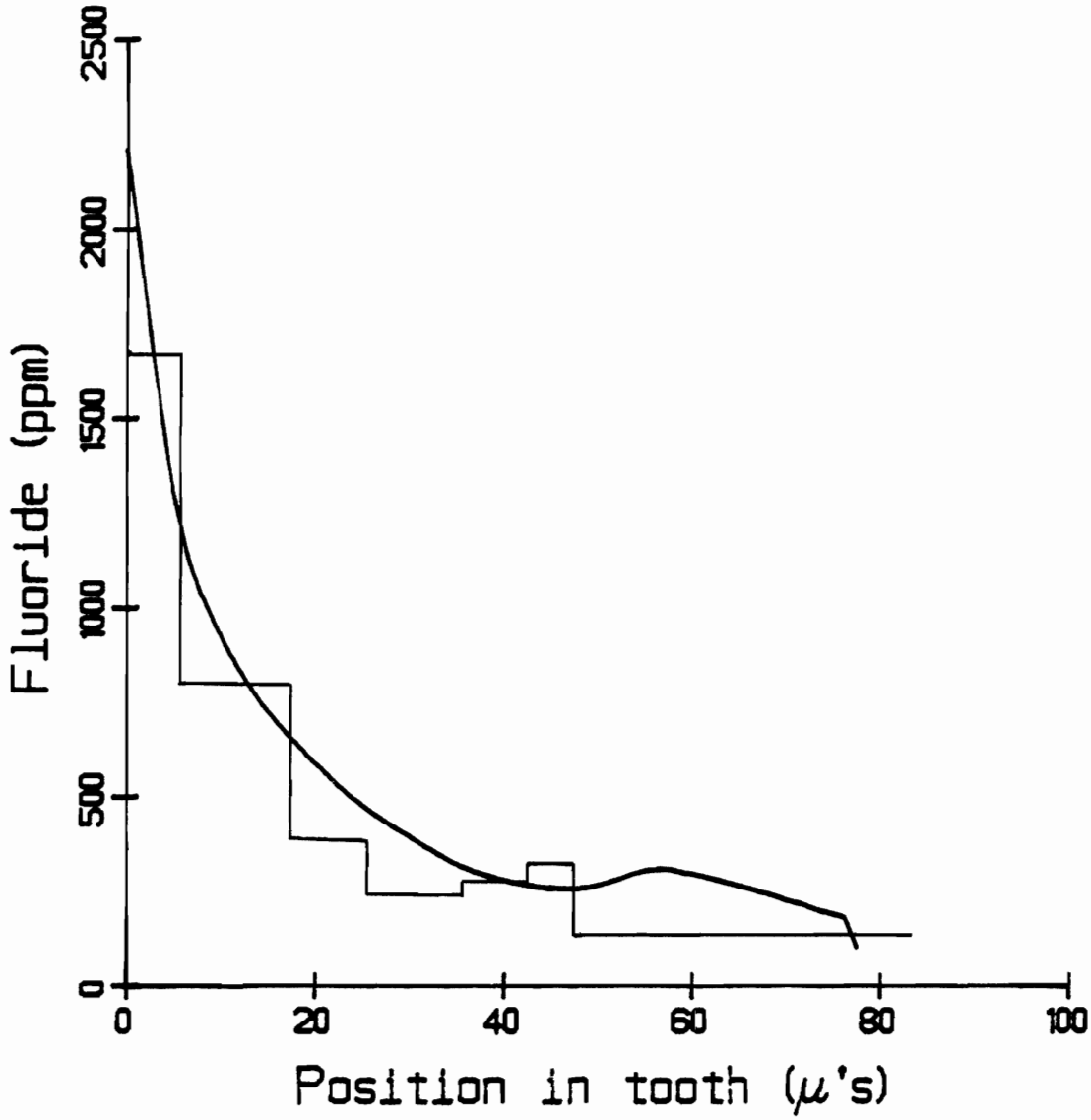

Fig. 5.12. Adsorbed fluoride distribution of dissolution for 12 hours case in pK_{FAP}= 114.53 buffer at 10 rpm, h = 227 micrometers. The smooth curve represents the fluoride profile corrected for mineral density and the histogram represents the raw data.

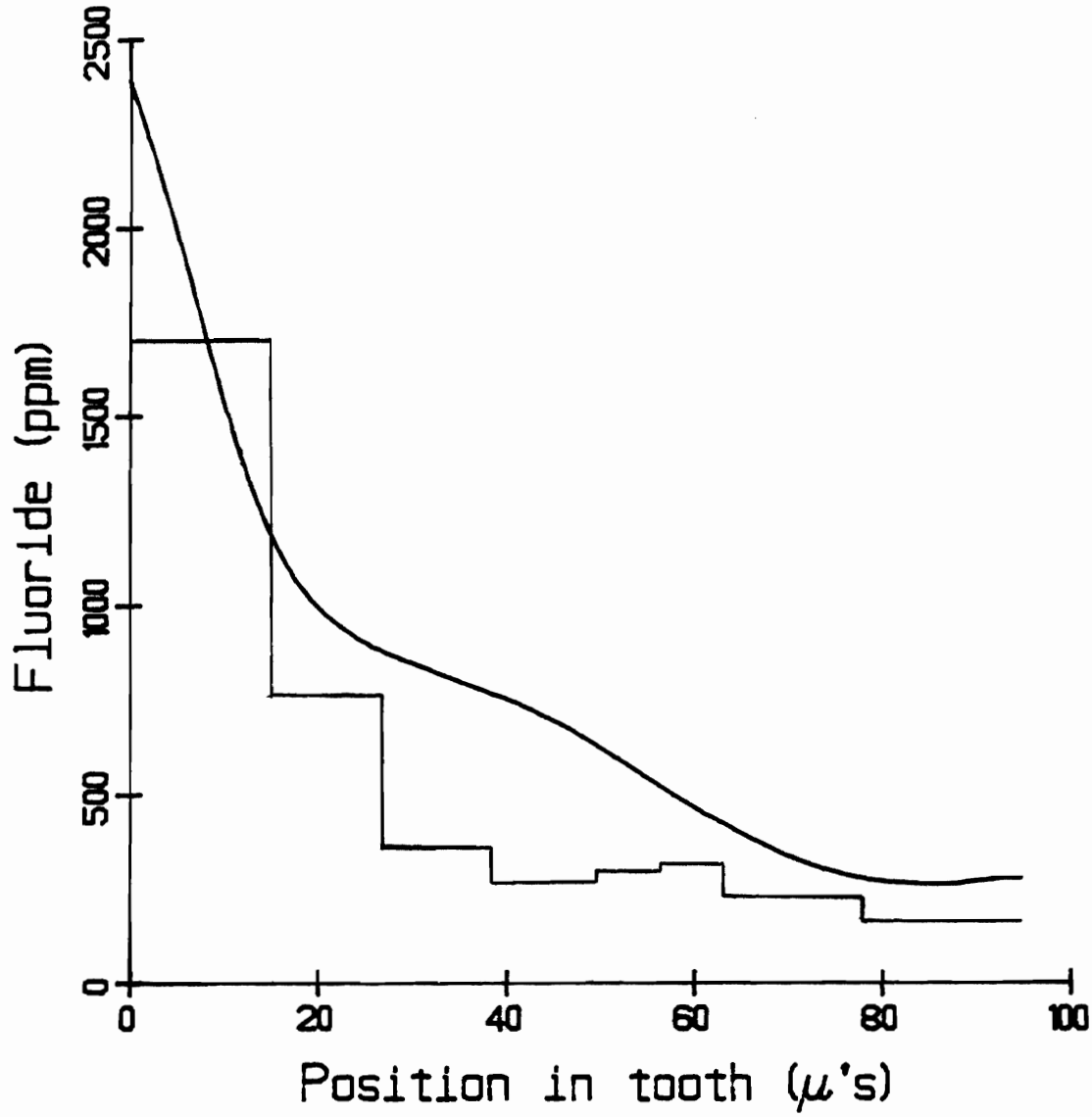

Fig. 5.13. Adsorbed fluoride distribution of dissolution for 24 hours case in pK_{FAP}= 114.53 buffer at 10 rpm, h = 227 micrometers. The smooth curve represents the fluoride profile corrected for mineral density and the histogram represents the raw data.

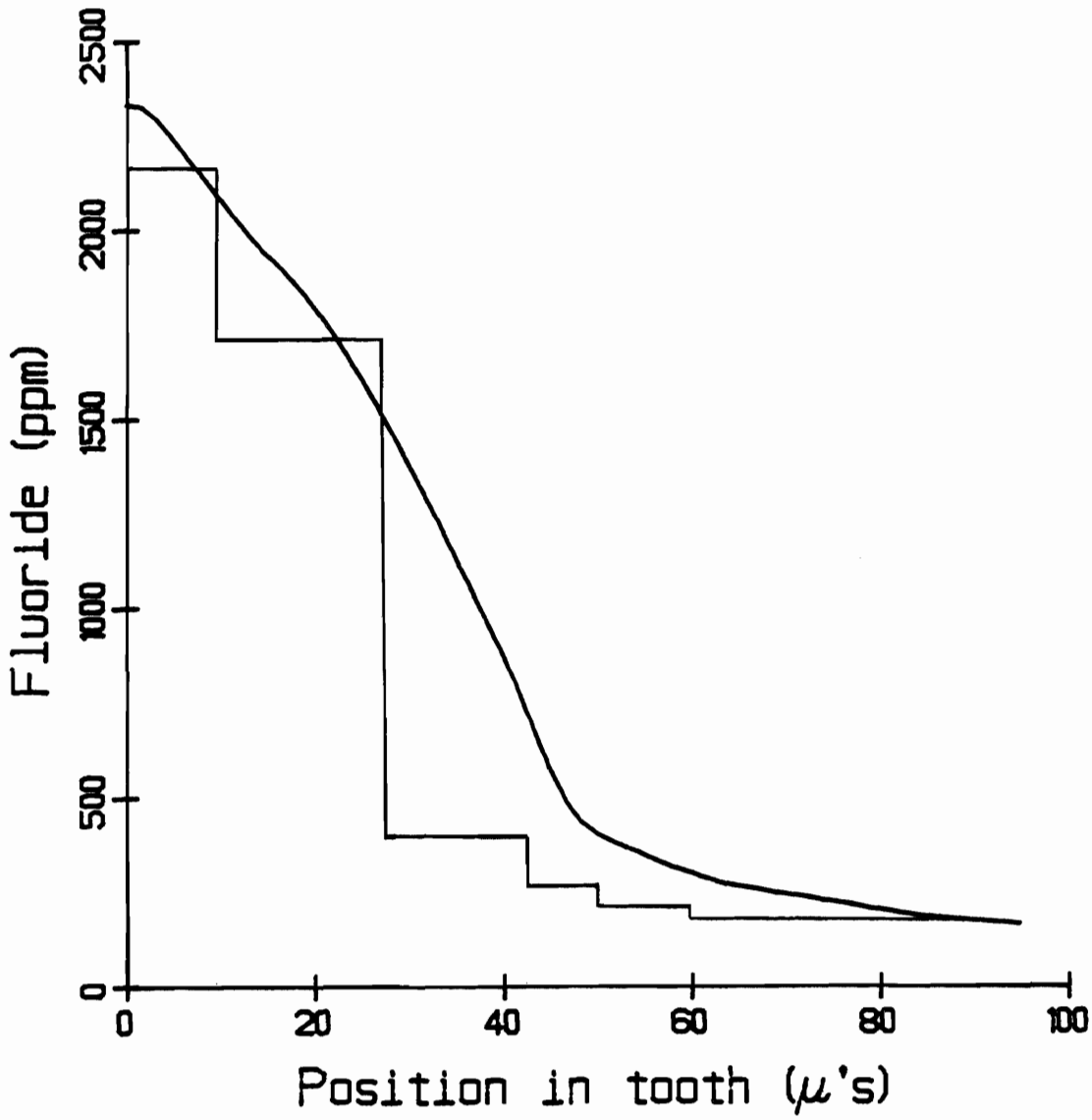

Fig. 5.14. Adsorbed fluoride distribution of dissolution for 24 hours case in pK_{FAP}= 114.53 buffer at 500 rpm, h = 32.1 micrometers. The smooth curve represents the fluoride profile corrected for mineral density and the histogram represents the raw data.

tion fluoride was unfeasible, adsorption experiments and theoretical calculations were designed to allow calculation of prevailing microenvironmental solution conditions.

Hydrodynamic Influences on the Uptake and Adsorption of Fluoride

It was found that a decreased aqueous boundary layer thickness had the effect of increasing the extent and depth of adsorbed fluoride for the same experimental time as compared to the thick boundary layer situation, (Figure 5.13 versus 5.14). However, the maximum levels of bound fluoride are not affected, as expected, since there are a limited number of adsorption sites available. The influence of the varied hydrodynamics in the presence of solution is examined in a subsequent section.

Fluoride Adsorption on Hydroxyapatite

To determine, at least conceptually, the extent of adsorption at the very low levels of solution fluoride concentration expected at the advancing front of fluoride diffusing into the enamel, synthetic hydroxyapatite of known surface area was used to generate equilibrium adsorption isotherms of fluoride for UM-A hydroxyapatite. The relative affinities of F^- and OH^- for hydroxyapatite were determined by varying the pH. The adsorption isotherm of hydroxyapatite for fluoride ion in the presence of a competing species (hydroxyl) is given by the equilibrium expression:

$$F_{ADS} = \frac{N_{sites} \cdot \frac{k_1}{k_2} \cdot F_{soln}}{1 + \frac{k_1}{k_2} \cdot F_{soln} + \frac{k_3}{k_4} (OH)_{soln}} \qquad (5.3)$$

where F_{ADS} is the amount of fluoride adsorbed (moles/meter^2), F_{soln} is the equilibrium concentration of fluoride in solution (moles/liter), $(OH)_{soln}$ is the equilibrium concentration of hydroxyl in solution (moles/liter), k_1/k_2 is the adsorption coefficient of fluoride ion for hydroxyapatite (liters/mole) and k_3/k_4 is the adsorption coefficient of hydroxyl ion for hydroxyapatite; N_{sites}, the number of available sites for adsorption (moles/meter^2).

The best fit of the experimental data at pH 7 and pH 8 by the nonlinear least squares method is represented by the solid line in Figure 5.15. The values of the three parameters N_{sites}, k_1/k_2, and k_3/k_4 are presented in Table 5.3. The affinity of hydroxyl for the apatitic surface is roughly 50 times that of fluoride. Extrapolation of this pH 7 and pH 8 data (where little or no dissolution occurs) to pH 4.5, the experimental condition used in the other studies, indicates that significant (~ 50% surface coverage) adsorption occurs at levels of solution fluoride around 1×10^{-8} M..

Interestingly, at very low equilibrium concentrations of solution fluoride the experimental data fell consistently and significantly above the isotherm predicted from the higher solution concentration equilibrium fluoride adsorption data (Figure 5.16). This suggests that approximately 20% of the hydroxyapatite crystal surface has a higher affinity for fluoride than the bulk of the crys-

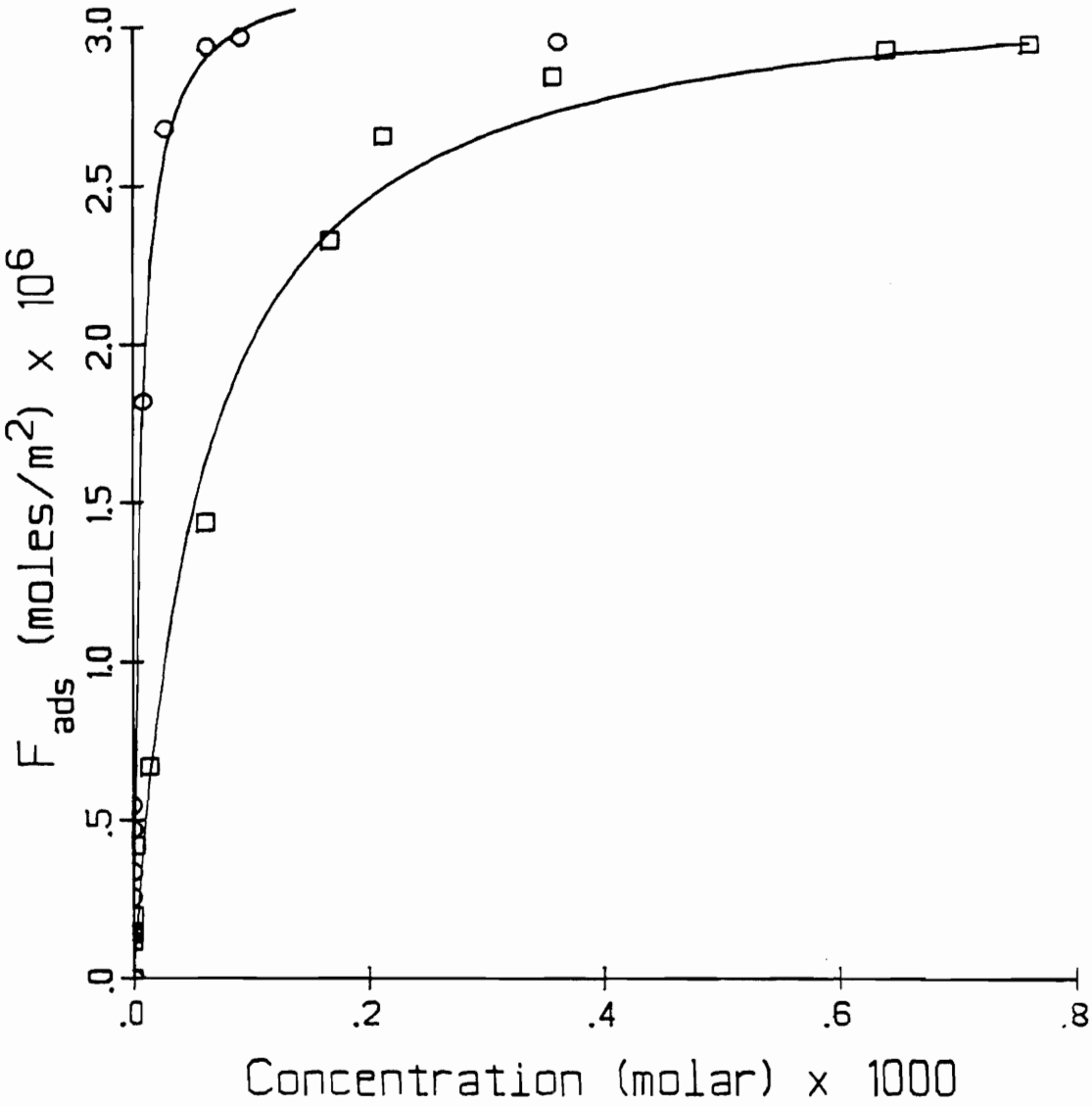

Fig. 5.15. Equilibrium fluoride adsorption isotherms, UM-A hydroxyapatite, 0.01 M barbital buffer, at pH = 7.0 (○) and pH = 8.0 (□). The smooth curve represents the isotherm calculated according to equation 5.3.

TABLE 5.3

BEST FIT VALUES FOR FLUORIDE ADSORPTION PARAMETERS*

N_{sites} (moles/meter^2)	k_1/k_2 (liter/mole)	k_3/k_4 (liter/mole)
3.2×10^{-6}	2.8×10^{6}	1.7×10^{8}

*UM-A hydroxyapatite, 0.01 M Barbital buffer at pH = 7 and 8.

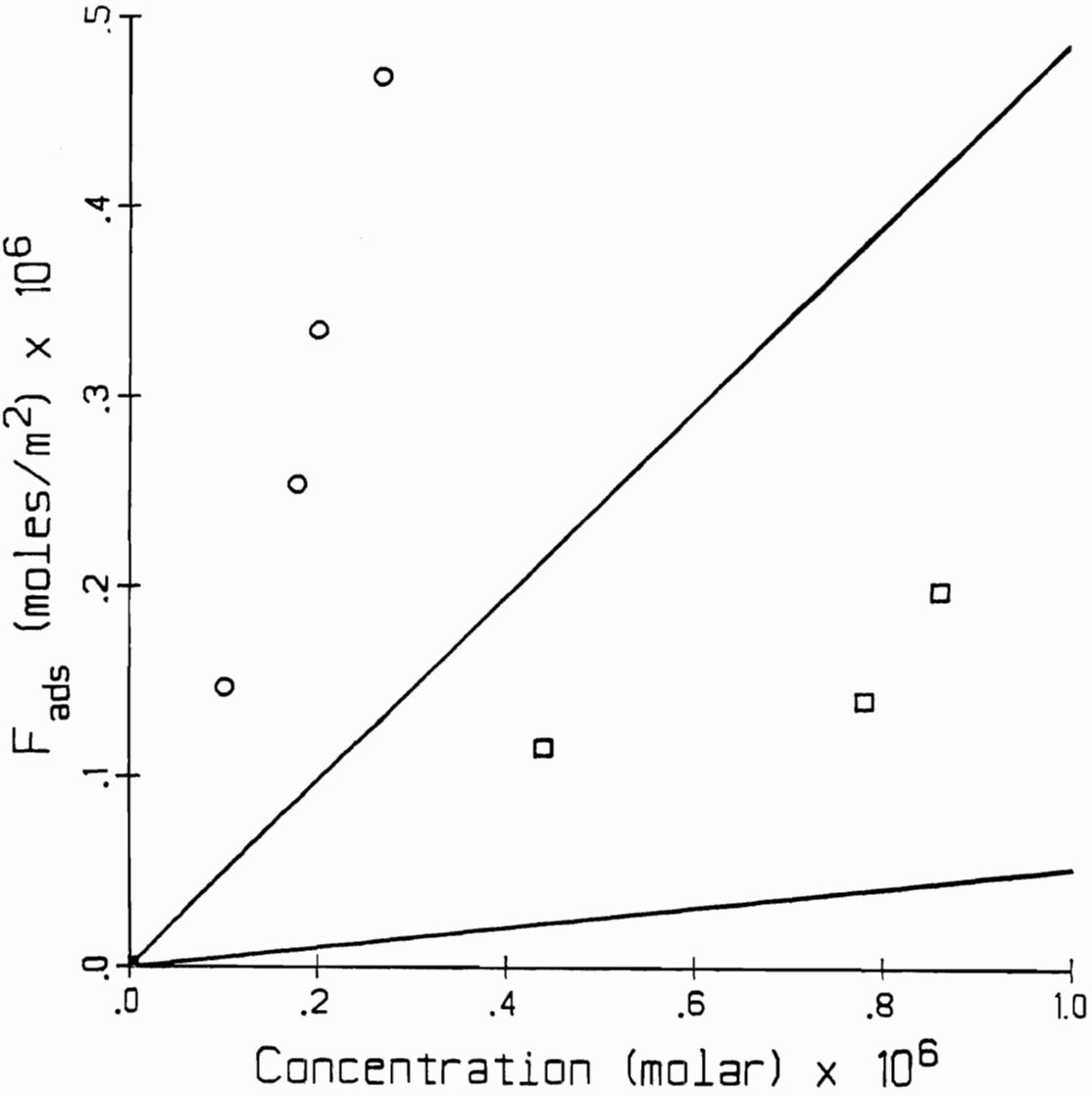

Fig. 5.16. Equilibrium fluoride adsorption isotherms, UM-A hydroxyapatite, 0.01 M barbital buffer, at pH = 7.0 (○) and pH = 8.0 (□). The smooth curve represents the isotherm calculated according to equation 5.3.

tal. A possible scenario describing this physically is that at very low solution fluoride concentrations the hydroxyapatite will contain fluoridated sites and nonfluoridated sites, with the relative abundancies of each related to the extent of surface adsorption of fluoride. Each site might be controlled by its own ion activity product and thereby have its own dissolution driving force, hence dissolution rate.

From these adsorption isotherm data it is concluded that the concept of a significant extent of adsorption (50%) can be occurring at very low levels of solution fluoride ($\sim 10^{-8}$M) at pH 4.5 is reasonable.

Determination of Apparent Solubility of Bovine Enamel From Dissolution Kinetic Data

In the absence of solution fluoride. Using the dissolution model put forth by Wu (1975) and estimating the dissolution rate from area above the curve measurements in the quantitative microradiographic methodology, the dissolution kinetics of bovine enamel are adequately described by a "one-site" kinetic model over a wide range of bulk solution condtions.

Treating the bovine enamel dissolution rate data (Figure 5.17) by the Wu model allows determination of the apparent driving force for dissolution and the kinetic rate constant. Briefly, Wu's model considers dissolution of a one component solute described by Fick's Second Law modified to include a term for the surface reaction component.

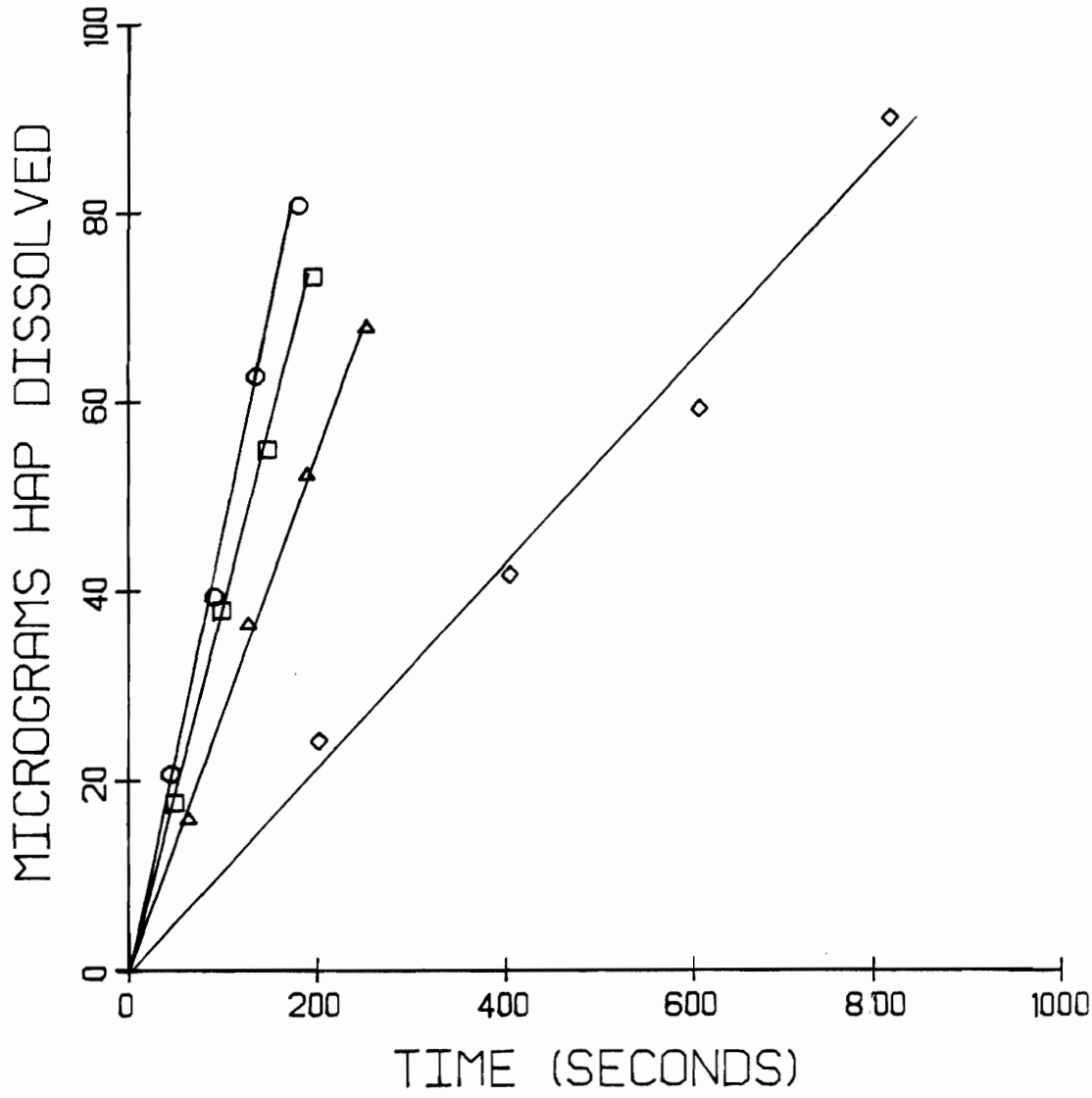

Fig. 5.17. Dissolution of bovine enamel under sink conditions; ◊ 50 rpm, △ 100 rpm, □ 300 rpm and ○ 600 rpm.

$$\frac{\partial C}{\partial t} = D' \frac{\partial^2 C}{\partial t^2} + k(C_s - C) \tag{5.4}$$

C_s is the apparent solubility, k is the apparent first order surface reaction rate constant, D' is the effective diffusivity within the enamel, C is the solution concentration in the pores of the enamel at time t and position x.

Assuming steady-state and including diffusional aspects within the aqueous boundary layer, under the appropriate boundary conditions the working equation is obtained.

$$\frac{h}{D} = \frac{A}{J} \cdot (C_s - C_h) - k' \tag{5.5}$$

D is the aqueous diffusivity, h is the effective aqueous boundary layer thickness, J is the dissolution rate and A is the surface area of reactant. Plotting h/D versus A/J will yield a straight line with slope equal to $(C_s - C_h)$ and the negative y intercept being k' (Figure 5.18). Therefore, C_s and k' can be determined since the other parameters are known or experimentally determined. Analysis of the experimental data with this theoretical treatment yields a K_{HAP} for bovine enamel of $10^{-117.0 \pm 0.5}$ and a k' value of $3.5 \pm .25 \times 10^2$ sec./cm.

In the presence of solution fluoride. Data for the dissolution of bovine enamel in weak acid buffer in the presence of low level solution fluoride are presented in Figures 5.19 - 5.22. Analyzing the data by the previously described method allows extraction of the

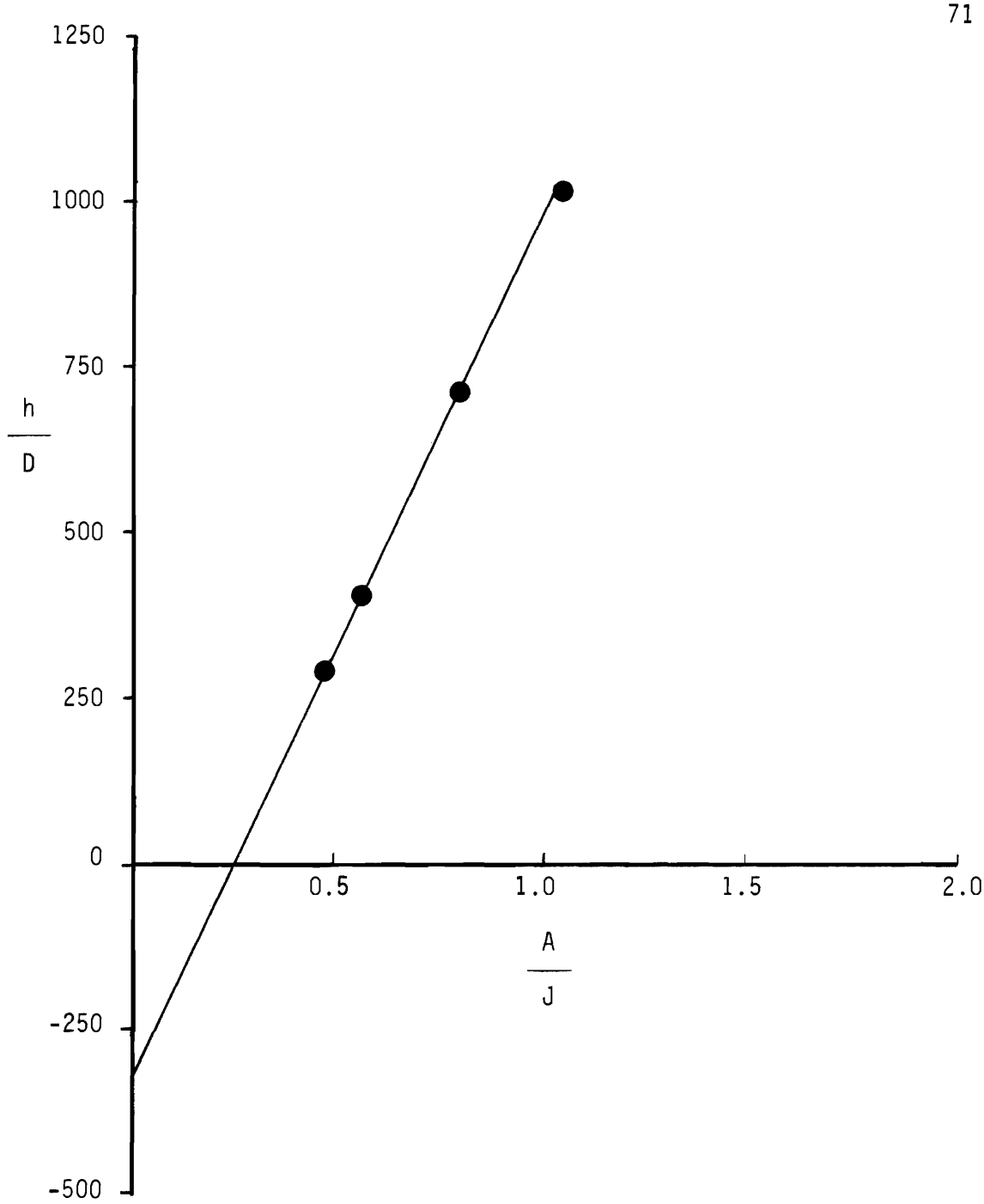

Fig. 5.18. h/D versus A/J plot from which C_s - C is obtained from the slope according to equation 5.5 for the zero solution fluoride case.

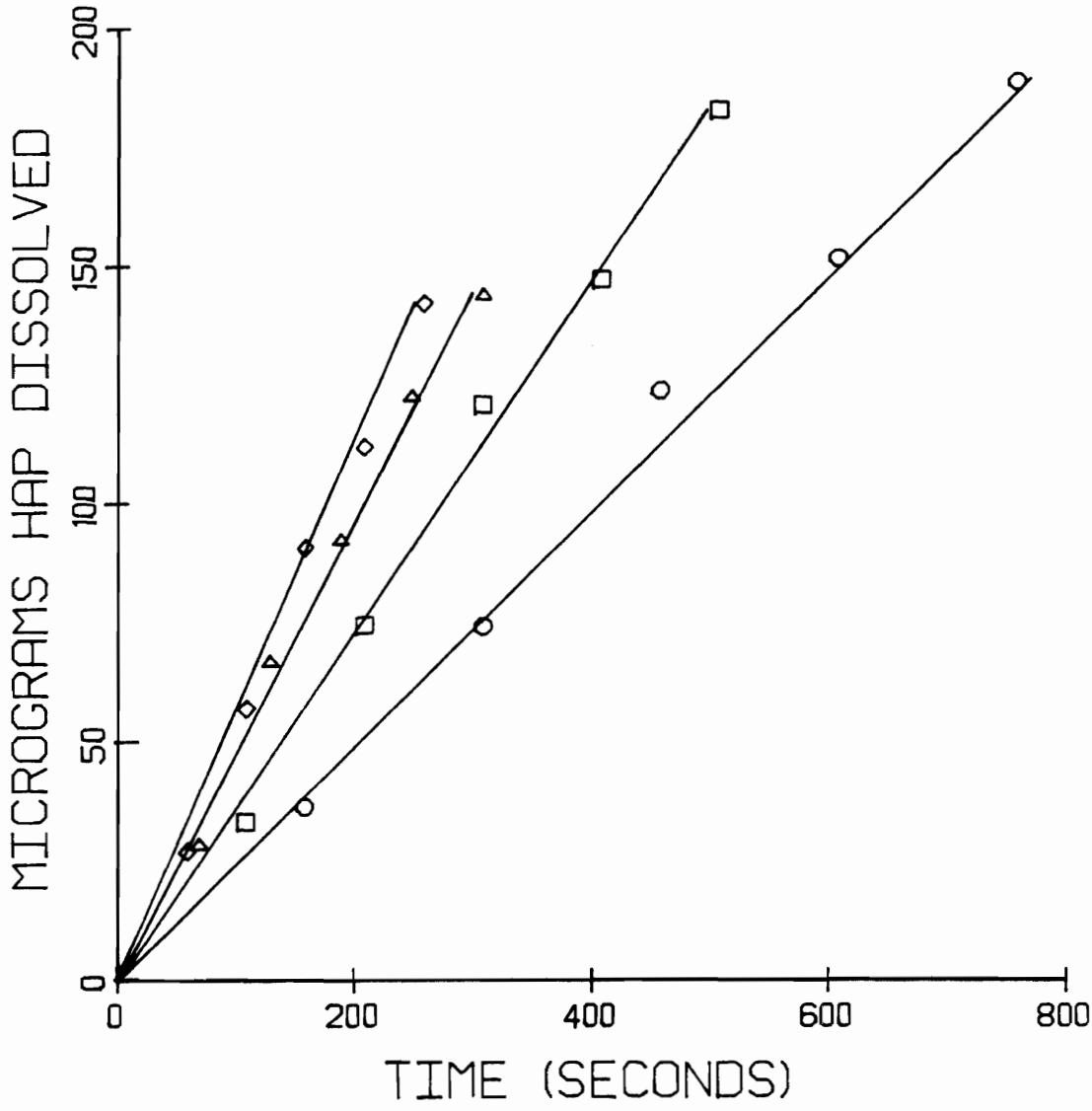

Fig. 5.19. Dissolution of bovine enamel in dissolution media containing 0.001 ppm F; ○ 50 rpm, □ 100 rpm, △ 300 rpm and ◇ 600 rpm.

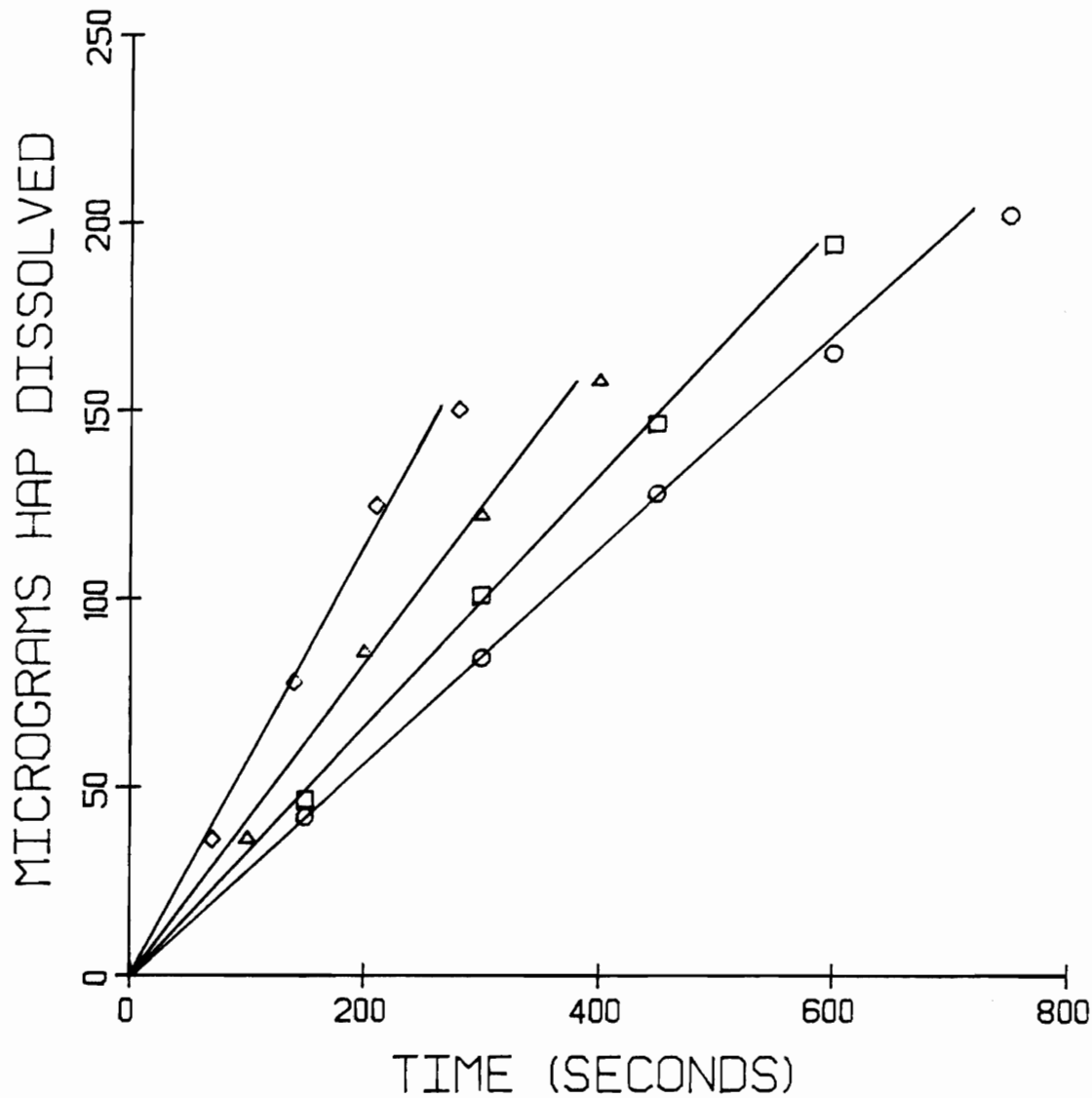

Fig. 5.20. Dissolution of bovine enamel in dissolution media containing 0.01 ppm F; ○ 50 rpm, □ 100 rpm, △ 300 rpm and ◇ 600 rpm.

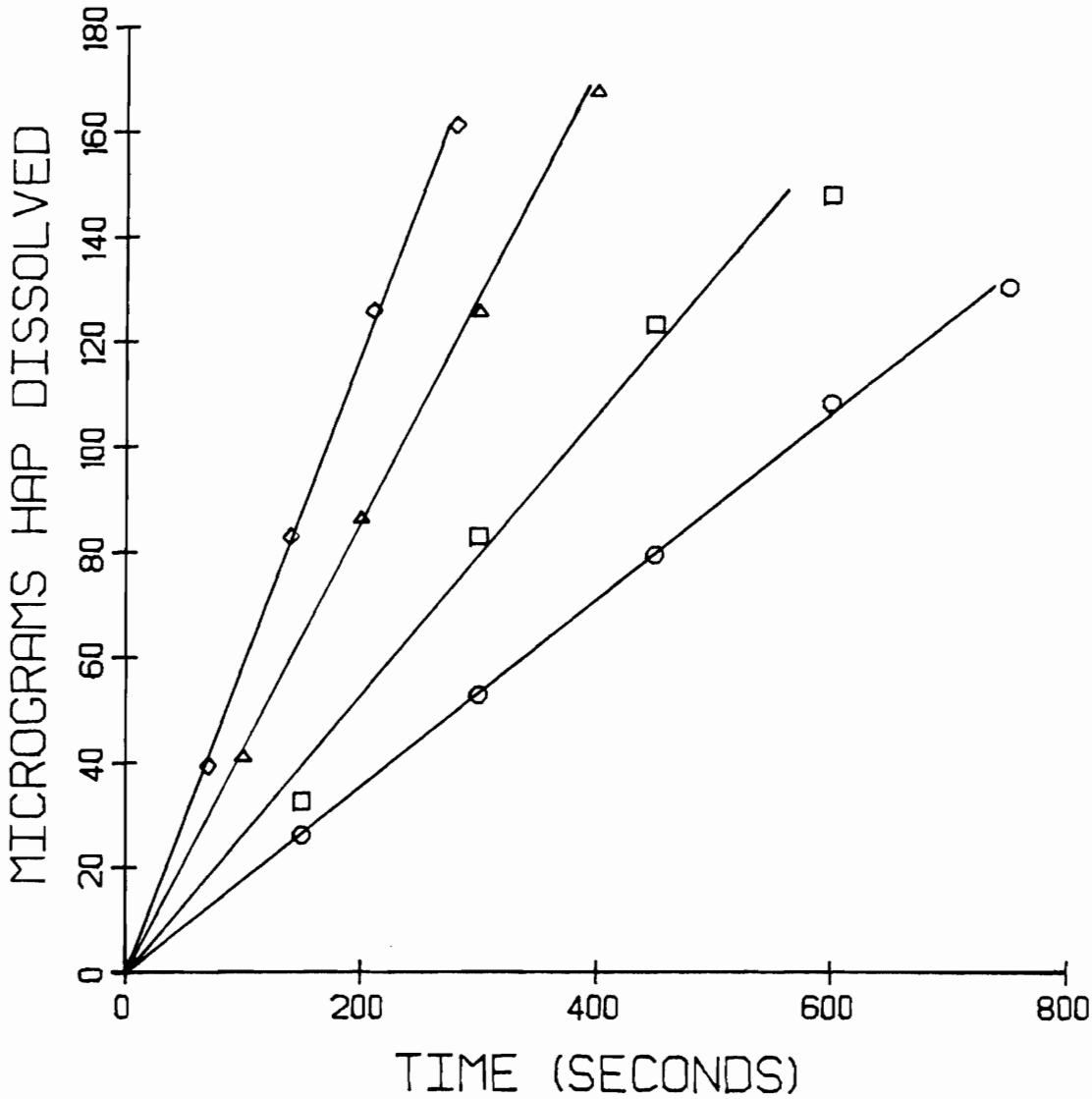

Fig. 5.21. Dissolution of bovine enamel in dissolution media containing 0.1 ppm F; ○ 50 rpm, □ 100 rpm, △ 300 rpm and ◇ 600 rpm.

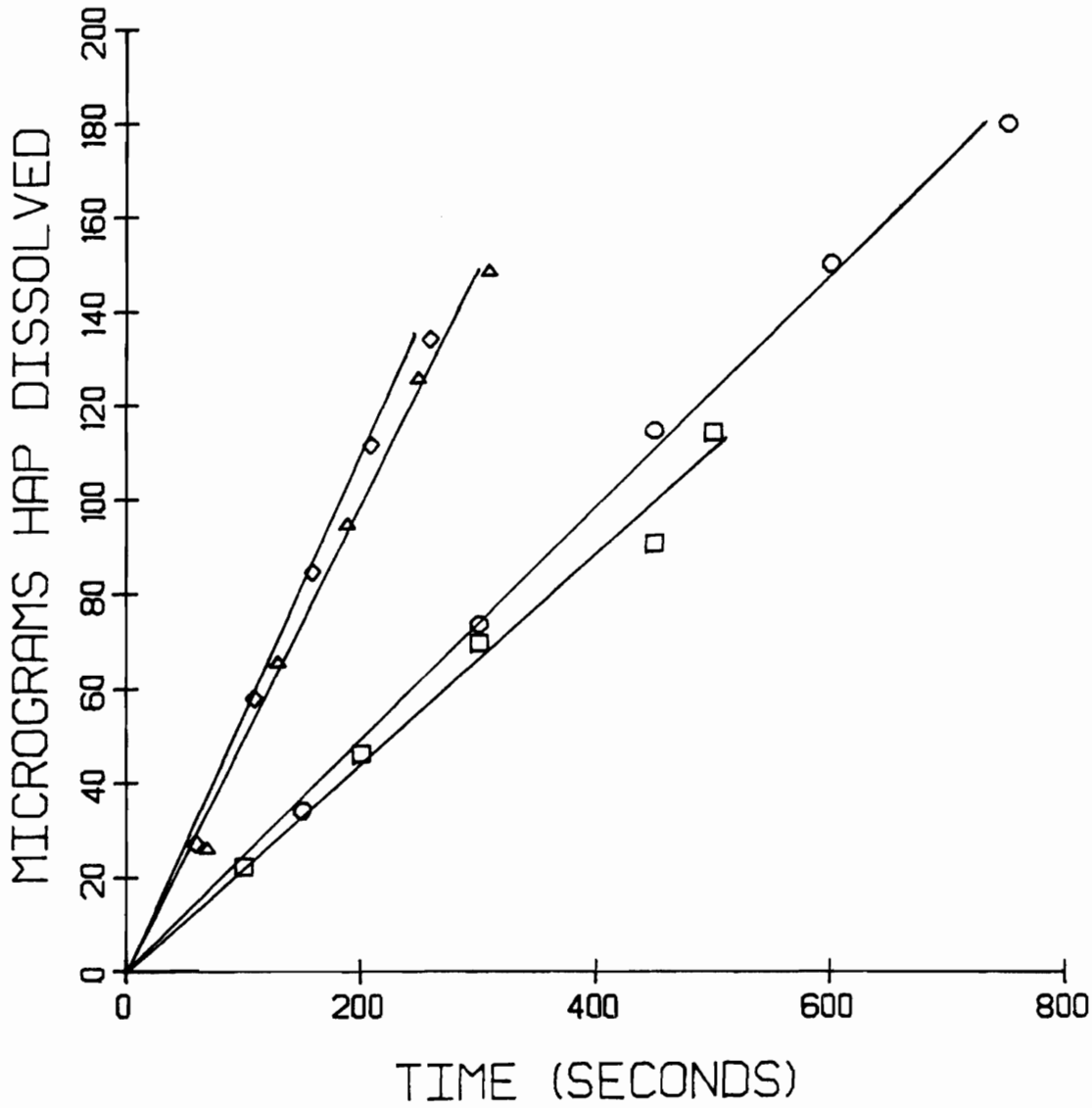

Fig. 5.22. Dissolution of bovine enamel in dissolution media containing 1.0 ppm F; ○ 50 rpm, □ 100 rpm, △ 300 rpm and ◇ 600 rpm.

apparent driving force for dissolution in the presence of solution fluoride and the corresponding kinetic rate constant (Figure 5.23). It should be noted that implicit in the Wu model is the assumption of a constant bulk solution fluoride concentration. In the present study a gradient exists in the solution fluoride concentration from the bulk solution to a given depth in the enamel. The consequence of this is that the parameters deduced from the experimental data treated with this model, K_{FAP} and k', represent a first approximation only. The best fit values for these parameters were determined to be $K_{FAP} = 10^{-115 \pm 1.0}$ and $k' = 2.25 \pm 0.25 \times 10^2$ sec./cm.

The apparent solubilities and surface reaction rate constant parameters, in the absence and presence of fluoride are summarized in Table 5.4.

Carbonate Apatite Dissolution Rate in the Presence of Solution Fluoride

Studies into the dissolution rate behavior of synthetic carbonate containing apatite powders, chemically similar to hydroxyapatite of bovine enamel, exhibited a pronounced dependence upon the ion activity product of the dissolution media, (Ludwig, et al., 1983). It was found that the dissolution rate of these apatitic powders, in the presence of low level solution fluoride, decreased and approached zero as the solution ion activity product (K_{FAP}) neared 10^{-114} or 10^{-115} (Figure 5.24).

The relevance of these findings to the present study using bovine enamel as the model hydroxyapatite system is that, as in the carbon-

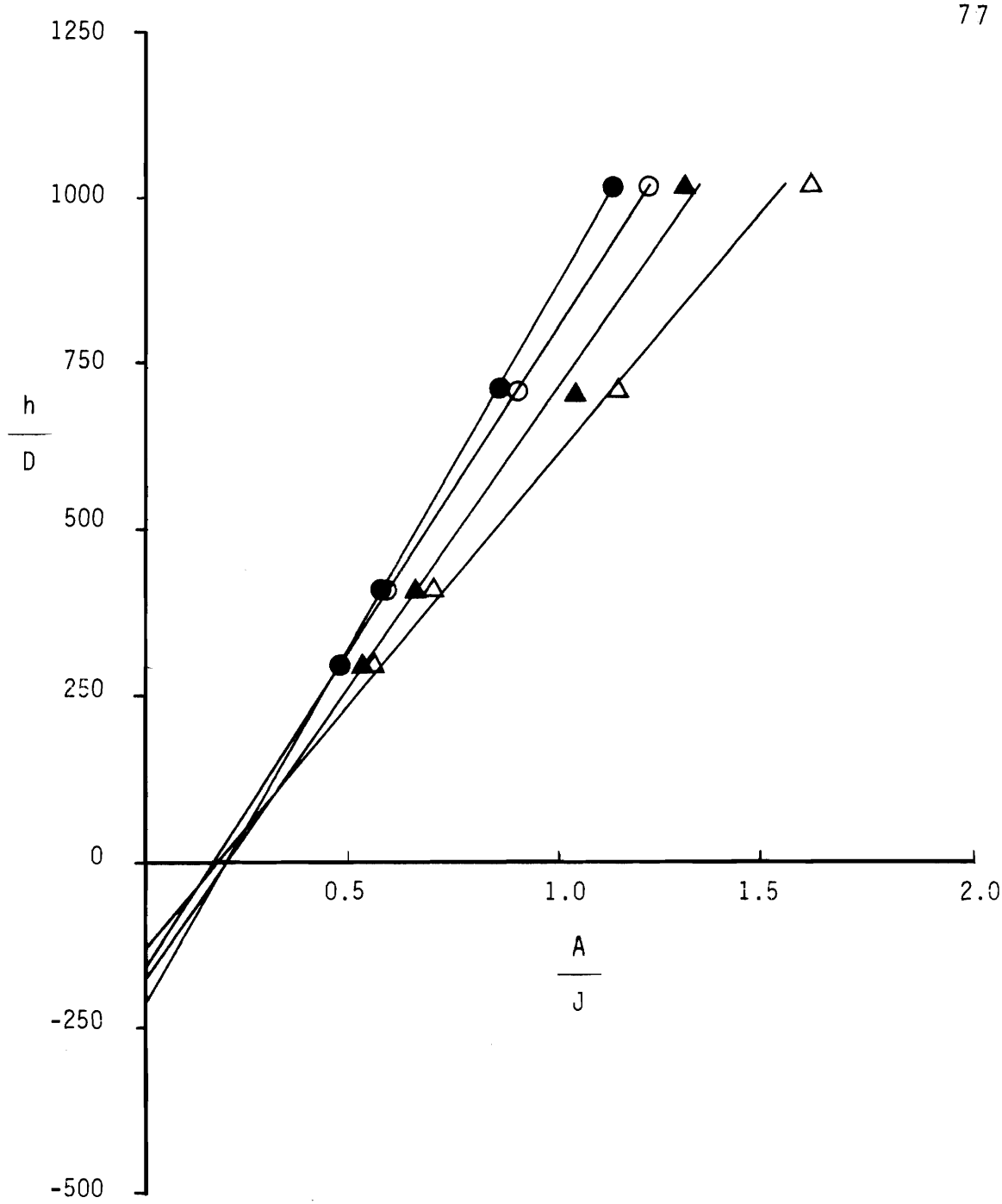

Fig. 5.23. h/D versus A/J plot from which $C_s - C$ is obtained from the slope according to equation 5.5 in the presence of solution fluoride; ● 0.001 ppm F, ○ 0.01 ppm F, ▲ 0.1 ppm F and △ 1.0 ppm F.

TABLE 5.4

BOVINE ENAMEL DISSOLUTION MODEL PARAMETERS

PHASE	DISSOLUTION THRESHOLD ION ACTIVITY PRODUCT	KINETIC CONSTANT (sec./cm)
Hydroxyapatite	$1 \times 10^{-117 \pm 0.5}$	350 ± 25
Fluorapatite	$1 \times 10^{-115 \pm 1.0}$	225 ± 25

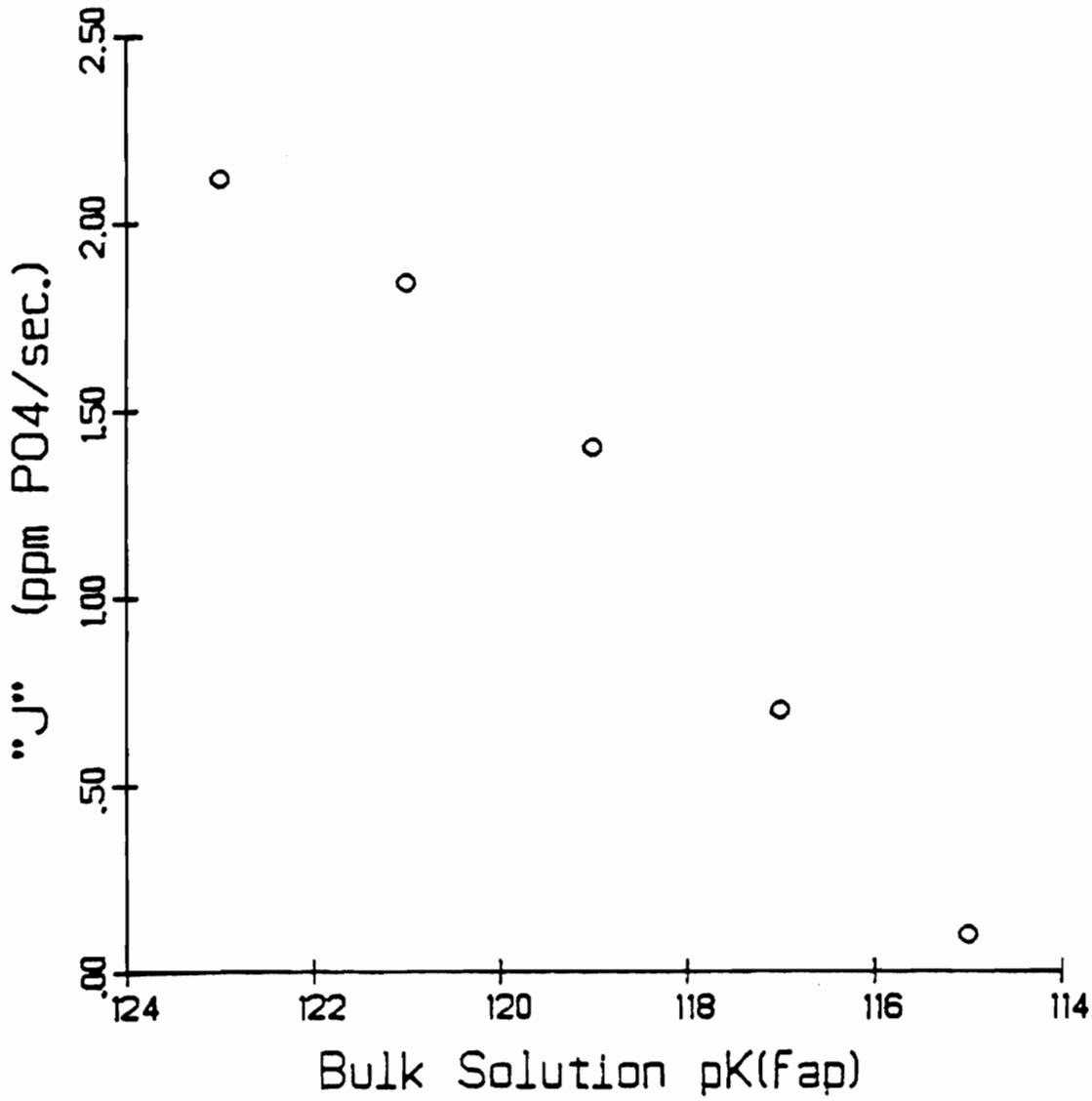

Figure 5.24. Inhibition of carbonate-apatite dissolution rate as the bulk solution ion activity product (pK_{FAP}) approaches a value of 114 or 115.

ate-apatite powder case, the dissolution rate of a bovine enamel hydroxyapatite crystallite should approach zero when the ambient solution has an ion activity product (K_{FAP}) of 10^{-114} or 10^{-115}.

Hydrodynamic Effect on Enamel Dissolution Behavior in Buffers Containing Fluoride

The dissolution rate behavior of bovine enamel blocks in weak acid buffers containing fluoride under two different hydrodynamic conditions was assessed by quantitative microradiographic analysis as a function of time and aqueous boundary layer thickness. The anticipated effect of an increased dissolution rate with a decreased aqueous boundary layer thickness was not observed.

Under bulk conditions known to give rise to intact surface layer formation (high Ca, PO_4, F; low pH) with subsurface dissolution, the extent of dissolution, as measured by mineral loss, decreases when the effective aqueous boundary layer thickness is decreased, i.e., high rpm. Figures 5.25 - 5.28 show the mineral density profiles obtained for 3, 6, 12 and 24 hours of dissolution at 10 rpm where the aqueous boundary layer thickness is 227 micrometers. Figures 5.29 - 5.32 are representative of dissolution under conditions of a thin boundary layer, 32 micrometers, where dissolution normally is expected to be greater. Table 5.5 shows the amount of mineral dissolved, expressed as equivalent micrometers of enamel, as a function of time and aqueous boundary layer thickness. This phenomenon has been observed reproducibly and is considered in terms of the reverse gradients that exist for calcium and phosphate ions leaving the enamel matrix and fluoride

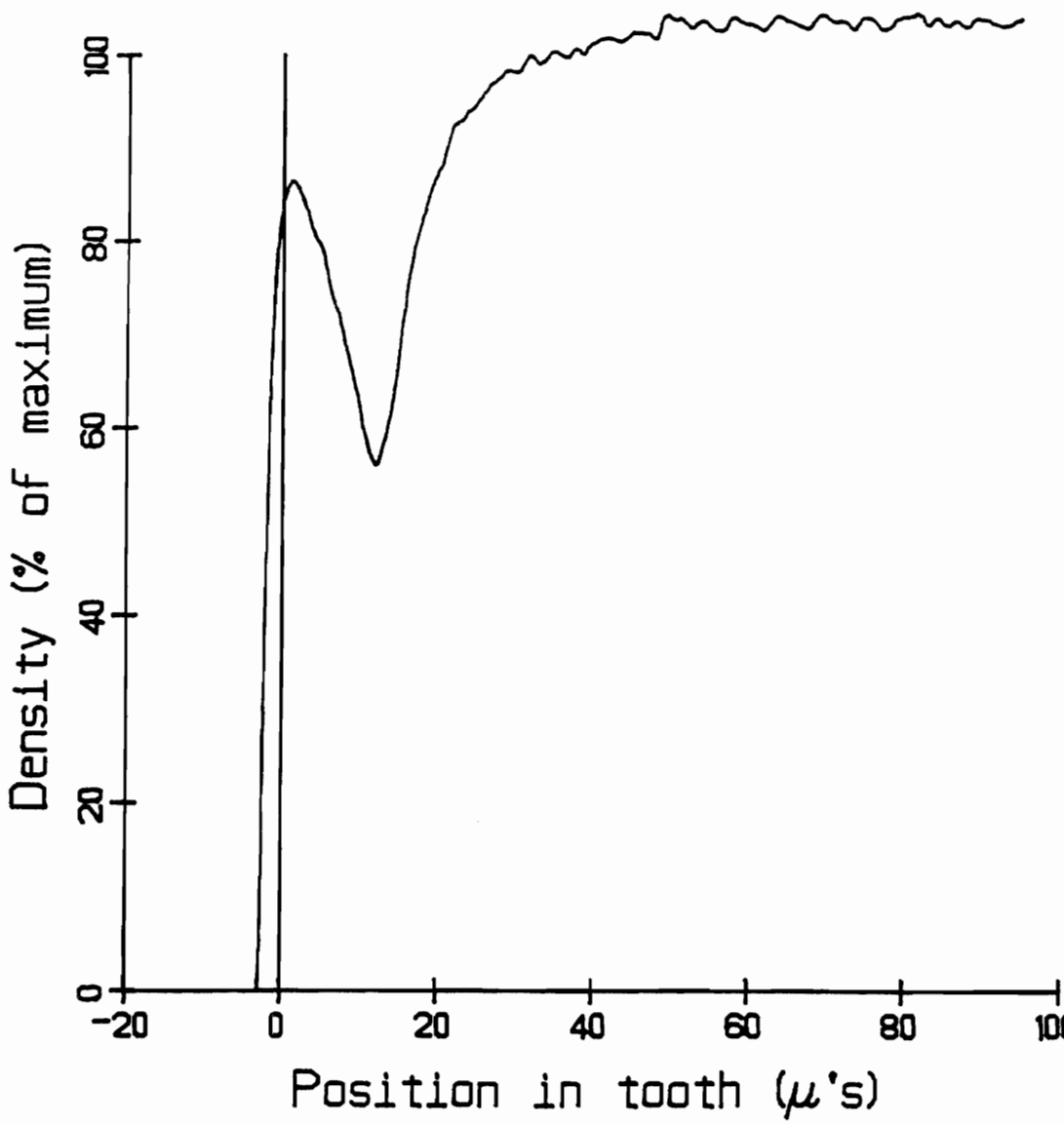

Fig. 5.25. Mineral density profile of bovine enamel dissolution for 3 hours in pK_{FAP}= 114.53 buffer at 10 rpm, h = 227 micrometers, 7.55 equivalent micrometers of enamel dissolved.

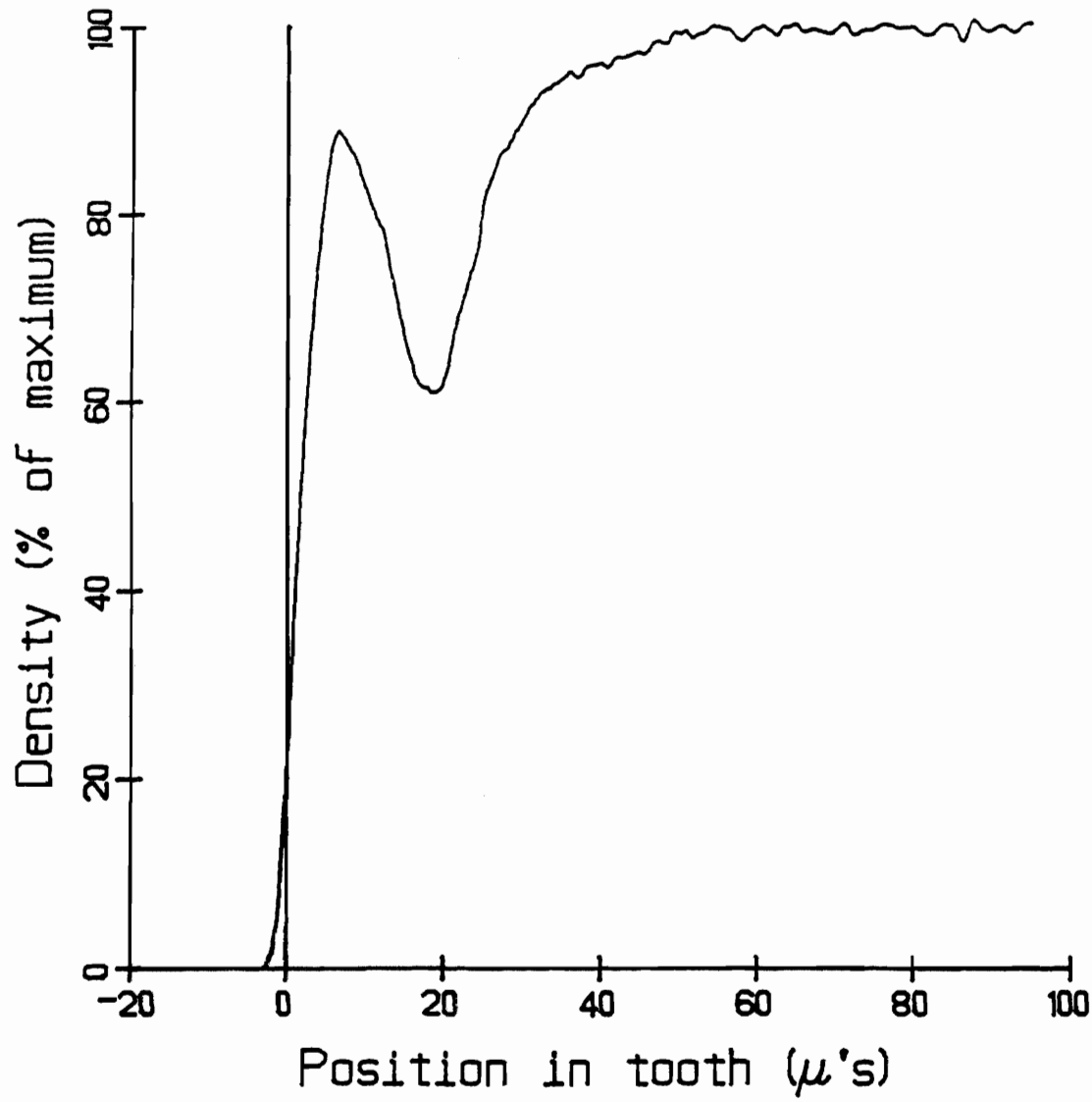

Fig. 5.26. Mineral density profile of bovine enamel dissolution for 6 hours in pK_{FAP}= 114.53 buffer at 10 rpm, h = 227 micrometers, 13.9 equivalent micrometers of enamel dissolved.

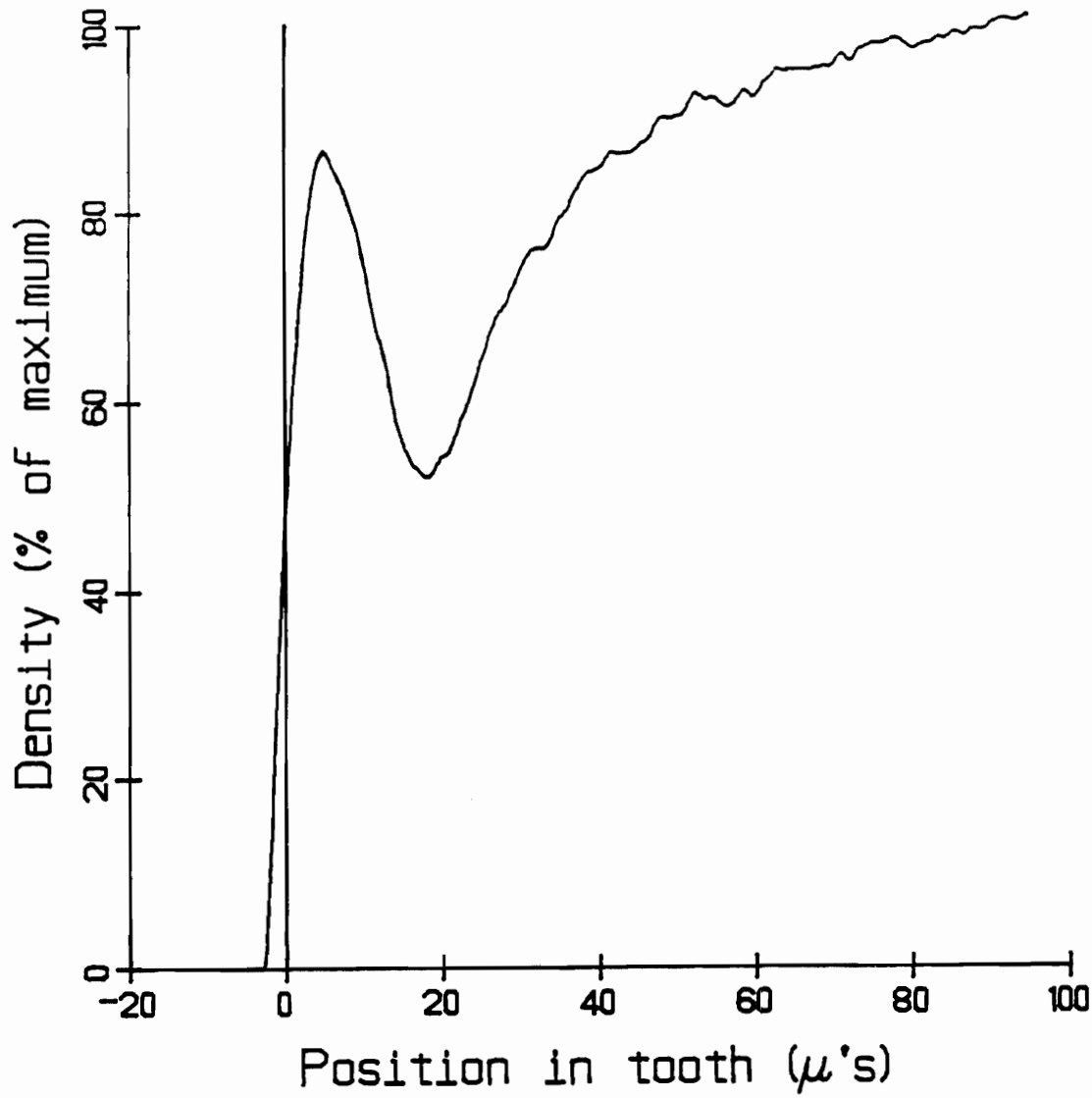

Fig. 5.27. Mineral density profile of bovine enamel dissolution for 12 hours in pK_{FAP}= 114.53 buffer at 10 rpm, h = 227 micrometers, 19.3 equivalent micrometers of enamel dissolved.

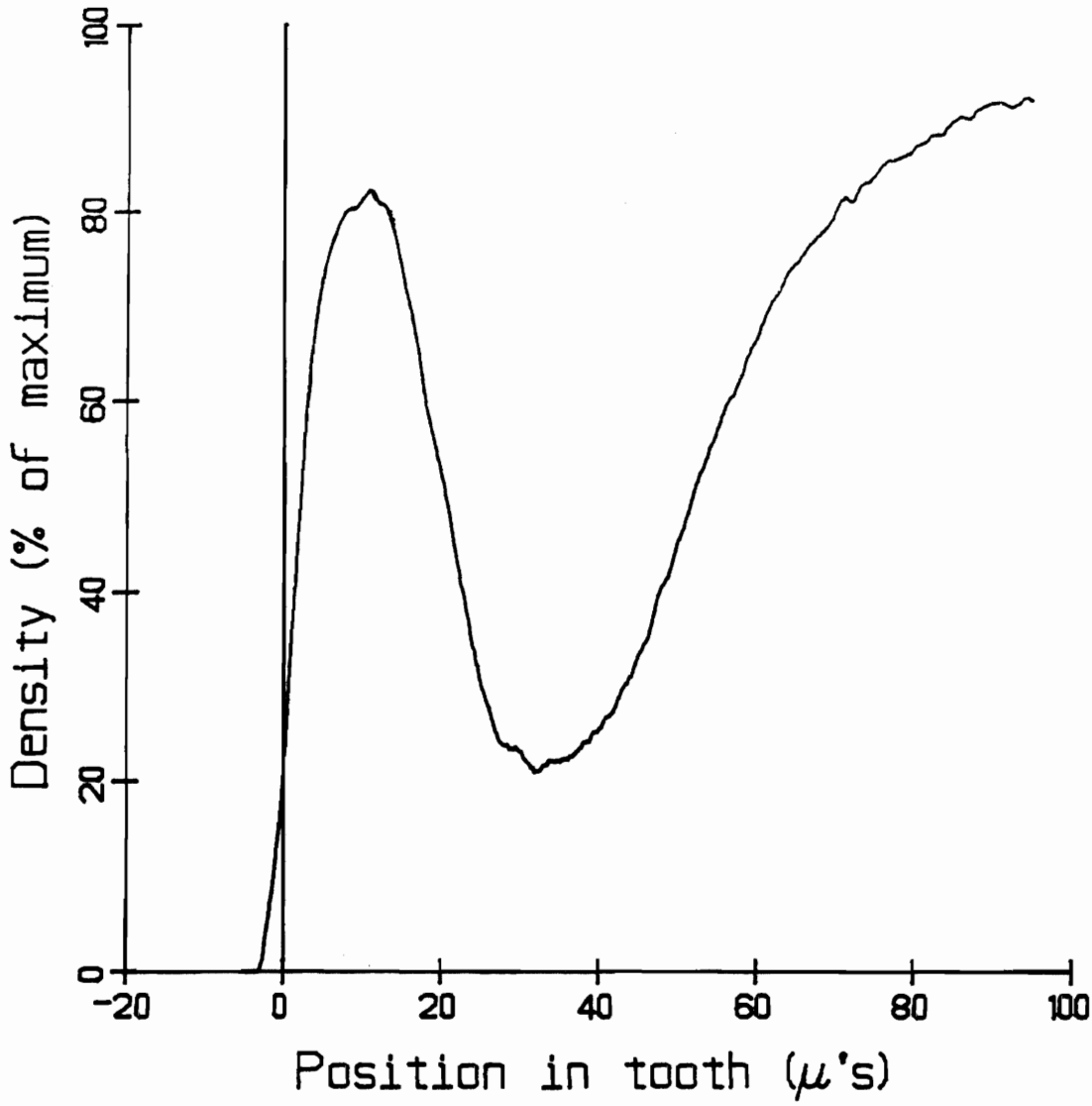

Fig. 5.28. Mineral density profile of bovine enamel dissolution for 24 hours in pK_{FAP}= 114.53 buffer at 10 rpm, h = 227 micrometers, 42.1 equivalent micrometers of enamel dissolved.

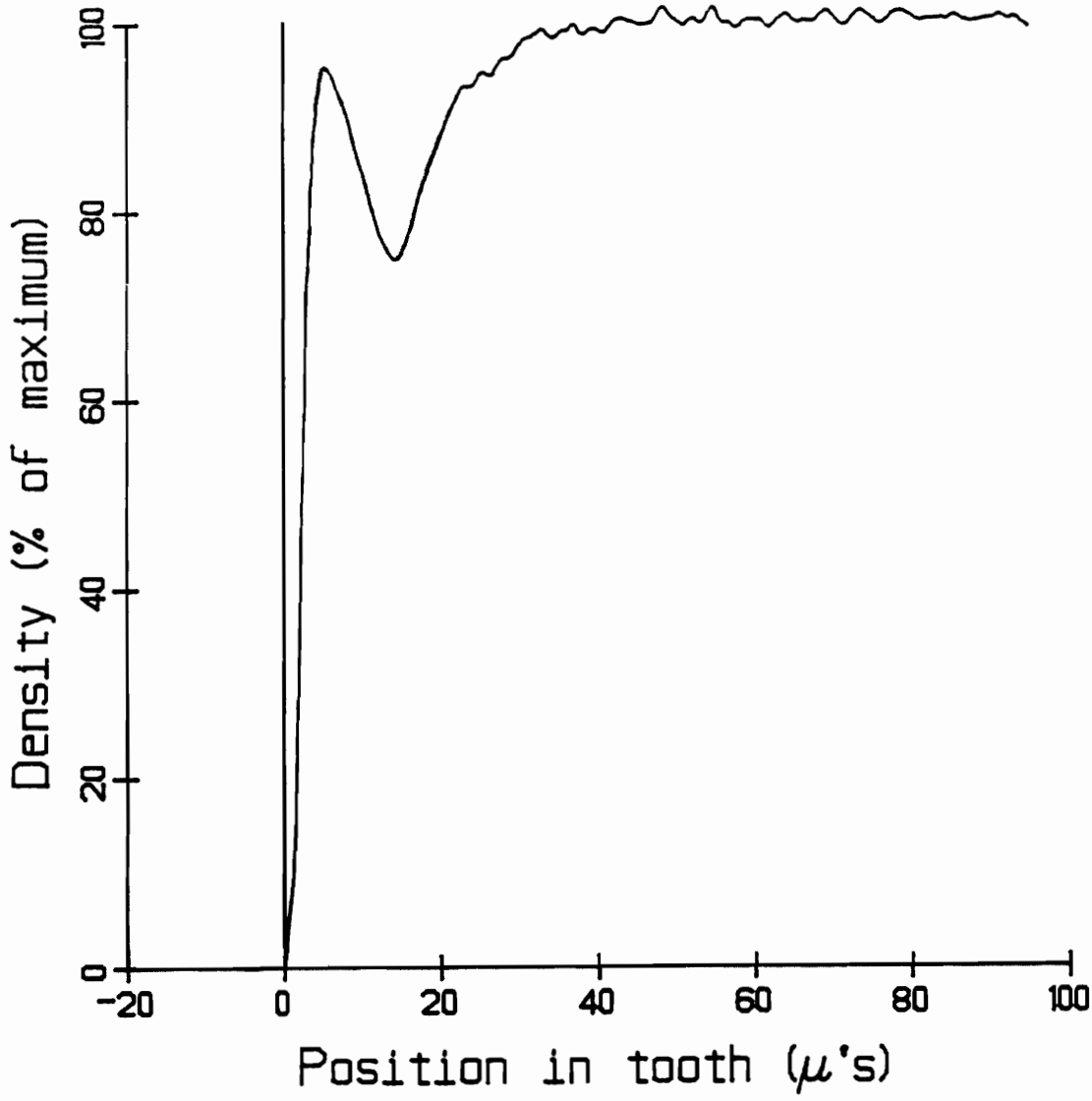

Fig. 5.29. Mineral density profile of bovine enamel dissolution for 3 hours in pK_{FAP}= 114.53 buffer at 500rpm, h = 32.1 micrometers, 10.5 equivalent micrometers of enamel dissolved.

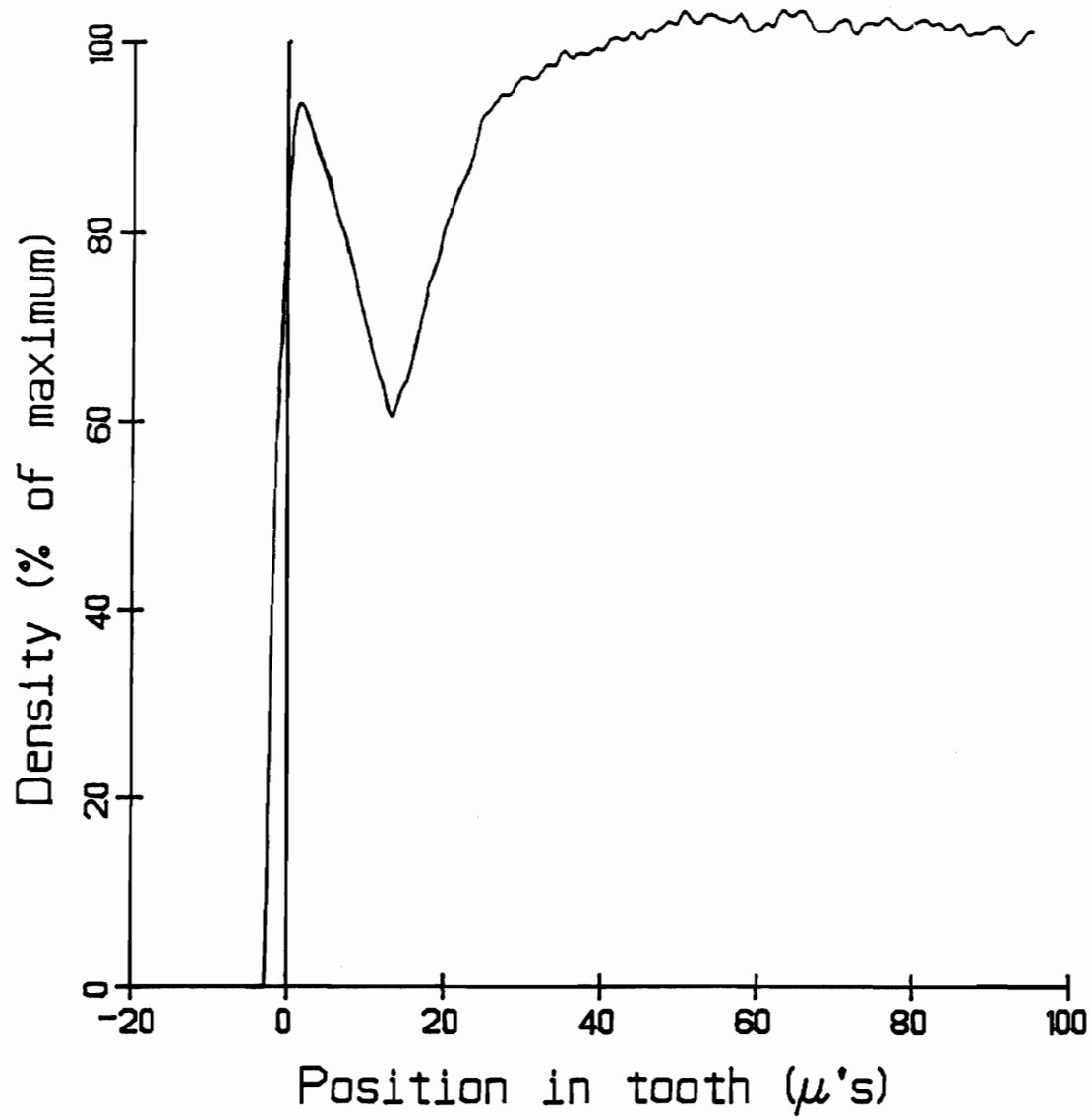

Fig. 5.30. Mineral density profile of bovine enamel dissolution for 6 hours in pK_{FAP}= 114.53 buffer at 500 rpm, h = 32.1 micrometers, 11.3 equivalent micrometers of enamel dissolved.

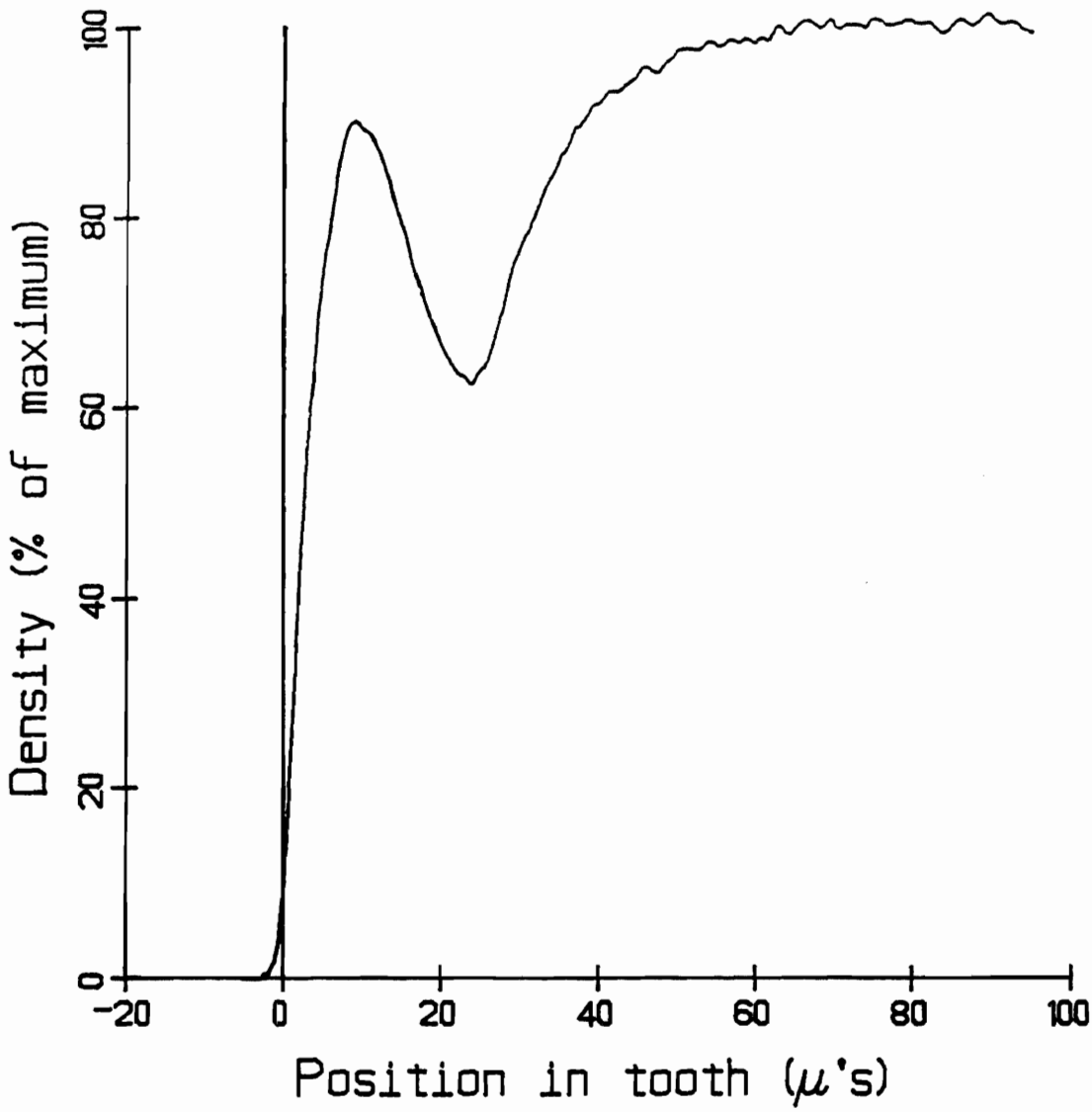

Fig. 5.31. Mineral density profile of bovine enamel dissolution for 12 hours in pK_{EAP} = 114.53 buffer at 500 rpm, h = 32.1 micrometers, 15.8 equivalent micrometers of enamel dissolved.

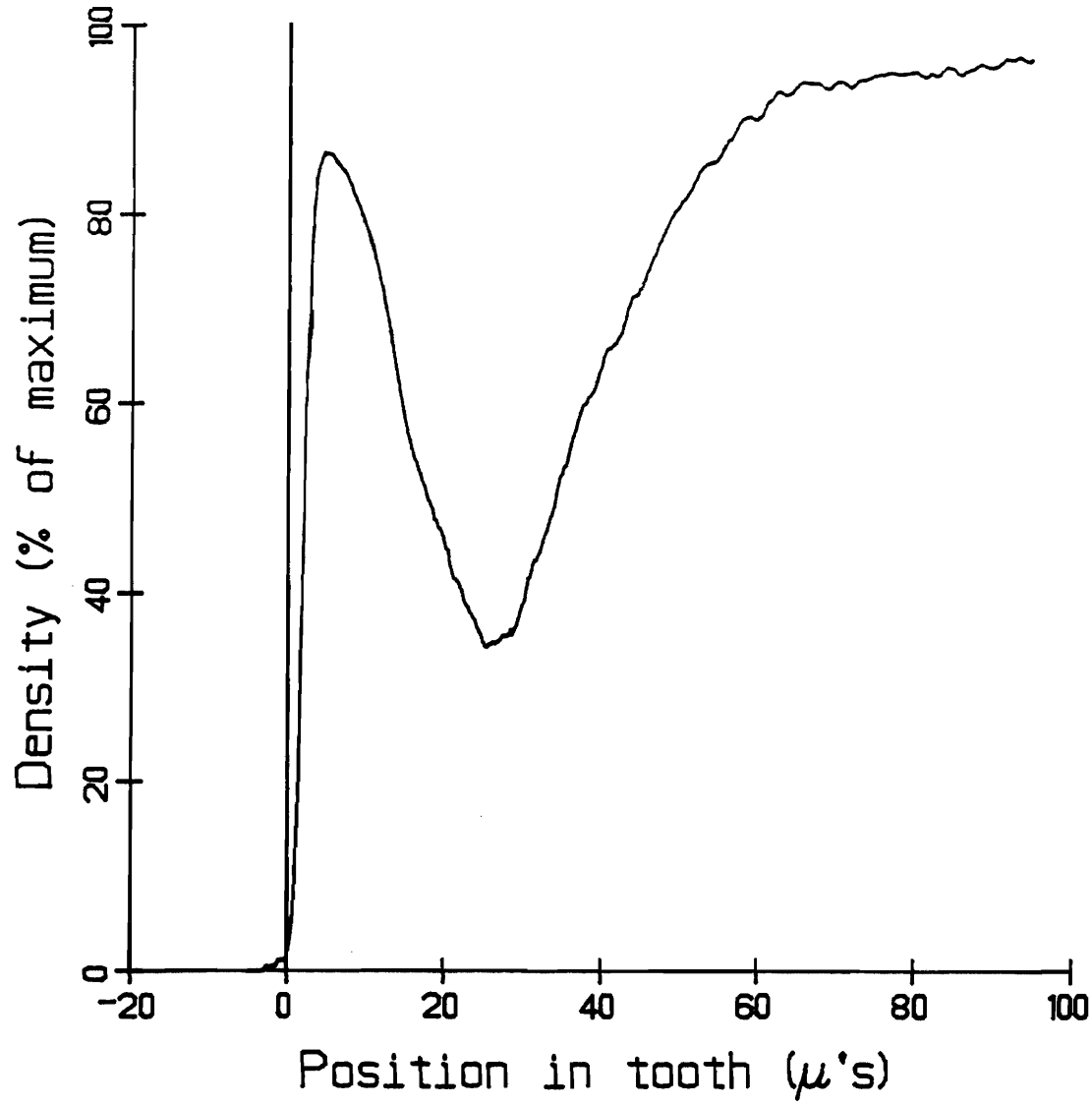

Fig. 5.32. Mineral density profile of bovine enamel dissolution for 24 hours in pK_{FAP} = 114.53 buffer at 500 rpm, h = 32.1 micrometers, 29.1 equivalent micrometers of enamel dissolved.

TABLE 5.5

EFFECT OF VARIED HYDRODYNAMICS ON THE DISSOLUTION RATE IN SOLUTION CONTAINING FLUORIDE*

Dissolution time (hours)	Equivalent micrometers of enamel dissolved (10 rpm)	Equivalent micrometers of enamel dissolved (500 rpm)
3	8.5	10.4
6	13.1	11.0
12	15.9	16.5
24	41.6	29.9

*Bulk solution pK_{FAP} = 114.53; average of duplicate experiments.

ions diffusing in from the bulk. The outward flux of calcium and phosphate is intercepted by the inward perfusion of the enamel surface and intercrystalline voids with bulk solution fluoride ion. The driving force for this infusion of fluoride is the concentration drop across the boundary layer, the gradient of which increases as the effective aqueous boundary layer thickness is decreased. The net result is that the prevailing microenvironmental solution ion activity product is elevated above a critical point. This is further evidence that the microenvironmental solution fluoride has a pronounced effect on the dissolution rate within the enamel matrix. A more comprehensive discussion of this mechanism will be presented in Chapter 6.

Dissolution of Preformed Intact Surface Layer

Dissolution experiments performed in the presence of low levels of solution fluoride have shown that bulk solution fluoride concentration decreases due to fluoride uptake and adsorption by enamel surface hydroxyapatite crystallites. Abrasion and chemical analysis of the biopsy have shown that a steep gradient exists in the levels of bound fluoride with the highest levels of fluoride found in the surface 10 to 20 micrometers of enamel.

Dissolution of enamel with preformed intact surface layers was performed in the standard buffer system (pK_{HAP} = 120) that is considered to be fluoride free. The dissolution of enamel under these conditions was assessed both by following the release of fluoride into the bulk solution and by quantitative microradiograpic analysis of the resulting mineral density changes within the enamel. The purpose of

these experiments was to determine whether it was the bound fluoride being responsible for the formation of an intact surface layer or whether it was the solution fluoride that was important by maintaining the microenvironmental solution ion activity product sufficiently high so as to retard the dissolution rate in this surface region preserving the surface layer and allowing subsurface dissolution to occur.

Figure 5.33 shows the fluoride release profile for 35 hours obtained from dissolving an enamel slab with an intact layer preformed over 24 hours in a pK_{FAP} = 111.9 buffer solution. Fluoride is initially released at a rate of 0.0179 microgram F/hour. The calculated surface K_{FAP} for this flux value is 1×10^{-112}, sufficiently high to maintain the intact surface layer. At later times, after 12 to 15 hours the flux decreases and results in a corresponding decrease in the surface K_{FAP} to 1×10^{-117}. This being less than a $K_{FAP} = 1 \times 10^{-115}$ allows dissolution to occur and maintenance of the intact surface layer is no longer possible.

Densitometric analysis of the microradiographs, Figures 5.34 - 5.37, depict the mineral density changes that occur when dissolution occurs under conditions designed to maintain essentially sink conditions with respect to bulk fluoride concentration. The intact surface layer formed (Figure 5.34) is absent after 24 and 48 hours of subsequent dissolution in a near zero concentration fluoride environment. In fact, surface recession is evident after 24 hours and in particular after 48 hours. Dissolution for 48 hours under identical conditions of buffer composition and hydrodynamics, except that the solution

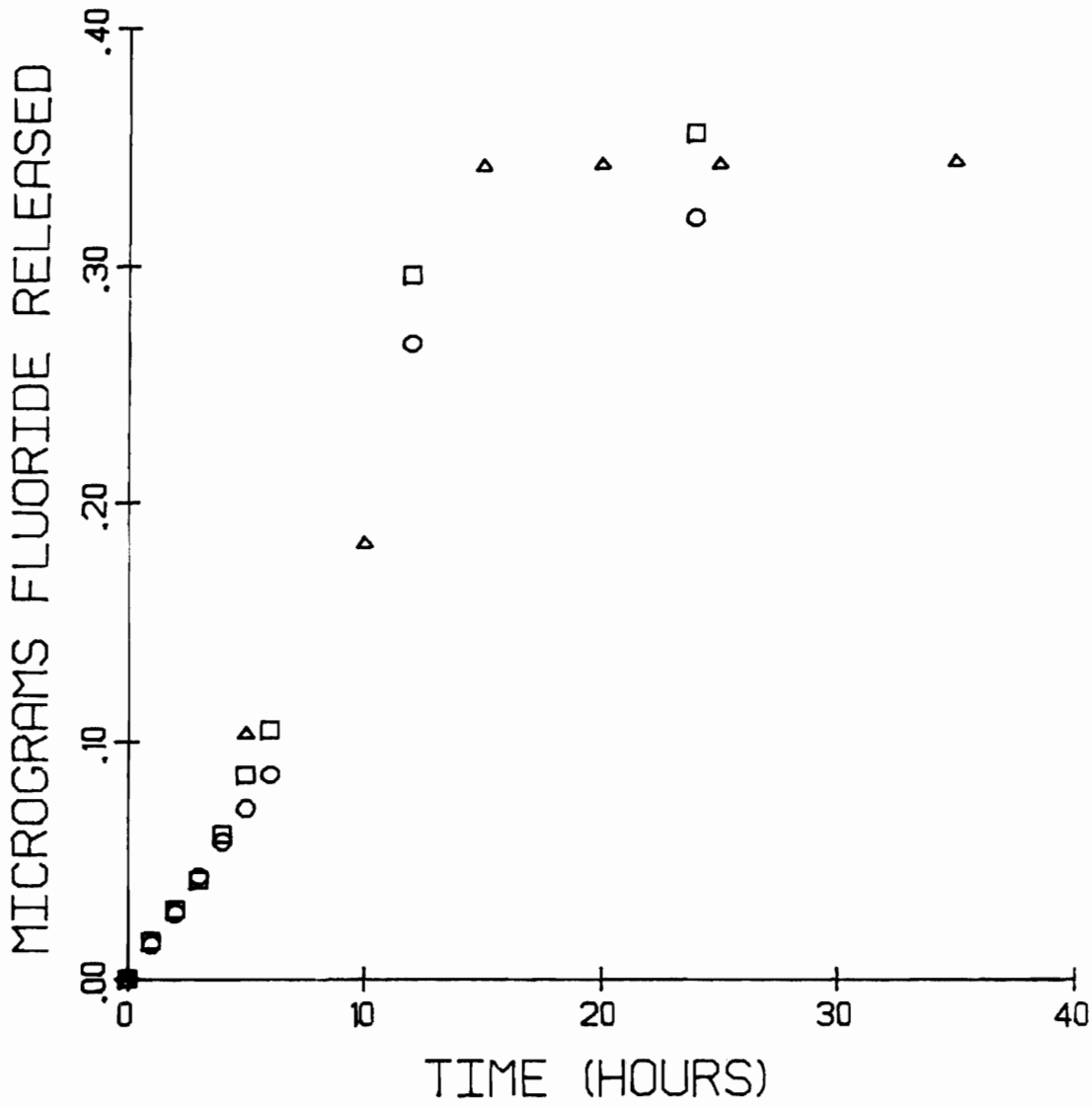

Fig. 5.33. Amount of fluoride released to bulk solution during dissolution of an intact surface layer preformed over 24 hours in a buffer having a pK_{FAP}= 111.93 at 10 rpm.

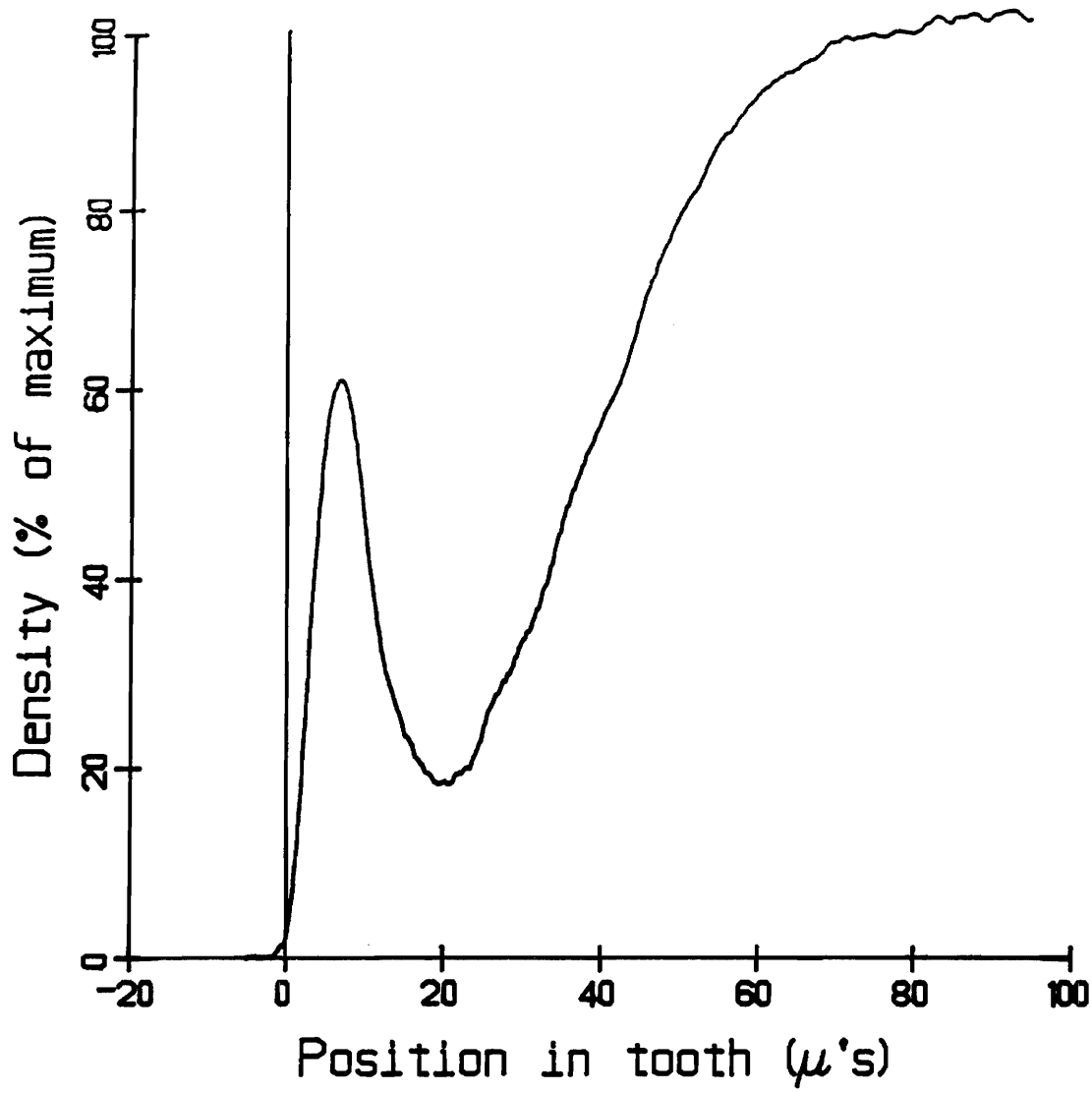

Fig. 5.34. Mineral density profile showing intact surface layer formed over 24 hours in a pK_{FAP}=111.93 buffer solution at 10 rpm.

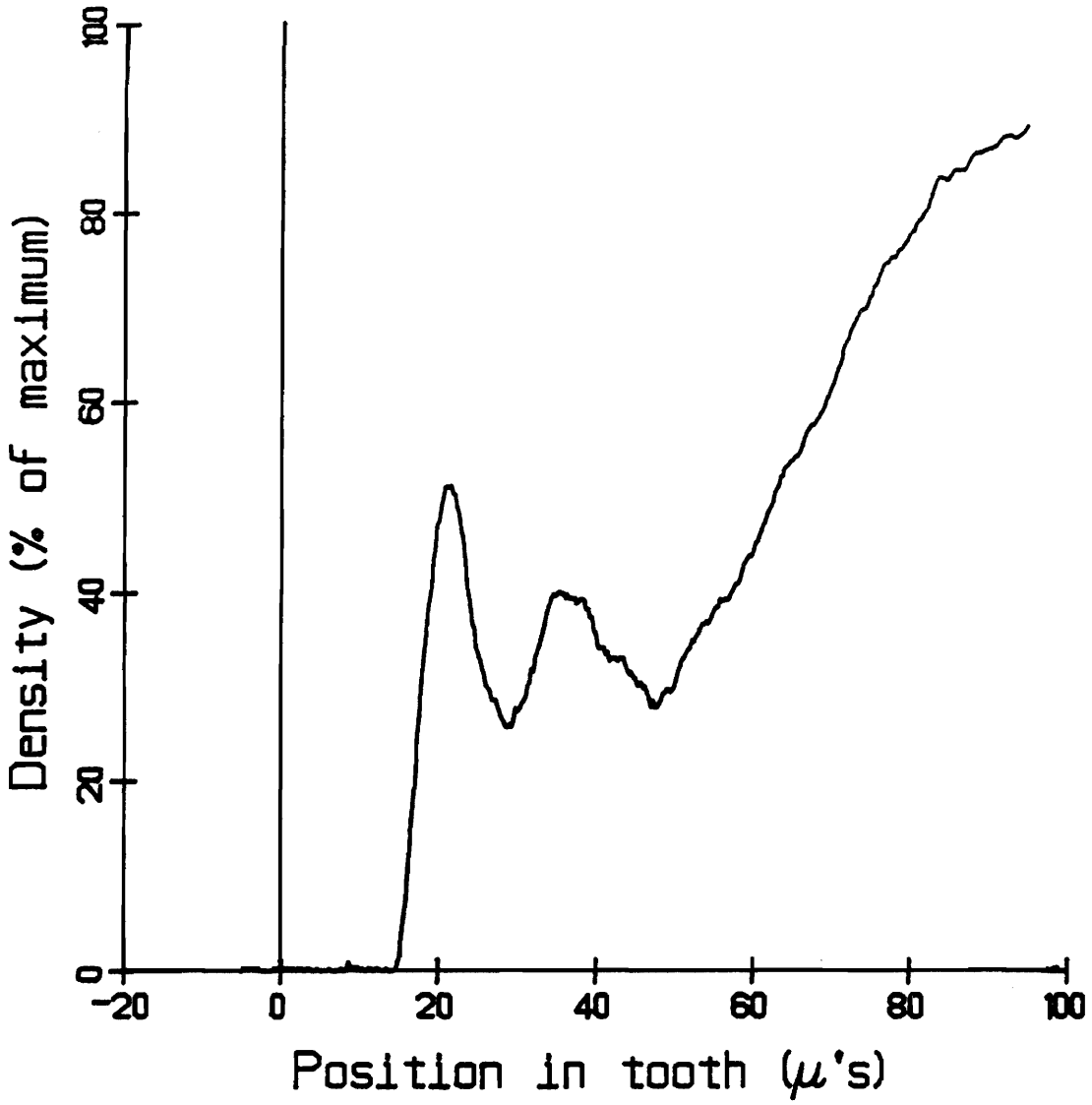

Fig. 5.35. Mineral density profile depicting the surface recession evident after 24 hours of dissolution of a preformed intact surface layer in a bulk solution having a pK_{HAP}= 120.0.

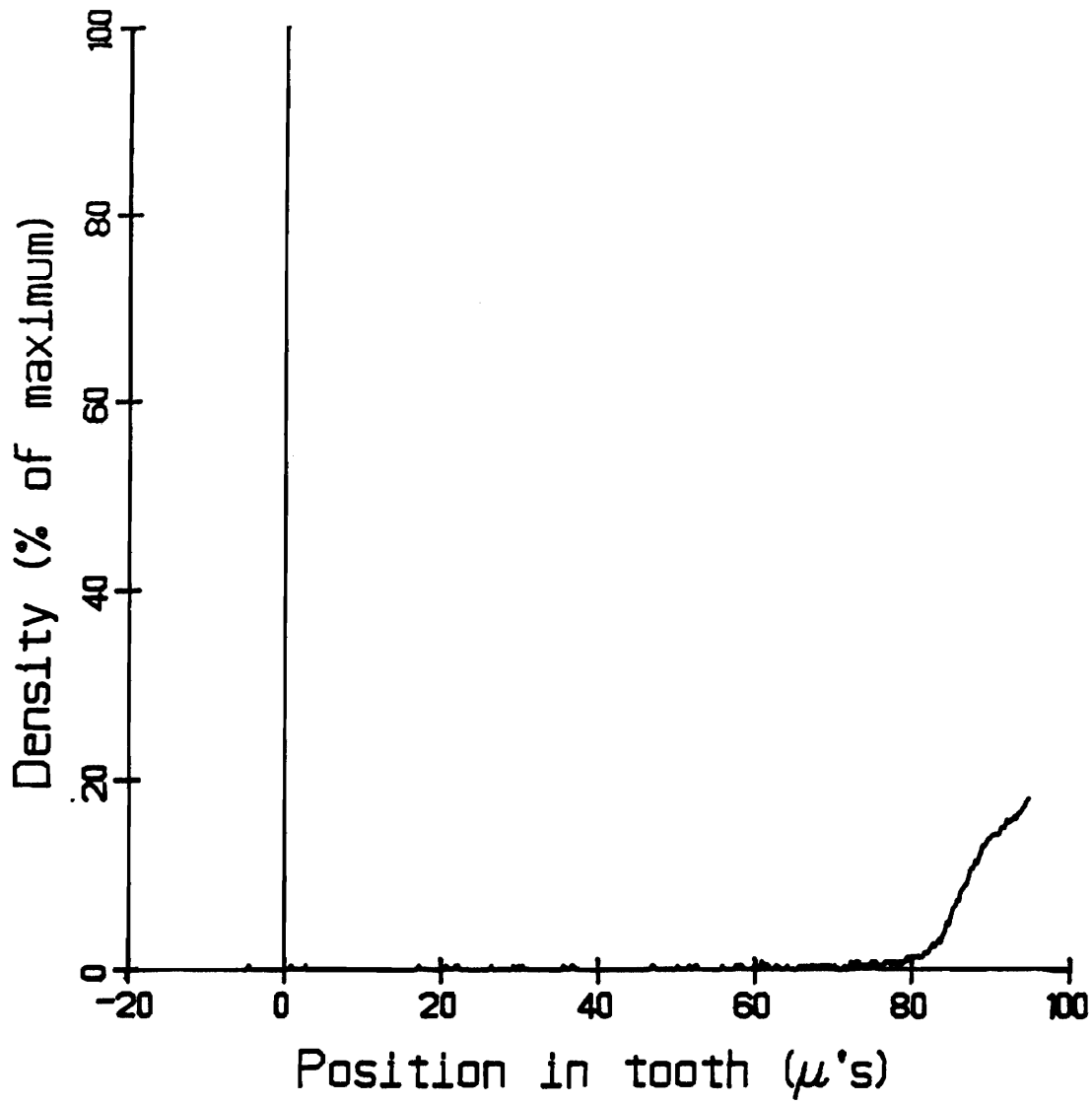

Fig. 5.36. Mineral density profile depicting the surface recession evident after 48 hours of dissolution of a preformed intact surface layer in a bulk solution having a pK_{HAP}= 120.0

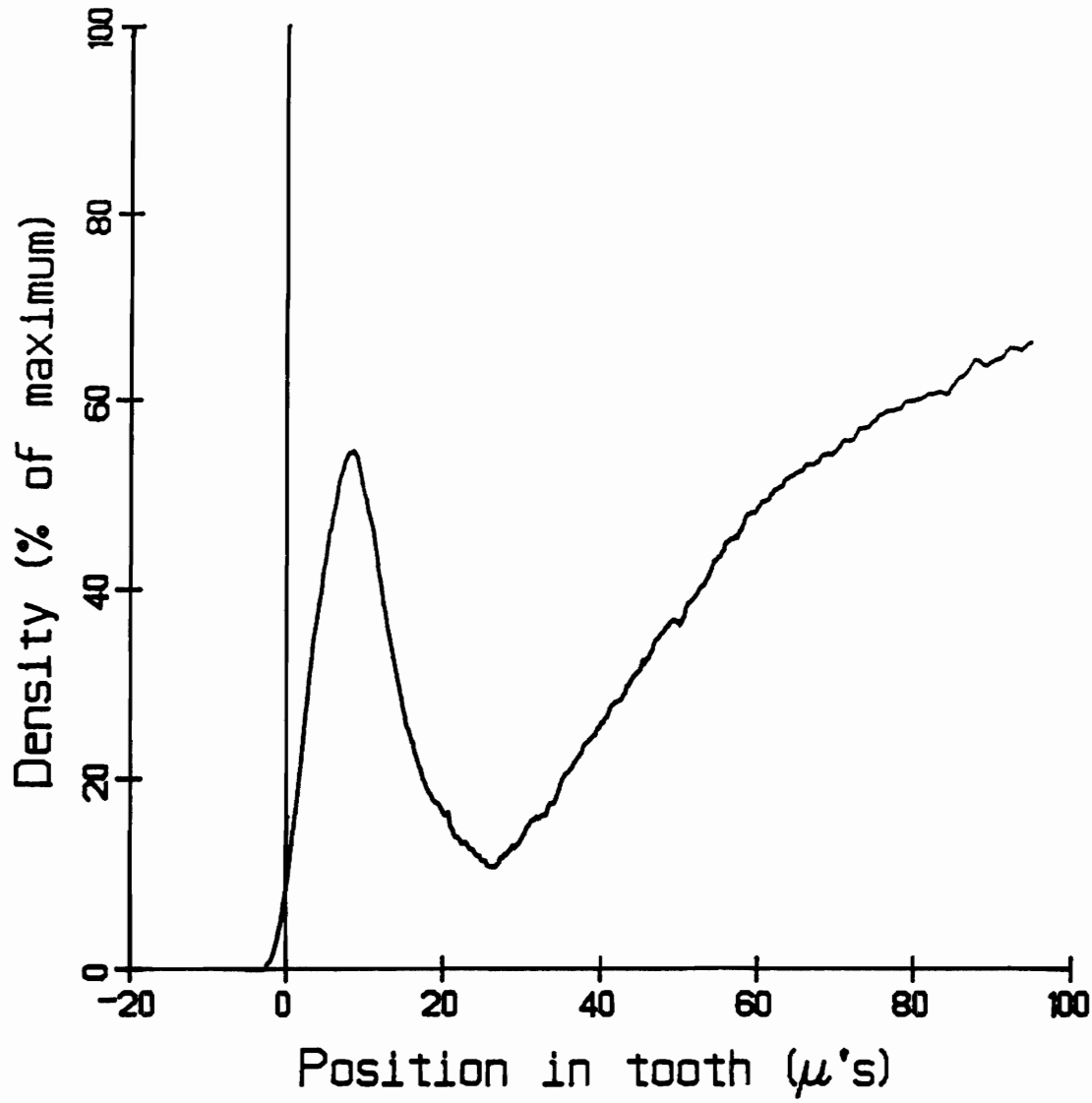

Fig. 5.37. Mineral density profile depicting preservation of the intact surface layer after 48 hours of dissolution of a preformed intact surface layer when the bulk solution fluoride was allowed to approach 0.01 ppm.

volume was 10 ml and not replaced during the experiment, resulted in maintenance of a high degree of mineralization at the enamel surface. This is due to the initial release of fluoride elevating the level of bulk fluoride concentration to inhibit dissolution by maintaining the prevailing microenvironmental solution ion product at a sufficiently high value.

The results of a similar experiment performed for a shorter period of time, Figures 5.38 - 5.41 indicate that the intact layer remains stable for at least the first 12 hours of dissolution and then as before; 24 hours of dissolution results in loss of the intact surface layer with resultant surface recession. Solution analysis for fluoride in the 10 ml, 24 hour sample (Figure 5.41) yields a fluoride concentration of nearly 0.01 ppm. A drop of even an order of magnitude across the aqueous boundary layer would still result in the solution immediately adjacent to the enamel surface being saturated with respect to an ion product of $K_{FAP} = 10^{-115}$. The result then is that dissolution of the surface region of the enamel would not occur (Figure 5.41).

The significance of these findings is that they are strong evidence supportive of the hypothesis that it is not the bound fluoride making the surface region inert to acid dissolution that results in intact surface layer formation, but rather it is maintenance of a significant level of fluoride in solution maintaining the microenvironmental solution ion activity product $K_{FAP} = a_{Ca}^{10} \cdot a_{PO_4}^{6} \cdot a_F^2$ at a sufficiently high value.

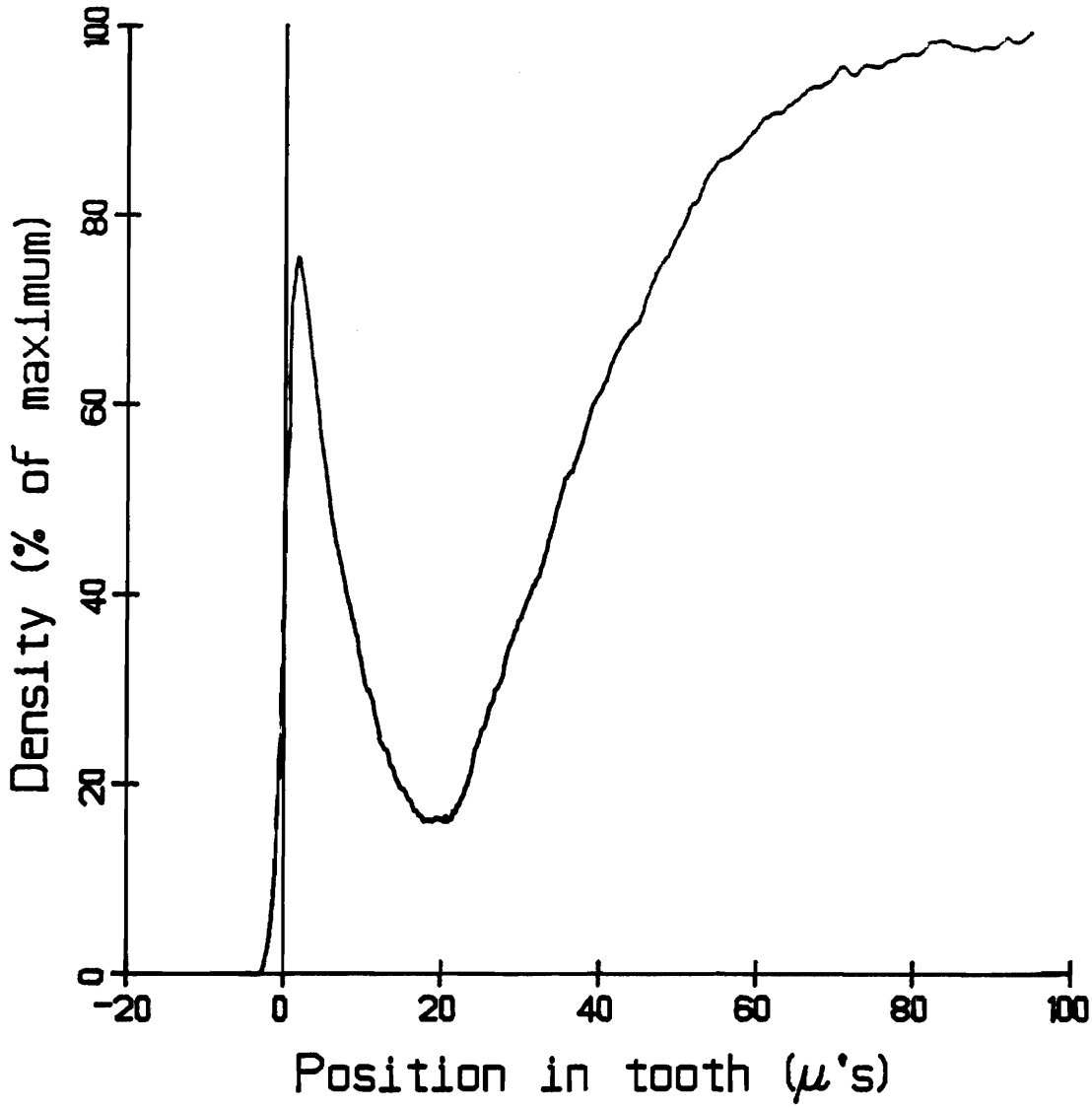

Fig. 5.38. Mineral density profile showing intact surface layer formed over 24 hours in a pK_{FAP}= 111.93 buffer solution at 10 rpm.

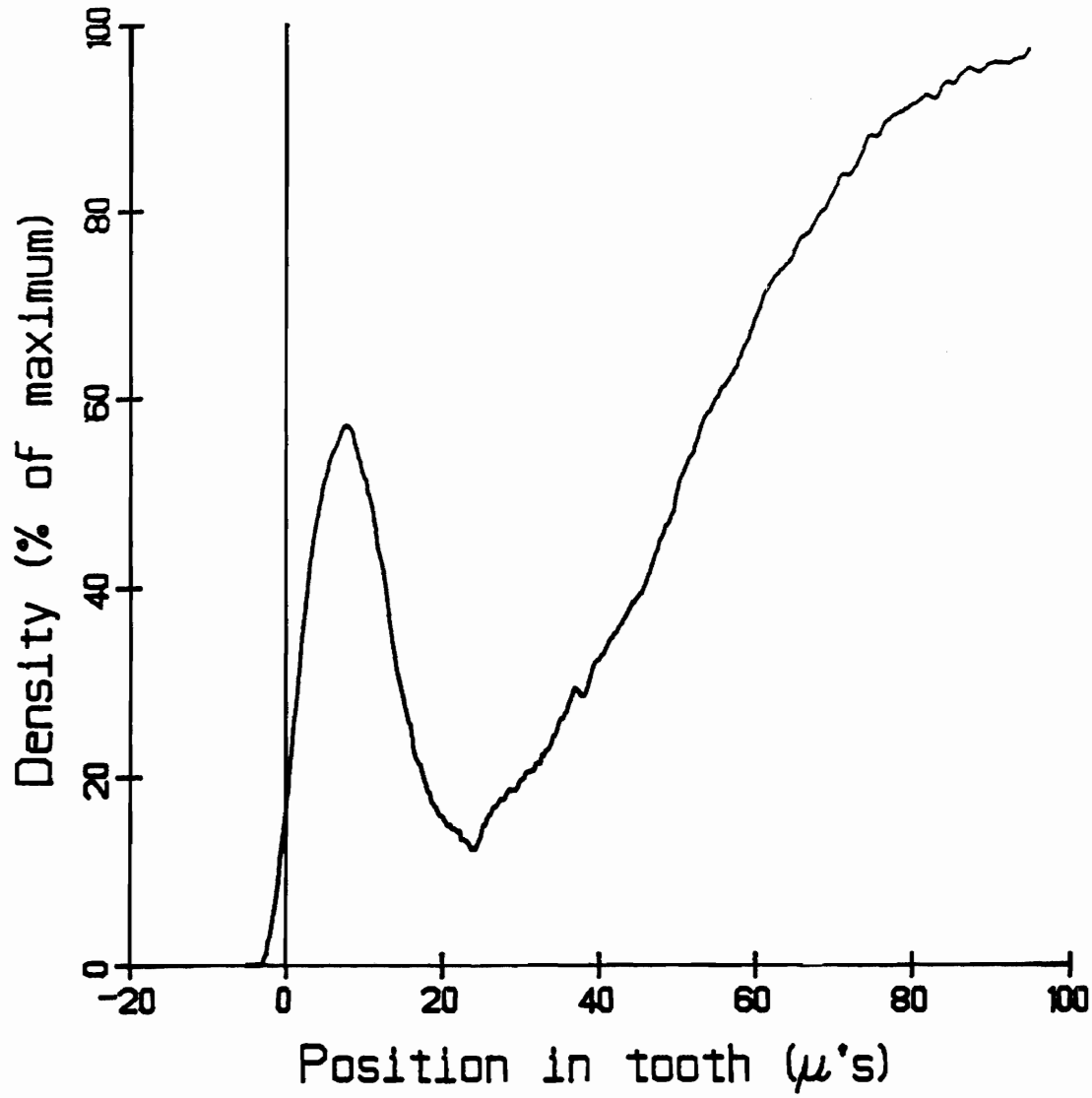

Fig. 5.39. Mineral density profile showing maintenance of intact surface layer after 12 hours of dissolution of a preformed intact surface layer in a bulk solution having a pK_{HAP}= 120.0

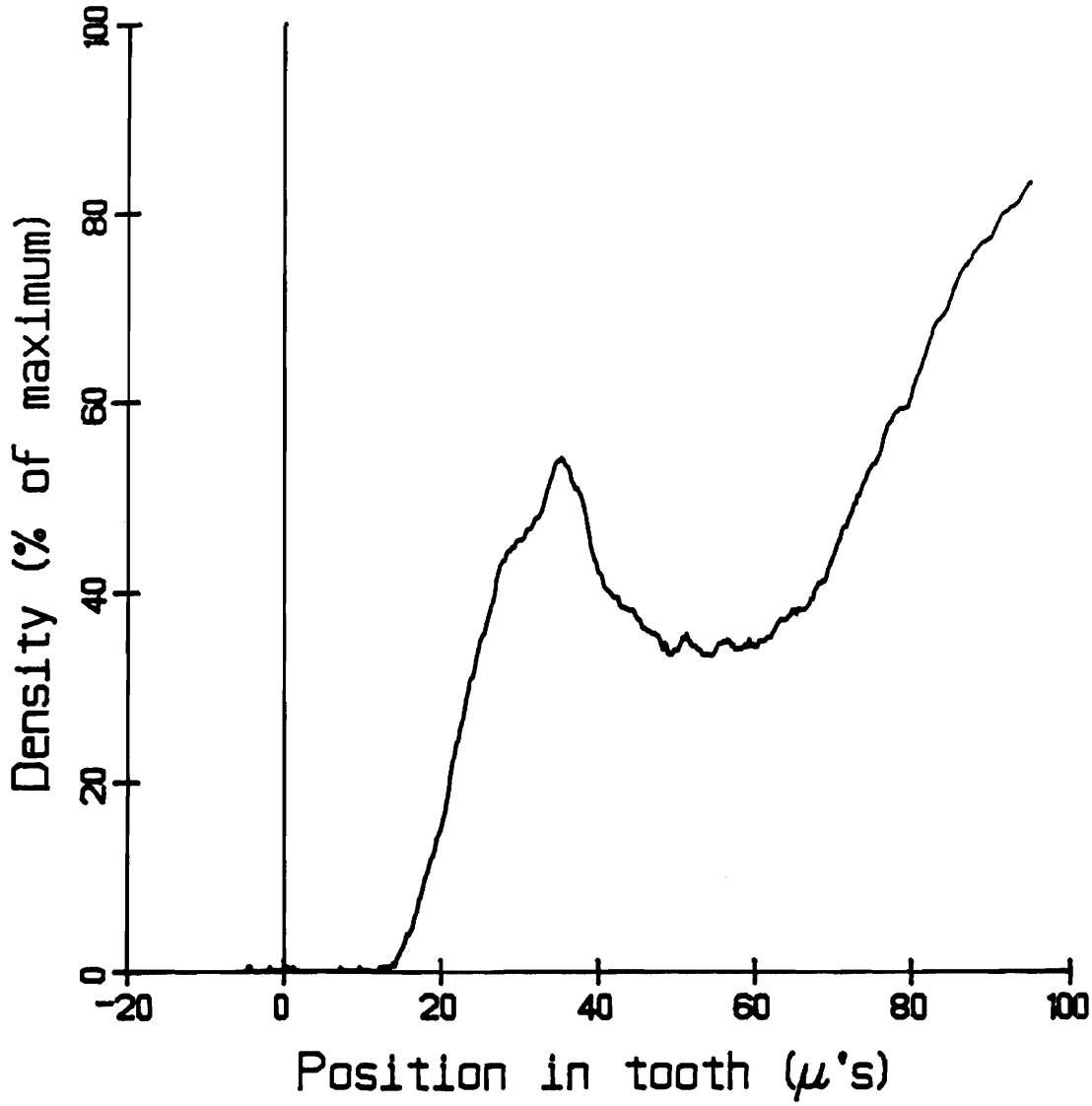

Fig. 5.40. Mineral density profile depicting the surface recession evident after 24 hours of dissolution of a preformed intact surface layer in a bulk solution having a pK_{HAP}= 120.0.

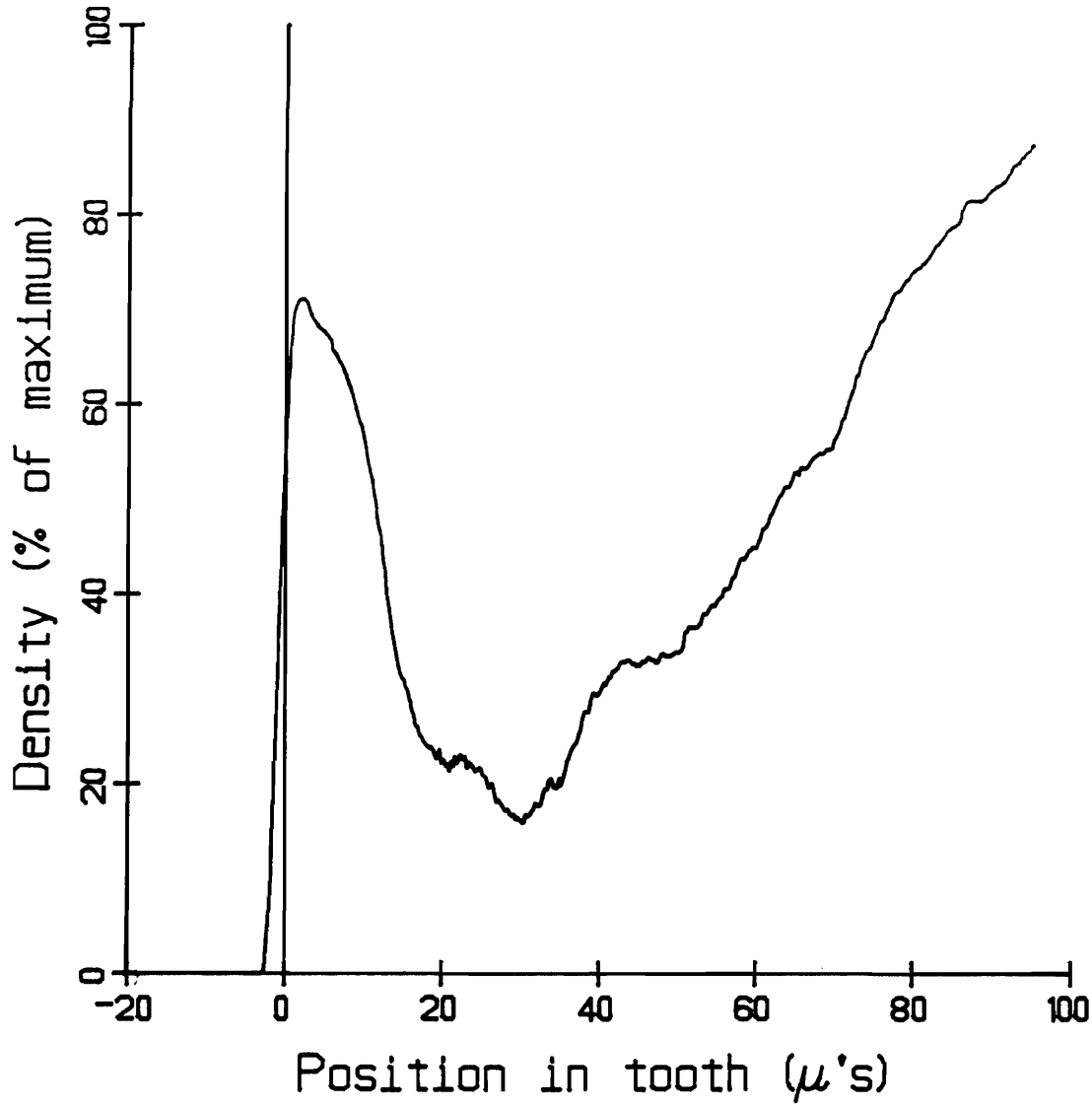

Fig. 5.41. Mineral density profile depicting preservation of the intact surface layer after 24 hours of dissolution of a preformed intact surface layer when the bulk solution fluoride was allowed to approach 0.01 ppm.

CHAPTER 6

MICROENVIRONMENTAL DIFFUSION, CHEMICAL REACTION AND MULTIPLE SOLUTION EQUILIBRIA CALCULATIONS

The development of a physical model describing the behavior of fluoride as it diffuses into the enamel matrix and its interaction with intercrystalline solution calcium and phosphate has led to formulation of a rigorous solution to the appropriate diffusion, reaction and solution equilibria equations (Chapter 4). From these calculations it is possible, considering variable porosity within the enamel, to rigorously determine the activities of the individual species in solution within the enamel matrix and consequently the dissolution governing solution ion activity product, K_{HAP} or K_{FAP}, as a function of position.

It has been determined from independent experimental calculations (Chapter 5) that the apparent solubility or dissolution threshold of bovine enamel in the absence of solution fluoride has a $pK_{HAP} = 117 \pm 0.5$. In the presence of low level solution fluoride the corresponding pK_{FAP} value is 115 ± 1.0. This value for the K_{FAP} is in excellent agreement with the value obtained for the inhibition of dissolution of carbonate-apatite powders in the presence of solution fluoride presented in Figure 5.24 where the dissolution rate tends toward zero as the solution ion activity product approaches a $pK_{FAP} = 115.0$.

In order to test the model parameters determined from experi-

ments, i.e., K_{HAP}, K_d and an assumed value of 3% for the initial porosity, the calculation was carried out and the results are presented in Figures 6.1 - 6.5. Figure 6.1 depicts the initial steady-state solution profile achieved within seconds (< 10 seconds) after exposure to a dissolution media having an ion activity product (K_{HAP}) of 10^{-120} under conditions giving an aqueous boundary layer of 227 micrometers. Also shown is the initial mineral density profile of uniform density with distance. Figures 6.2 - 6.4 are analogous calculations showing the solution concentration profiles and resultant mineral density changes after 3, 6, and 12 hours of dissolution respectively. Apparent from these calculated profiles, as well as from experimental results, is the absence of an intact surface layer (since fluoride was not present in the bulk solution) and also that dissolution of the enamel is occurring that is zonal in nature. Figure 6.5 represents the dissolution for 24 hours situation in which the mineral content has decreased to near zero at the original enamel surface and increases to near 100% at approximately 100 micrometers. It is evident from these calculations that as the mineral density decreases at the surface, there is also a corresponding change in the solution concentration profile. Comparison of Figure 6.5 and Figure 5.1, the actual experimental situation, shows excellent agreement between the theoretical calculation and experimental result. This excellent agreement allows use of the stated parameters with confidence of their being representative of the actual values.

Rigorous solution of the diffusion/reaction equation in the pre-

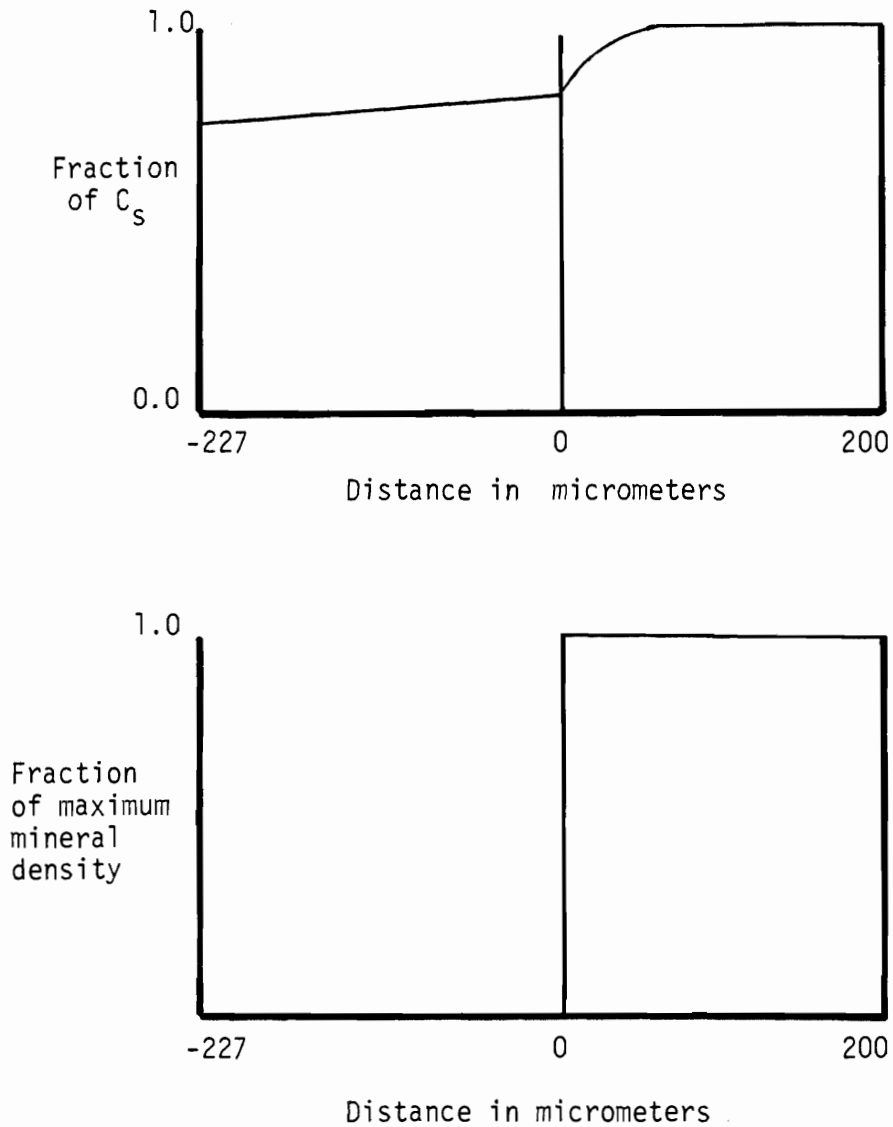

Fig. 6.1. Initial steady-state solution profile and the initial mineral density profile as a function of position for a bulk solution having a pK_{HAP}= 120.0 and h = 227 micrometers.

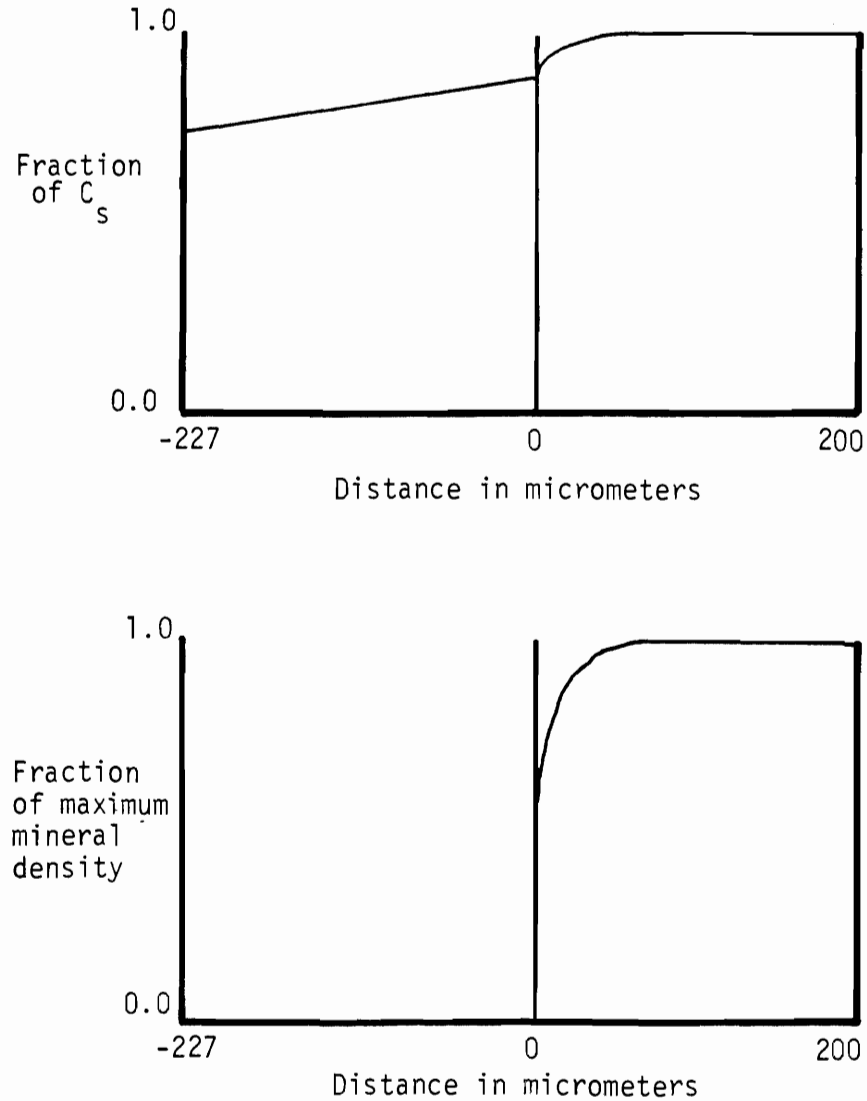

Fig. 6.2. Solution calcium and phosphate profile and the theoretical simulation of the mineral density profile after 3 hours of dissolution in pK_{HAP}= 120.0 buffer where h = 227 micrometers.

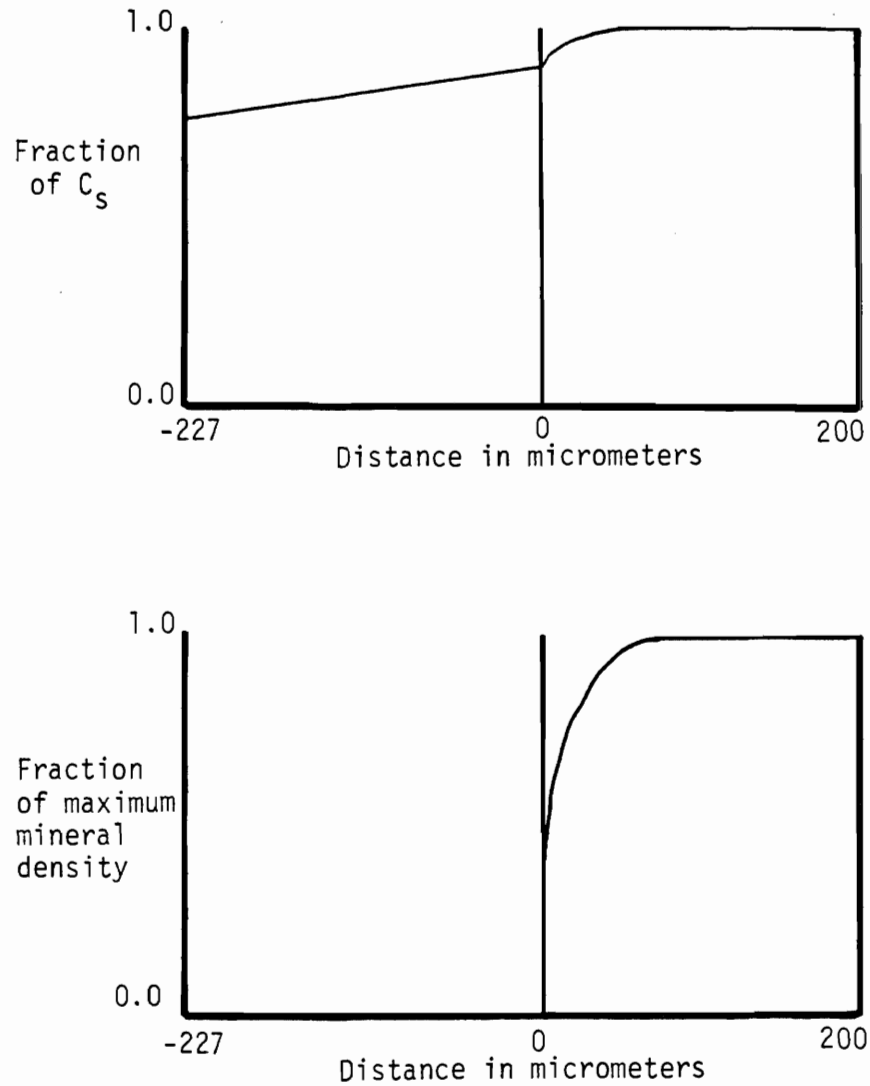

Fig. 6.3. Solution calcium and phosphate profile and the theoretical simulation of the mineral density profile after 6 hours of dissolution in pK_{HAP}= 120.0 buffer where h = 227 micrometers.

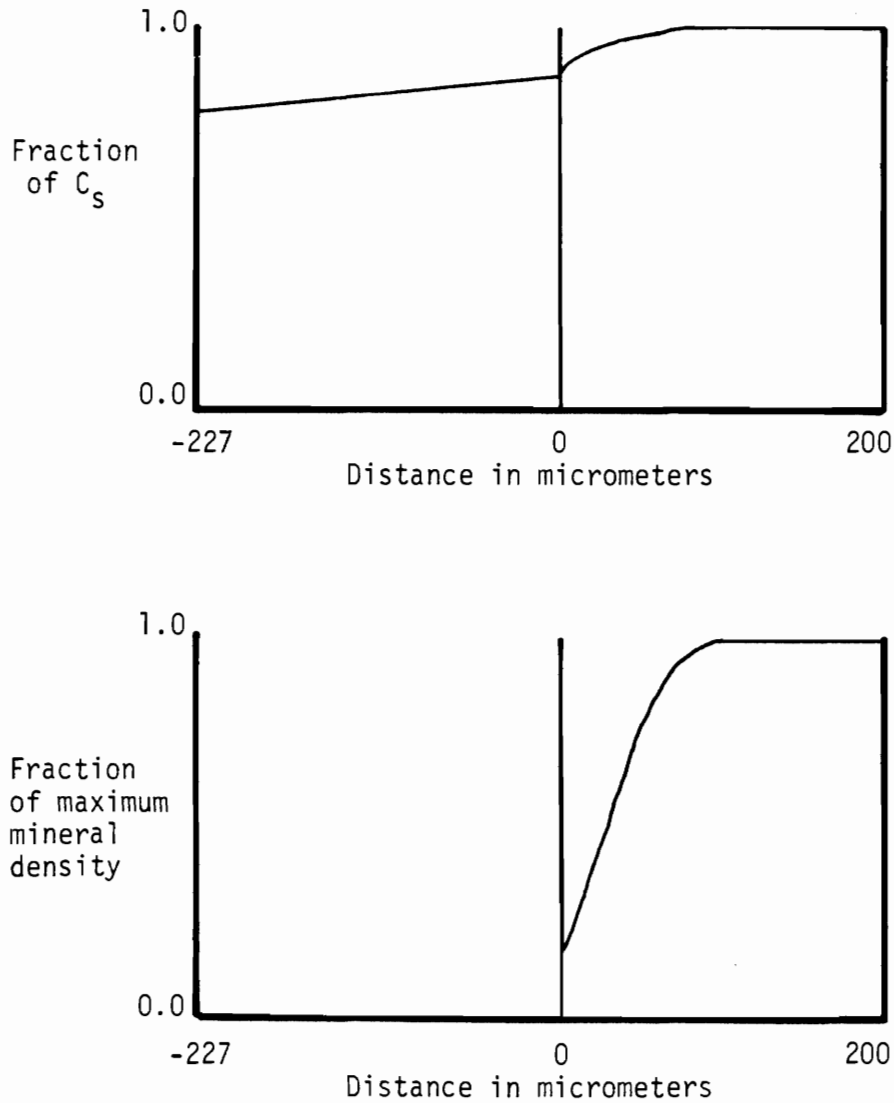

Fig. 6.4. Solution calcium and phosphate profile and the theoretical simulation of the mineral density profile after 12 hours of dissolution in pK_{HAP}= 120.0 buffer where h = 227 micrometers.

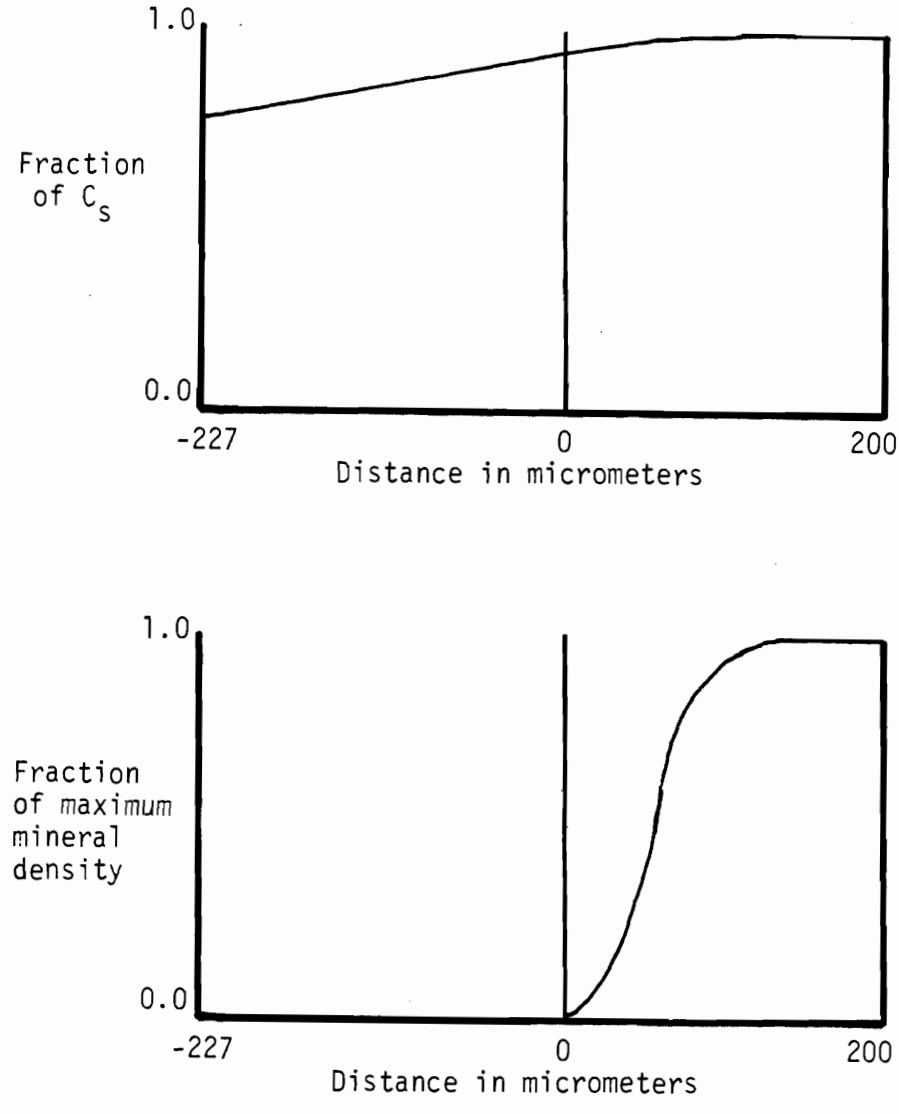

Fig. 6.5. Solution calcium and phosphate profile and the theoretical simulation of the mineral density profile after 24 hours of dissolution in pK_{HAP}= 120.0 buffer where h = 227 micrometers.

sence of solution fluoride has been found to become unacceptably slow when the surface crystals become saturated with respect to fluoride adsorption. Presumably, the apparent diffusion coefficient becomes very small as the free fluoride concentration becomes several orders of magnitude less than the total fluoride concentration at the advancing fluoride front. Also, at this point in time the problem becomes one of a moving boundary problem and is not well represented by a finite number of spatially fixed stationary nodes. To overcome this problem an approximate formulation of the problem has been developed that is readily solved.

This analytic solution to the fluoride diffusion equation represents the solution fluoride profile (Figure 4.1) as a linear gradient. The nonlinear region at the advancing fluoride front is not approximated well by the analytic solution; however, calculations indicate that the solution fluoride concentrations in this nonlinear region have no significant effect on the mineral density profiles subsequently obtained.

Using the rigorous solution to the fluoride diffusion/adsorption equation, the solution fluoride concentration in this advancing nonlinear region is calculated. Figure 6.6 depicts the rigorous concentration profile as a function of position for a wide range of bulk solution fluoride concentrations and hydrodynamic conditions. The hydrodynamic conditions were chosen to evaluate the effect of the developing intact layer on the diffusional parameters determining the physical characteristics of the advancing nonlinear region. It can be

stated, with a reasonable degree of certainty, since the shape of the fluoride front and its sharp decrease is a function of the ability of hydroxyapatite to adsorb fluoride, it is expected that this rapid decrease in concentration persists at the advancing front for all time, much as it does in every single example rigorously examined (Fig. 6.6). It is evident from Figure 6.6 that the solution fluoride concentration decreases very rapidly within the advancing few micrometers of this nonlinear region. Most importantly, the concentration drops to approximately $10^{-9.5}$ molar in less than 5 micrometers, this being the value at which K_{HAP} would become the dissolution governing function. This 5 micron region at the advancing fluoride front represents the only uncertainty in the approximating solution to the fluoride diffusion equation. This region of uncertainty would, in fact, decrease with experimental time as the analytic solution better approximates the rigorous solution at longer time.

Under conditions known to give an intact surface layer there is a significant degree of mineralization at the enamel surface and throughout the intact layer; therefore the microenvironmental solution calcium and phosphate concentrations will be well represented by considering the intact layer to represent an additional diffusional barrier, the magnitude of which is calculated from intact surface layer thickness, porosity and diffusivity, the effect of which on the calcium and phosphate concentration profiles can be calculated as a function of time and thickness of the intact surface layer. Combining this quasi-steady-state profile with the calculated solution fluoride

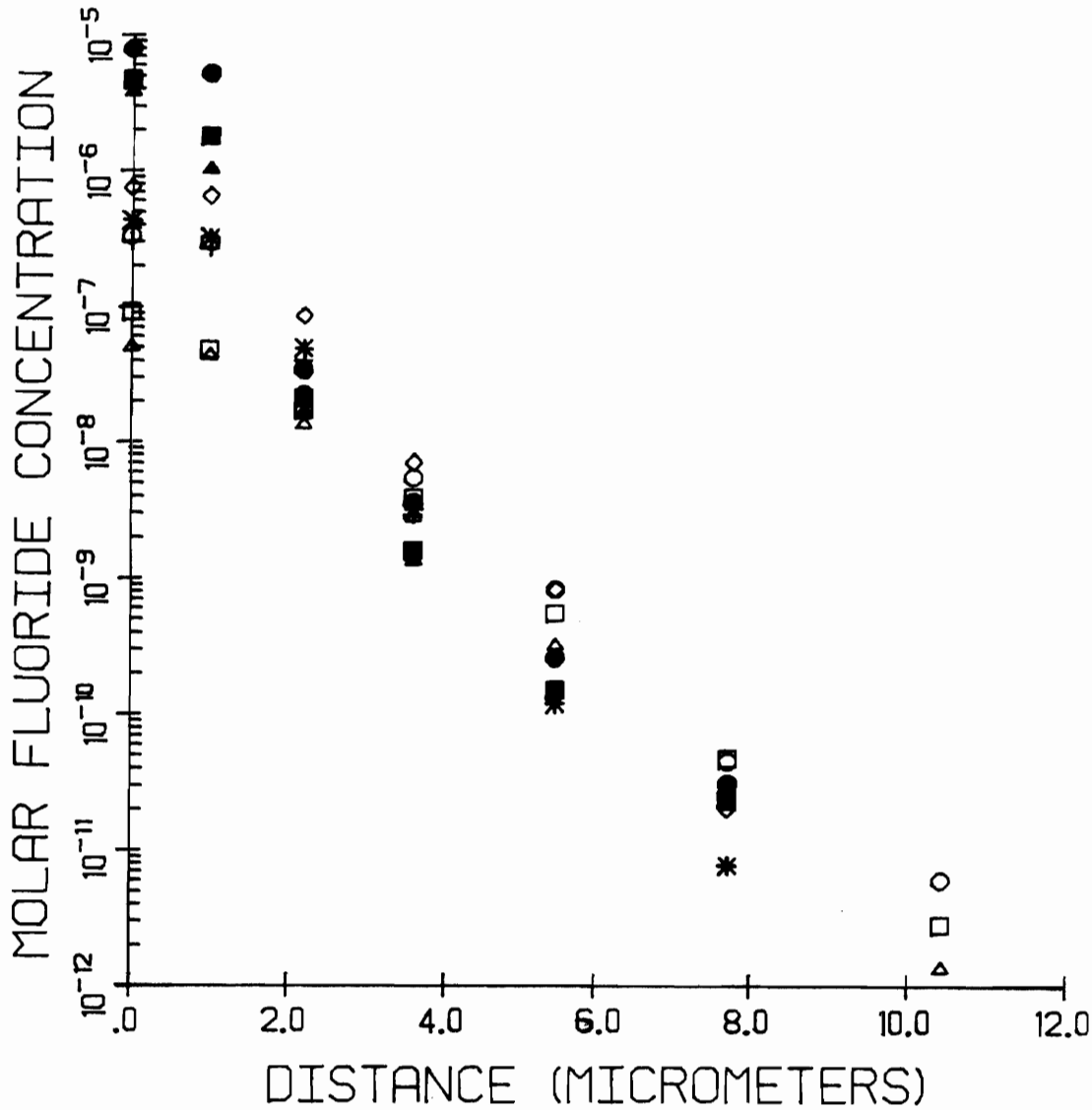

Fig. 6.6. Solution fluoride concentration in the nonlinear region of the rigorous solution to the fluoride diffusion equation for a range of bulk solution fluoride concentrations and effective aqueous boundary layer thicknesses; 0.01 ppm F: ○ h=32 , □ h=227 , △ h=277 ; 0.1 ppm F: ◇ h=32 , ✱ h=227 , x h=277 ; 0.5 ppm F: ● h=32 , ■ h=227 , ▲ h=277 micrometers.

profiles, it becomes possible to calculate, considering the multiple solution chemical equilibria, the prevailing microenvironmental solution ion activity product as a function of both time and position within the enamel matrix for different bulk solution chemistries and hydrodynamic conditions. In all cases presented, conditions known to result in intact surface layer formation with preservation of the original enamel surface, saturation or supersaturation with respect to the pK_{FAP} value of 115 ± 1 exists in the surface region and is maintained a distance in the enamel before rapidly becoming unsaturated as the solution fluoride levels fall to zero at sufficient depth. At each point in time, when the microenvironmental solution conditions are saturated with respect to a $pK_{FAP} = 115$, inhibition of dissolution would occur as predicted by previous bovine enamel kinetic and carbonate-apatite powder data presented in Chapter 5; at the same time and sufficient depth, as predicted by the quasi-steady-state solution profile for the calcium and phosphate concentrations, dissolution would be occurring at an interior position.

In order to determine the maximal effect that neglecting the advancing nonlinear region would have on the resultant calculated mineral density profiles, the calculations were performed with an initial condition of a 2.5 and 5.0 micrometer nonreactive zone at the advancing fluoride front. Figure 6.7 is the theoretical simulation of the mineral density changes that occur with time using the approximating solution to represent the advancing fluoride front where the bulk solution had a $pK_{FAP} = 111.93$ and the effective aqueous boundary layer

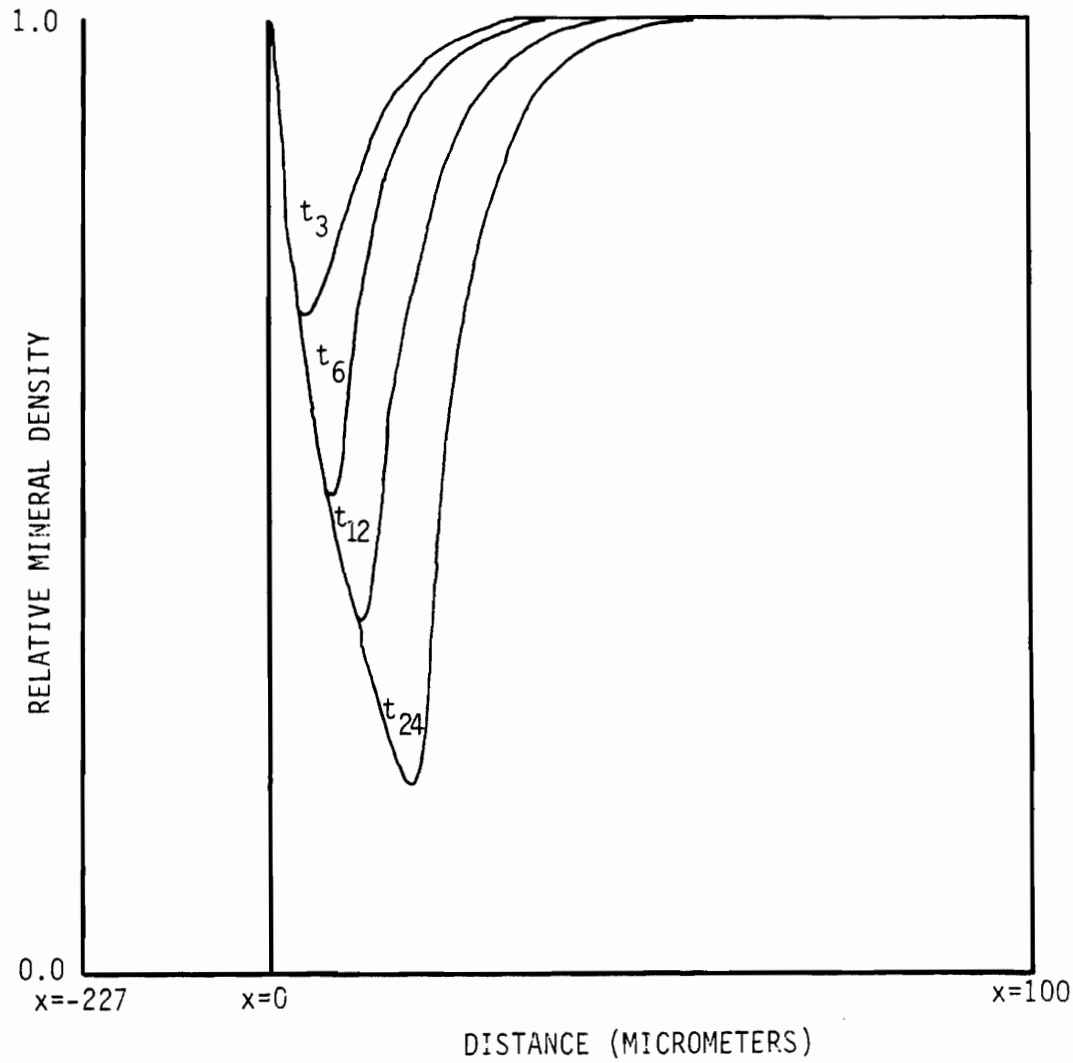

Fig. 6.7. Theoretical simulation of subsurface dissolution for 3, 6, 12 and 24 hours at 10 rpm, 3% initial porosity and bulk solution pK_{FAP}= 111.93.

was 227 micrometers. In comparing this theoretical simulation with the analogous experimental situation (Figure 5.43), it is seen that there is good agreement between the two cases. The mineral density profiles calculated by the approximating function for fluoride diffusion predict 100% mineral density at the enamel surface. It is observed experimentally that surface dissolution occurs to a limited extent before fluoride inhibition of the surface enamel dissolution rate occurs. This shortcoming of the approximating function is recognized, however, no serious influence on the conclusions result. Figures 6.8 and 6.9 are the simulated mineral density profiles obtained when the initial conditions were chosen to give a 2.5 and 5.0 micrometer nonreactive zone at the advancing fluoride front. Comparison of these two cases with experiment and Figure 6.7 where the simulation did not include this nonreactive zone indicates that the effect on the simulated mineral density profiles of this nonlinear region in the rigorous solution fluoride concentration solution is, at most, minimal and may therefore be neglected without seriously distorting the theoretical simulation of the mineral density profiles.

The initial porosity used in these simulations is 3%. In order to determine the appropriateness of this value, simulations at 1% and 10% initial porosity were performed, Figures 6.10 and 6.11. The effect seen is principally upon the dissolution component. Since excellent agreement was seen between experimental and simulation using 3% initial porosity and based on these mineral density profiles, it is concluded that the choice of 3% initial porosity is reasonable and

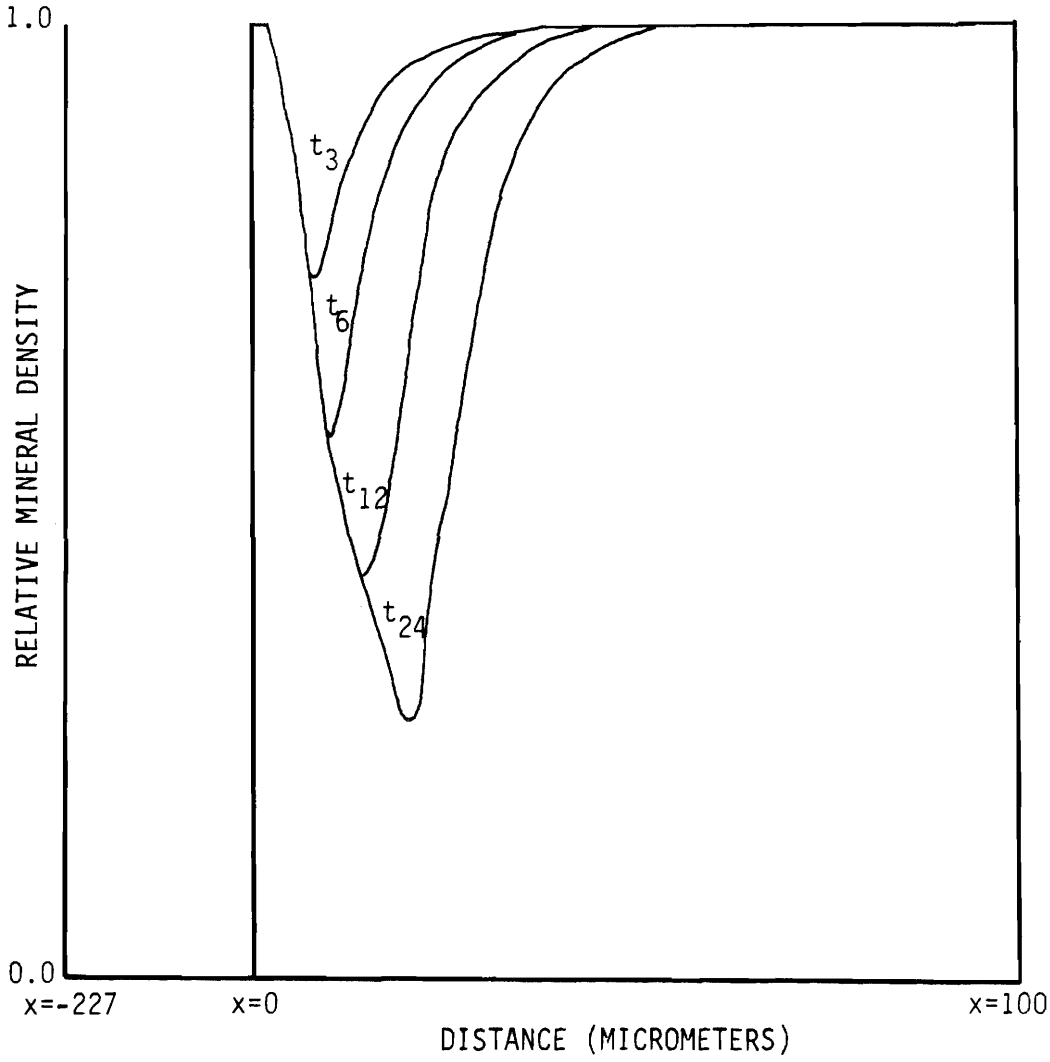

Fig. 6.8. Theoretical simulation of subsurface dissolution with the initial condition of a nonreactive zone of 2.5 micrometers for 3, 6, 12 and 24 hours at 10 rpm, 3% initial porosity and bulk solution pK_{FAP}= 111.93.

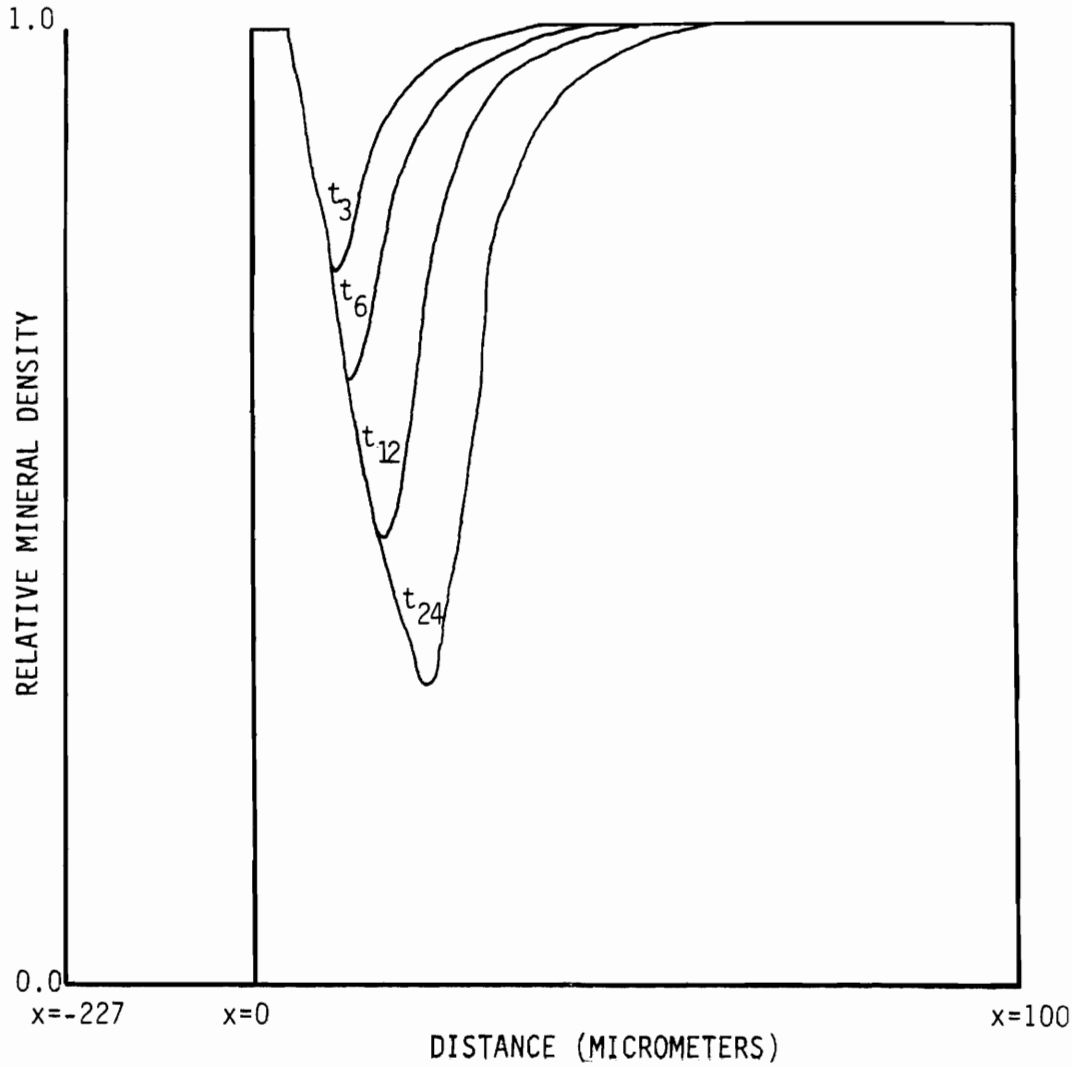

Fig. 6.9. Theoretical simulation of subsurface dissolution with the initial condition of a nonreactive zone of 5.0 micrometers for 3, 6, 12 and 24 hours at 10 rpm, 3% initial porosity and bulk solution pK_{FAP}= 111.93.

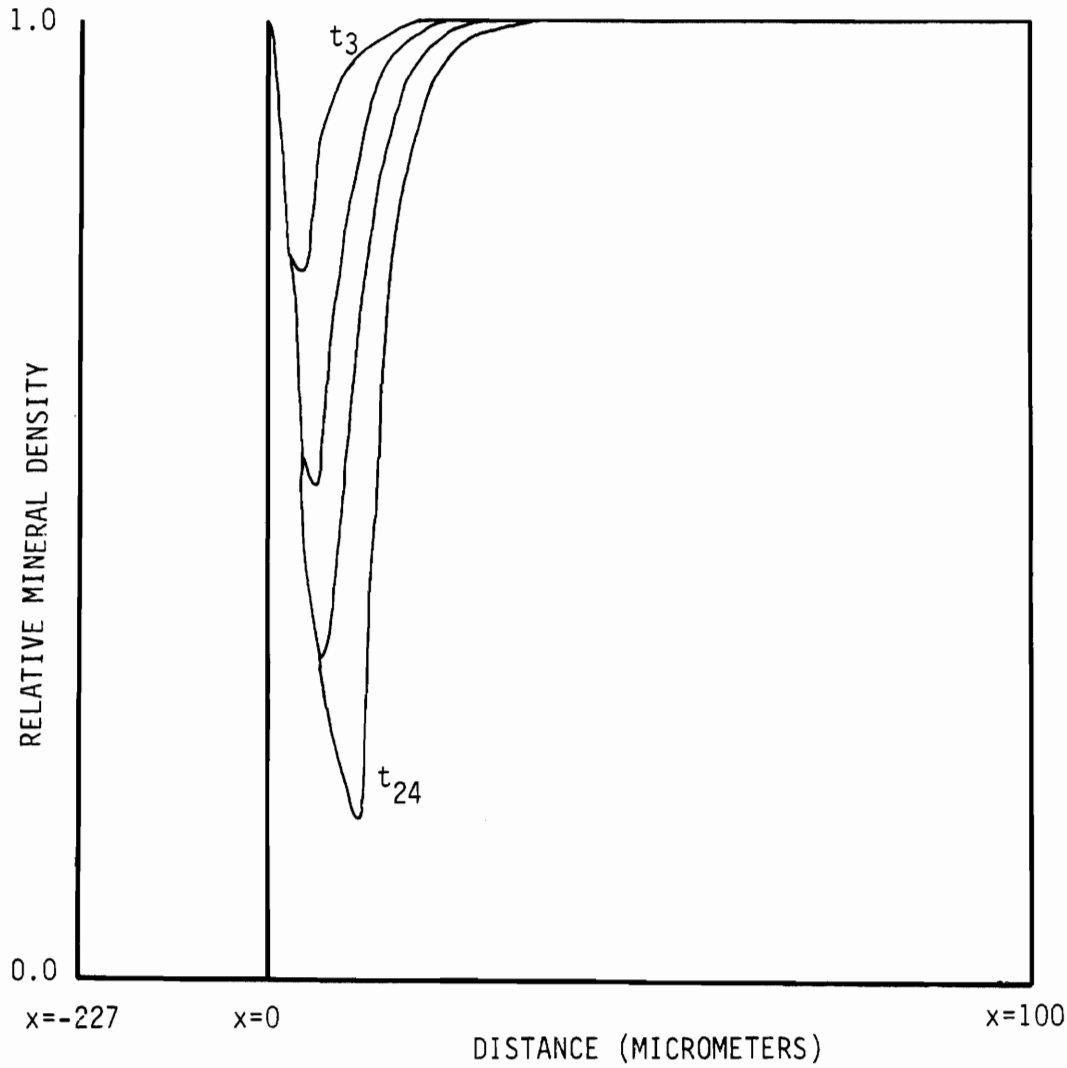

Fig. 6.10. Theoretical simulation of subsurface dissolution for 3, 6, 12 and 24 hours at 10 rpm, 1% initial porosity and bulk solution pK_{FAP}= 111.93.

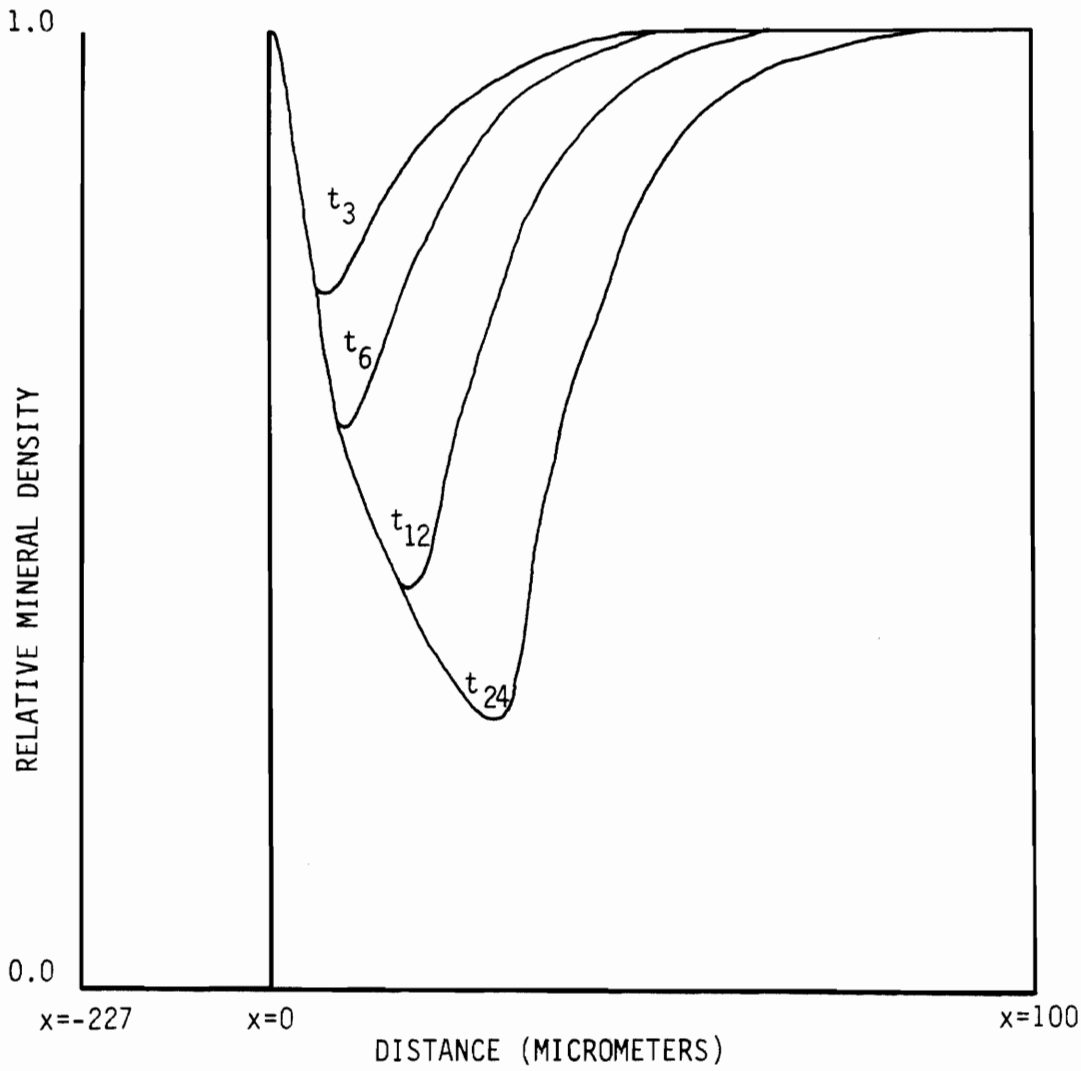

Fig. 6.11. Theoretical simulation of subsurface dissolution for 3, 6, 12 and 24 hours at 10 rpm, 10% initial porosity and bulk solution pK_{FAP} = 111.93.

more appropriate than 1% and certainly 10%.

In order to further evaluate the generality of the proposed model, theoretical simulations were performed for additional bulk solution chemistries and hydrodynamics and then compared with analogous experimental results.

Figures 6.12 and 6.13 represent the mineral density profiles for the thick and thin aqueous boundary layer situations generated by the computer simulation. Figures 5.25 - 5.28 and 5.29 - 5.32 depict the mineral density profiles obtained experimentally under identical conditions as those used to generate the theoretical profiles of Figures 6.12 and 6.13. Comparison of these 4 sets of data indicate that in general there is reasonably good agreement between theory and experiment. Interestingly, even perhaps suprisingly, these results show both experimentally and theoretically, an unexpectedly small effect of the aqueous boundary layer thickness on the resultant mineral density profiles as a function of time. In the absence of solution fluoride and an intact surface layer, it would be expected that there would be more than a 7-fold increase in the dissolution rate when the aqueous boundary layer is decreased from 227 micrometers to 32 micrometers. Table 5.5 depicts the amount of mineral dissolved as a function of time for the experimental situation as determined by integration of the corresponding mineral density profiles. The data indicate that the enamel dissolution rate is relatively insensitive to the hydrodynamics of the system under these conditions. In order to examine this lack of, or modest, effect of agitation on the dissolu-

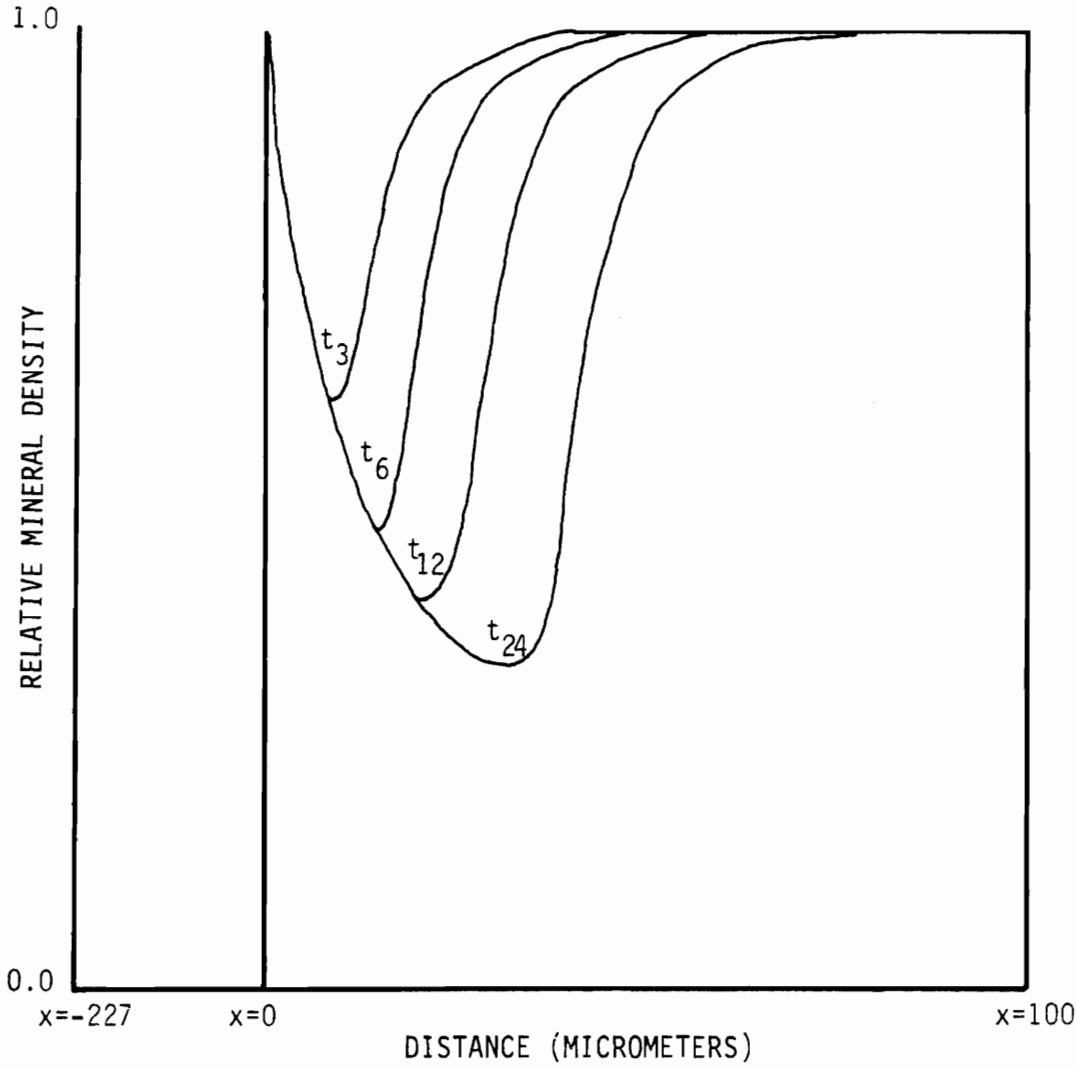

Fig. 6.12. Theoretical simulation of subsurface dissolution for 3, 6, 12 and 24 hours at 10 rpm, 3% initial porosity and bulk solution pK_{FAP}= 114.53.

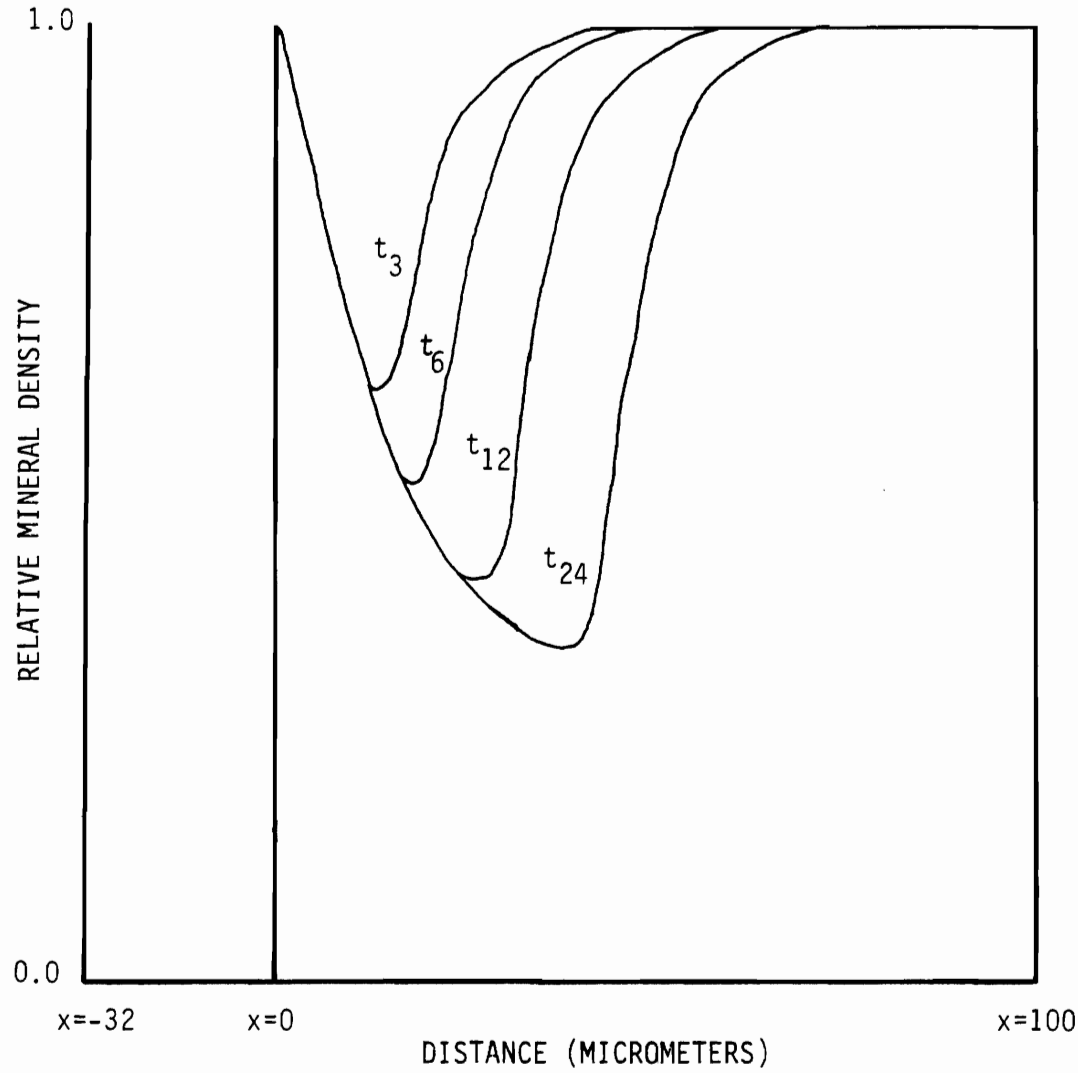

Fig. 6.13. Theoretical simulation of subsurface dissolution for 3, 6, 12 and 24 hours at 500 rpm, 3% initial porosity and bulk solution pK_{FAP}= 114.53.

tion rate, further theoretical calculations were performed. The corresponding theoretical model calculated values of the dissolution rate are presented in Table 6.1. The lack of sensitivity of the dissolution rate to changes in aqueous boundary layer thickness is clearly shown in Tables 5.5 and 6.1, for the experimental and theoretical cases respectively. It is apparent that for both the experimental and theoretical cases the results are far from the expected 7-fold increase in dissolution rate when the aqueous boundary layer is decreased from 227 micrometers to 32 micrometers.

The following discussion examines more closely the results presented in Figures 5.25 - 5.32 and the lack of stirring dependence on the demineralizaion behavior of bovine enamel under these experimental conditions. There are two opposing influences that govern the dissolution behavior when surface solution fluoride is maintaining the intact surface layer. These are one, the surface solution fluoride concentration itself and two, the surface solution pK_{HAP}. The influence of an increased stirring rate is to simultaneously increase the surface solution fluoride concentration and decrease the surface ion activity product (K_{HAP}). Therefore, under the conditions of the present experiments the two effects tend to cancel each other giving rise to a lack of stirring dependence in the overall demineralization behavior.

Figure 6.14 presents the approximate model calculated solution fluoride concentration profiles within the enamel. The data represent the profiles obtained for 4 cases of different bulk solution fluoride

TABLE 6.1

EFFECT OF VARIED AQUEOUS BOUNDARY LAYER THICKNESS ON THEORETICAL CALCULATED AMOUNT DISSOLVED VERSUS TIME

Dissolution time (hours)	Equivalent Micrometers of Enamel Dissolved (h = 227 micrometers)	Equivalent Micrometers of Enamel Dissolved (h = 32 micrometers)
3	5.0	6.2
6	8.7	9.1
12	14.2	15.1
24	22.9	23.1

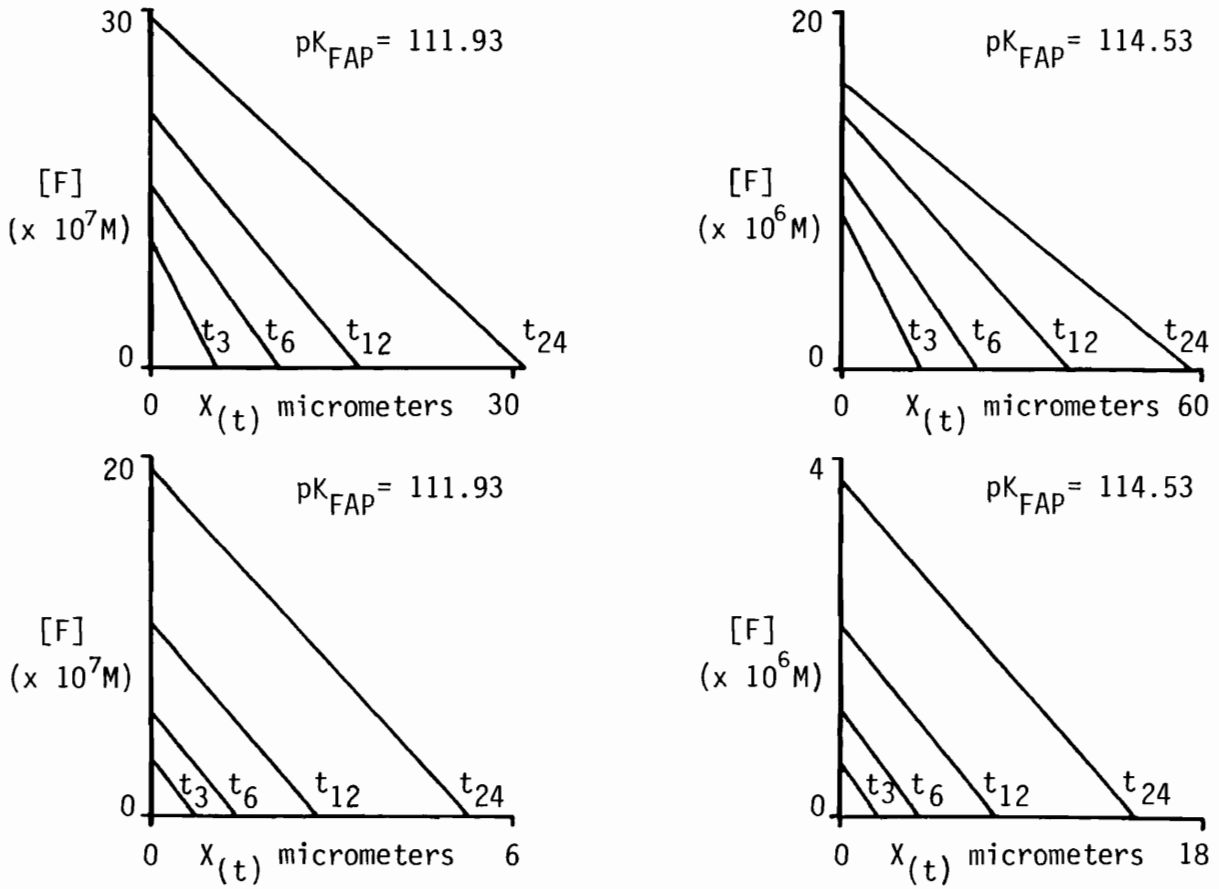

Figure 6.14. Hydrodynamic influence on the calculated solution fluoride concentration profiles as a function of time (hours) for bulk solution $pK_{FAP's}$ = 111.93 and 114.53.

concentrations and hydrodynamic conditions as a function of time. For the given bulk solution fluoride concentrations, there is a clear hydrodynamic influence on the surface fluoride concentration. In fact, for a given time, decreasing the aqueous boundary layer from 227 micrometers to 32 micrometers results in increasing the surface fluoride concentration by a factor of 5 or 6. Totally independent of these theoretically calculated solution fluoride concentration profiles are the experimentally determined fluoride uptake data presented in Figures 5.8 and 5.9. From these experimental data, and together with the theoretical calculations of Figure 6.14 at $x = 0$, the corresponding fluoride uptake fluxes may be plotted as a function of time (Figure 6.15). The results presented in Figure 6.15 indicate relatively good agreement between the calculated and experimentally determined fluoride uptake flux values. This good agreement suggests that use of the approximate fluoride function (equation 4.11) to calculate the fluoride profiles of Figure 6.14 is quite valid, as demonstrated by comparison of theory and experiment in Figure 6.15.

The lack of a stirring dependence on the dissolution rate of bovine enamel in the presence of fluoride observed in these studies is most appropriately considered in terms of the prevailing surface solution ion activity product. Table 6.2 summarizes the calculated surface solution ion activity products (K_{HAP} and K_{FAP}) for two different bulk solution and hydrodynamic conditions as a function of time. It can be seen that a thicker aqueous boundary layer serves to increase the surface K_{HAP} values. The effect of stirring observed for

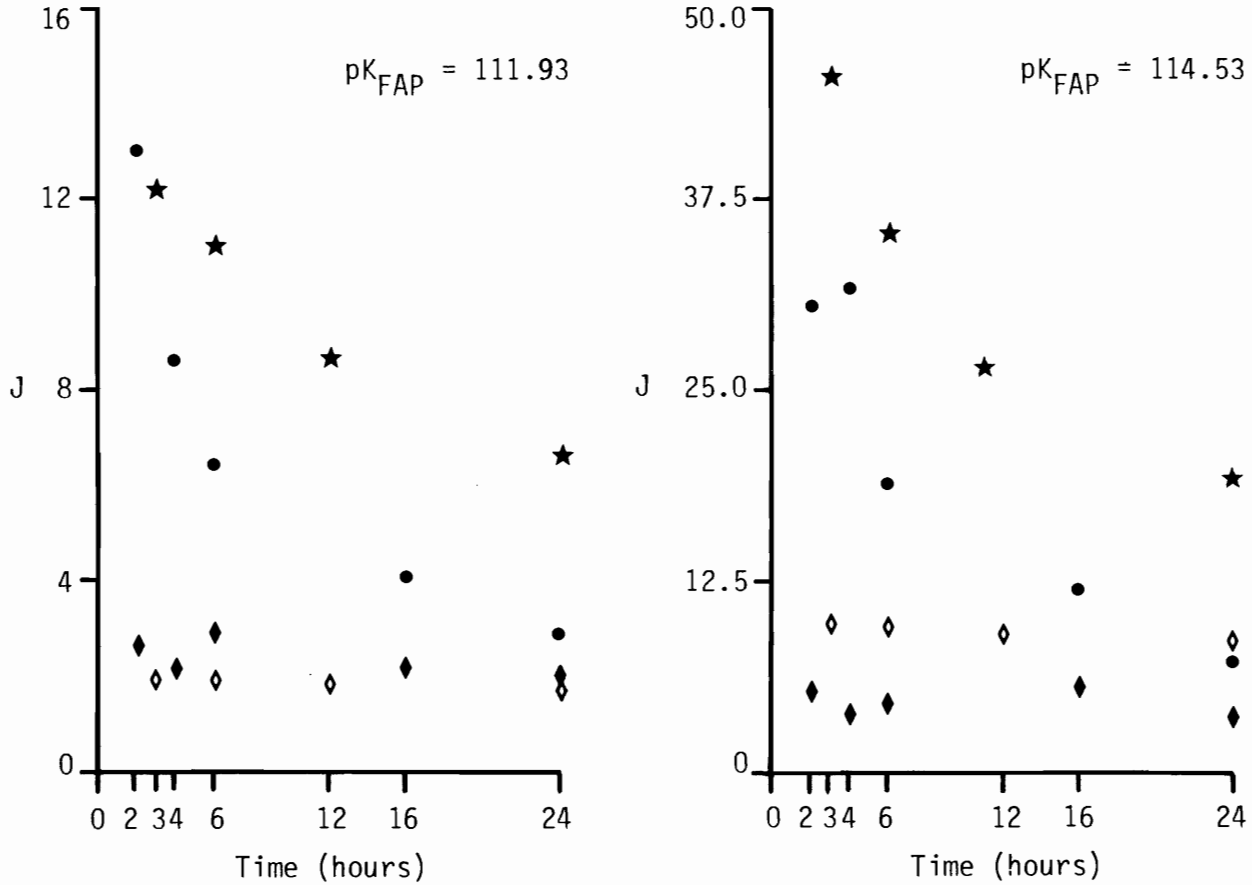

Fig. 6.15. Comparison of theoretical and experimental fluoride uptake flux values. h = 32 μm: (●) experimental, (★) theoretical; h = 227 μm: (♦) experimental, (◊) theoretical; J x 10^{10} mmoles/cm^2·sec.

TABLE 6.2

SURFACE SOLUTION ION ACTIVITY PRODUCTS

	Bulk Solution pK_{FAP} = 111.93	
	A.B.L. Thickness (micrometers)	
	227	32
Dissolution Time (hours)	$pK_{HAP/FAP}$	$pK_{HAP/FAP}$
3	118.69/114.04	119.56/112.82
6	118.70/113.47	119.63/112.48
12	118.73/112.93	119.69/112.21
24	118.77/112.44	119.77/112.05

	Bulk Solution pK_{FAP} = 114.53	
	A.B.L. Thickness (micrometers)	
	227	32
Dissolution Time (hours)	$pK_{HAP/FAP}$	$pK_{HAP/FAP}$
3	120.18/113.84	122.82/114.01
6	120.26/113.35	123.14/114.07
12	120.43/112.97	123.28/114.04
24	120.69/112.72	123.46/114.09

the surface fluoride concentrations (Figure 6.14) is, however, partially canceled by the effect of stirring on the surface pK_{HAP}. The net result of the two opposing forces is seen in Table 6.2 for the surface $pK_{FAP's}$ where it is observed that the decreased surface pK_{HAP} for the thinned boundary layer situation is partially compensated for by an increased surface fluoride concentration with the result being a rather constant surface pK_{FAP} for the two hydrodynamic conditions examined.

From the data presented in Table 6.2 it can be seen that in the pK_{FAP} = 111.93 bulk solution case, the effect of increasing the stirring rate on the solution fluoride concentration changes is slightly greater than the effect of an increased stirring rate on the surface solution ion activity product values. This effect can be seen in Table 6.2 by comparing the corresponding pK_{FAP} values at the two different stirring rates. On the other hand, in the pK_{FAP} = 114.53 bulk solution case, the effect of stirring on the surface solution K_{HAP} is slightly greater than it is for the surface solution fluoride concentration. The result of this is a greater surface solution K_{FAP} at the higher stirring rate. In either case, even though the magnitude of the effects is not that great, and also the fact that there is a partial cancellation between them, the conclusion is that the influence of stirring, under these conditions, would have at most a minimal effect on the enamel demineralization behavior. These conclusions are consistent with the good experimental observations (Figures 5.25 - 5.32) and the theoretical simulations

(Figures 6.12 and 6.13) the results of which are summarized in Tables 5.5 and 6.1 depicting the amount of hydroxyapatite dissolved as a function of time.

These interesting findings clearly demonstrate the complex nature of the role that solution fluoride plays in subsurface dissolution of dental enamel, validating the theoretical physical model and its assumptions. The proposed model can adequately account for all experimental observations related to the effect of solution fluoride on the formation and maintenance of an intact surface layer formed during bovine enamel demineralization. Furthermore, the analysis demonstrates the very complex nature of the intact surface layer/subsurface dissolution phenomenon from the physical chemistry standpoint.

To summarize the proposed theoretical physical model, it is important to recognize the importance of the intercrystalline solution ion activity product as being the important criteria determining where and under what conditions an intact surface layer will form in this bovine enamel system, at least. This is a consequence of the inability of fluoride to diffuse to the deep recesses of the enamel because of the adsorption/depletion mechanism and concurrently, the ability of acid to be able to diffuse to these deeper regions. The net result is that of the subsurface dissolution observed experimentally (Figures 5.25 - 5.32) and theoretically decribed by the proposed model. The unifying criteria for the formation and maintenance of an intact surface layer then is that all of these factors influence the dynamics in the system and must, in the net, lead to the situation where the

solution surface K_{FAP} is greater than 1×10^{-115} or 1×10^{-114}. As previously discussed, the solution calcium, phosphate, fluoride and hydrodynamics are all variables that must be defined.

The intercrystalline solution ion activity product model for predicting where and under what conditions subsurface dissolution will occur has been tested over a wide range of bulk solution chemistries and hydrodynamic conditions and has been found to adequately simulate the experimental results in a quantitative manner.

CHAPTER 7

SUMMARY

A physical and mathematical model has been proposed that adequately describes, at least, the early stages of subsurface dissolution in bovine enamel and, perhaps, human enamel as well. The development of this model was predicated on the experimental observation of an inhibition of the dissolution rate of hydroxyapatite when the dissolution media contained trace levels of fluoride ion. The purpose of the present study was to directly assess the inhibitory effect of fluoride on the dissolution rate of the crystallites in the surface region of bovine enamel by considering the appropriate diffusion equations and calculating the prevailing intercrystalline solution ion activity product. Calculation of the solution threshold for dissolution as a function of position in the enamel has allowed prediction of when and at what position in the enamel subsurface dissolution would occur. The major findings of the study completed may be summarized as follows:

1. A microradiographic technique has been developed that allows quantitative determination of experimentally observed mineral density changes occurring within the enamel matrix as a function of time and position.

2. Solution fluoride, in the presence of sufficient calcium and phosphate in the microenvironmental pores of the surface region of

enamel is a necessary condition for subsurface, rather than surface, dissolution to occur.

3. An advancing front of solution fluoride within the enamel infrastructure occurs, limited by adsorption of fluoride by the surface crystallites. The levels of bound fluoride in the surface region indicate a monolayer coverage of fluorapatite rather than gross precipitation of a new fluorapatitic phase.

4. Hydrodynamic considerations have indicated an enhanced uptake of fluoride by the enamel when the aqueous boundary layer is thin as seen by following the bulk solution chemistry changes as well as in the bound fluoride distribution profiles. This effect is also exemplified in the microradiographic kinetic studies where the dissolution rate decreased, or stayed nearly the same, when the aqueous boundary layer thickness was decreased by a factor of approximately 7. A similiar effect is observed in the calculated flux values obtained from a theoretical treatment of the problem.

5. Theoretical calculations have yielded a microenvironmental solution ion activity product (K_{HAP}) of 10^{-114} or 10^{-115} as representing the solution condition at which an intact surface layer is maintained or where subsurface dissolution proceeds at an appreciable rate.

6. A quantitative computer simulation of the mineral density changes occurring within the enamel matrix as a function of time and position has been achieved. Theoretically simulated mineral density profiles depicting the experimentally observed zonal dissolution (in

the absence of solution fluoride) and the subsurface dissolution with concomitant intact surface layer formation observed experimentally in the presence of low level solution fluoride is now possible.

REFERENCES

Armstrong, W.D. and Brekhus, P.J., Possible relationship between the fluorine content of enamel and resistance to dental caries. J. Dent. Res., 17 (1938) 393-399.

Aoba, T., Okazaki, M., Takahashi, J. and Moriwaki, Y., X-ray diffraction study on remineralization using synthetic hydroxyapatite pellets. Caries Res., 12 (1970) 223-230.

Bartheld, F. von, Decalcification in initial dental caries. Tijdschr Tandheelk, 65 (1958) 76-89.

Bartheld, F. von, Membrane phenomena in carious dissolution of the teeth. Arch. Oral Biol., special supplement, 6 (1961) 284-303.

Bibby, B.G., The use of fluorine in the prevention of dental caries, II. Effect of sodium fluoride applications. J. Am. Dent. Assoc., 31 (1944a) 317-321.

Bibby, B.G., Use of fluorine in the prevention of dental caries, I. Rationale and approach. J. Am. Dent. Assoc., 31 (1944b) 228-236.

Brown, W.E., Physicochemisity of apatite dissolution, Physico-chimie et Crystallographie des Apatites D'interet Biologigue, 230 (1978) 355-368.

Brudevold, F., Savory, A., Gardner, D.E., Spinelli, M. and Speirs, R., A study of acidulated fluoride solutions. Arch. Oral Biol., 8 (1963) 179-182.

Cate, J.M. ten and Duijsters, P.P.E., Influence of fluoride in solution on tooth demineralization. Caries Res., 17 (1983a) 193-199.

Cate, J.M. ten and Duijsters, P.P.E., Influence of fluoride in solution on tooth demineralization, II. Microradiographic data. Caries Res., 17 (1983b) 513-519.

Christoffersen, J. and Arends, J., Progress of artifical carious lesions in enamel. Caries Res., 16 (1982) 433-439.

Clarkson, B.H., Wefel, J.S. and Silverstone, L.M., Redistribution of enamel fluoride during white spot lesion formation: an in vitro study of human dental enamel. Caries Res., 15 (1981) 158-165.

Coolidge, T.B. and Jacob, M.H., Enamel carbonate in caries. J. Dent. Res., 36 (1957) 765-768.

Dean, H.T., Arnold, F.A. Jr. and Elvove, E., Domestic water and dental caries. Public Health Reports, 57 (1942) 1155-1179.

Dijk, J.W.E. van, Borggreven, J.M.P.M. and Driessens, F.C.M. Chemical and mathematical simulation of caries. Caries Res., 13 (1979) 169-180.

Driessens, F.C.M., The mineral in bone, dentin and tooth enamel. Bull. Soc. Chim. Belg., 89:8 (1980) 663-689.

Driessens, F.C.M. and Verbeeck, R.M.N., The probable phase composition of the mineral in sound enamel and dentine. Bull. Soc. Chim. Belg., 91:7 (1982) 573-597.

Falkenheim, M. and Hodge, H.C., A note on the mechanism of fluoride fixation. J. Dent. Res., 26 (1947) 241.

Fawzi, M.B., Fox J.L., Dedhiya, M.G., Higuchi, W.I. and Hefferren, J.J., A possible second site for hydroxyapatite dissolution in acidic media. J. Coll. and Int. Sci., 67:2 (1978) 304-311.

Featherstone, J.D.B., Duncan, J.F. and Cutress, T.W., Surface layer phenomenon in artifical early carious lesions of human enamel. Arch. Oral Biol., 23 (1978) 397-404.

Featherstone, J.D.B., Duncan, J.F. and Cutress, T.W., A mechanism for dental caries based on chemical processes and diffusion phenomenon during in vitro caries simulation on human tooth enamel. Arch. Oral Biol., 24 (1979) 101-112.

Featherstone, J.D.B., Melberg, J.R., Relative rates of progress of artificial carious lesions in bovine, ovine and human enamel. Caries Res., 15 (1981) 109-114.

Fox, J.L., Higuchi, W.I., Fawzi, M.B. and Wu, M., A new two-site model for hydroxyapatite dissolution in acidic media. J. Coll. and Int. Sci., 67:2 (1978) 312-330.

Fox, J.L., Muhammad, N.A., Bergstrom, D.H. and Higuchi, W.I., Fluoride profile in samples of nonuniform density. manuscript submitted to J. Pharm. Sci., 1984.

Francis, M.D., Briner, W.W. and Gray, J.A., Chemical agents in control of calcification processes in biological tissues. Hard tissue growth, repair and remineralization, A.S.P. Amsterdam, 1973, 57-90.

Gelinas, R.J., Doss, S.K. and Miller, K. The moving finite element method: application to general partial differential equations with multiple large gradients. J. Comp. Phys., 40 (1980) 202-249.

Gray, J.A., Kinetics of the dissolution of human dental enamel in acid. J. Dent. Res., 41 (1962) 633-645.

Gray, J.A. and Francis, M.D., Physical chemistry of enamel dissolution, in Mechanisms of hard tissue destruction, A.A.A.S. publication, 75 (1963) 213-260, Washington D.C.

Gray, J.A., Kinetics of enamel dissolution during formation of incipient caries-like lesions. Arch. Oral Biol., 11 (1966) 397-421.

Gray, J.A., Chemical events during cariogenesis. Proc. symp. on incipient caries of enamel, (1977) 69-92, Rowe ed., The University of Michigan.

Griffith, E.N., Katdare, A., Fox, J.L. and Higuchi, W.I., Transmission electron microscopic confirmation of the morphological predictions of the two site model for hydroxyapatite dissolution. J. Coll. and Int. Sci., 67:2 (1978) 331-335.

Groeneveld, A., Purdell-Lewis, D.J. and Arends, J., Influence of the mineral content of enamel on caries-like lesions produced in hydroxyethyl cellulose buffer solutions. Caries Res., 9 (1975) 127-138.

Gron, P., Spinelli, M., Trautz, O. and Brudevold, F., The effect of carbonate on the solubility of hydroxyapatite. Arch. Oral Biol., 8 (1963) 251-263.

Higuchi, W.I., Gray J.A., Hefferren, J.J. and Patel, P.R., Mechanisms of enamel dissolution in acid buffers. J. Dent. Res., 44 (1965) 330.

Higuchi, W.I., Cesar, E.Y., Cho, P.W. and Fox, J.L., Powder suspension method for critically re-examining the two-site model for hydroxyapatite dissolution kinetics. J. Pharm. Sci., 73:2 (1983) 146-153.

Hindmarsh, A.C. and Byrne, G.D. A polyalgorithm for the numerical solution of ordinary differential equations. ACM Trans. Math. Software 1, (1975) 71-96.

Holly, F.J. and Gray, J.A., Mechanism for incipient caries lesion growth utilizing a physical model based on diffusion concepts. Arch. Oral Biol., 13 (1968) 319-334.

Johansen, E., Ultrastructural chemical observations on dental caries. In A.A.A.S. publication, Mechanisms of hard tissue destruction. (1963) 187-211.

Koulourides, T.A. and Reed, J.L. Jr., Effects of calcium, phosphate and fluorine ions on the rate of softening and dissolution of tooth enamel. Arch. Oral Biol., 8 (1964) 585-594.

Langdon, D.J., Elliott, J.C. and Fearnhead, R.W., Microradiographic observation of acidic subsurface decaldification in synthetic apatite aggregates. Caries Res., 14 (1980) 359-366.

Larsen, M.J. and Fejerskov, O., Surface etching and subsurface demineralization of dental enamel induced by strong acids. Scand. J. Dent. Res., 85 (1977) 320-326.

Leach, S.A., Reactions of fluoride with powdered enamel and dentine. Brit. Dent. J., 106 (1959) 133.

Liang, Z.S., Kinetics and mechanism of fluoride uptake by hydroxyapatite. Ph.D. thesis, (1971) The University of Michigan, Ann Arbor, MI.

Little, M.F. and Barrett, K., Strontium and fluoride content of surface and inner enamel versus caries prevalence in the Atlantic coast of The United States of America. Caries Res., 10 (1976) 297-307.

Losee, F.L., Cutress, T.W. and Brown, R., Natural elements of the periodic table in human dental enamel. Caries Res., 8 (1974) 123-124.

Ludwig, A., Dave, S.C., Higuchi, W.I., Fox, J.L. and Katdare, A., Dissolution rate of apatite powders in acidic fluoride solutions and the relationship to hydroxyapatite disk and bovine enamel behavior. Int. J. Pharm., 16 (1983) 1-10.

Malaowalla, A. and Myers, H.M., Interaction of sodium fluoride and synthetic apatite. J. Dent. Res., 41 (1962) 413-419.

Miller, W.D., Acid dissolution in dental caries. J. Brit. Dent. Assoc., 5 (1884) 104.

Mir, N.A., The mechanism of action of solution fluoride upon the demineralization rate of enamel. Ph.D. thesis, (1967) The University of Michigan, (1967) Ann Arbor, MI.

Moreno, E.C. and Zahradnik. R.T., Chemistry of enamel subsurface demineralization in vitro. J. Dent. Res., 53 (1974) 226-235.

Neuman, W.F., Neuman, M.W., Main, E.K., O'Leary, J. and Smith, F.A., The surface chemistry of bone. J. Biol. Chem., 187 (1950) 655.

Saleeb, F.Z. and De Bruyn, P.C., Electrophoretic mobility study of human dental enamel. J. Electroanal. Chem., 37 (1972) 99.

Sincovec, R.F. and Madsen, N.K., Software for nonlinear partial differential equations. ACM Trans. Math. Software 1, (1975) 232-260.

Stalfors, A., Acid dissolution of enamel. Trans. Roy. Schools Stockholm and Umei, series 2:1 (1958) 52.

Stineman, R.W., A consistently well-behaved method of interpolation. Creative Computing, July (1980) 54-63.

Theuns, H.M., Dijk, van J.W.E., Driessens, F.C.M. and Groeneveld, A., Effect of time and degree of saturation of buffer solutions on artifical carious lesion formation in human tooth enamel. Caries Res., 17 (1983) 503-512.

Volker, J.F., Effect of fluorine on solubility of enamel and dentin. Proc. Soc. for Exp. Biol. and Med., 42 (1939) 725-727.

Weatherell, J.A., Robinson, C. and Hallsworth, A.S., Variations in the chemical composition of human enamel. J. Dent. Res., 53 (1974) 180-192.

White, W.D. and Nancollas, G.H., A rotating disk study of enamel dissolution in HEDP solution under simulated white spot conditions. J. Dent. Res., 59:7 (1980) 1180-1186.

Wu, M.S., Kinetics of hydroxyapatite dissolution and influence of foreign ions under sink conditions. Ph.D. thesis, (1975) The University of Michigan, Ann Arbor, MI.

Wu, M.S., Higuchi, W.I., Fox, J.L. and Friedman, M. Hydroxyapatite crystal dissolution in weak acid buffers using the rotating disk method. J. Dent. Res., 55:3 (1976) 496-505.

Zahradnik, R.T. and Moreno, E.C., Structural features of human dental enamel as revealed by isothermal water vapor sorption. Arch. Oral Biol., 20 (1975) 317-325.

Zahradnik, R.T., Moreno, E.C. and Burke, E.J., The effect of salivary pellicle on enamel subsurface demineralization in vitro. J. Dent. Res., 55 (1976) 664-670.